# The Use of Satellite-Model coupled System to Study Soil Moisture Effects on Mesoscale Circulations

By
Ingrid C. Guch

P.I. Roger A. Pielke

Department of Atmospheric Science
Colorado State University
Fort Collins, Colorado

Colorado State University

Department of Atmospheric Science

Paper No. 621

# THE USE OF A SATELLITE-MODEL COUPLED SYSTEM TO STUDY SOIL MOISTURE EFFECTS ON MESOSCALE CIRCULATIONS

Submitted by

Ingrid C. Guch

Department of Atmospheric Sciences

Fall 1996

ABSTRACT

THE USE OF A SATELLITE-MODEL COUPLED SYSTEM TO STUDY SOIL MOISTURE EFFECTS ON MESOSCALE CIRCULATIONS

It has been recognized that mesoscale circulations in numerical models are strongly influenced by soil moisture distributions. Because of the scarcity of *in-situ* soil moisture data, previous work has been done to use infrared heating rates observed from the GOES-7 satellite to derive approximate soil moisture amounts along with the Regional Atmospheric Modeling System (RAMS, version 3a). This research further studies this technique [the RAMS/GOES Data Assimilation (RGDA) method] by conducting sensitivity tests and analyzing several new case studies which involve different types of low level mesoscale circulations. Each case study was compared to a control run with homogeneous soil moisture initialization as well as to surface observations from National Weather Service stations and to microwave emissivity maps derived using data from the Defense Meteorological Satellite Program.

The effects of several surface parameters were studied. Among them were soil type, soil top layer depth, amount of vegetation, and deep level soil moisture. The RGDA method was found to be moderately sensitive to soil type, soil top layer depth and to the amount of vegetation. It was not sensitive to deep level soil moisture initialization for sandy clay loam. In general, the RAMS model appeared to evaporate the assimilated soil moisture quickly and RGDA runs had cooler air temperatures and higher humidities than control runs. Use of the RGDA method

improved values of surface relative humidity maximums in all case studies. However, temperatures in the control were about 0.5 K warmer than in the RGDA method and matched observations better.

All three case studies produced reasonable soil moisture fields from the RGDA method in cloud-free vegetated regions, as compared to microwave emissivity maps and recent rain events. The three cases using the RGDA method specifically studied breezes between wet cropland and lake regions (2 August 1991), breezes between wet cropland and dry grassland regions (6 August 1991), and breezes between wet cropland and dry cropland regions (11 September 1991). These breezes could not be modeled without the knowledge of soil moisture fields obtained from the RGDA method.

ACKNOWLEDGEMENTS

This research was funded by the DoD for Geosciences, Phase II, under grant #AAH04-94-G-0402.

*TABLE OF CONTENTS*

**INTRODUCTION** ..... **1**

1.1 OUTLINE OF RESEARCH ..... 1
1.2 BACKGROUND ..... 3
*1.2.1 The McNider et al. Method* ..... *5*
*1.2.2 A quantitative description of the RGDA method.* ..... *6*
1.3 RAMS ..... 10
*1.3.1 Lower Boundary Conditions as currently used in RAMS version 3a* ..... *10*
*1.3.2 RAMS Initialization and Configuration* ..... *11*
1.4 INSTRUMENTS AND STATION OBSERVATIONS USED IN CASE STUDIES. ..... 12
*1.4.1 Archived data used to initialize the RAMS model* ..... *12*
*1.4.2 GOES-7 Data* ..... *12*
*1.4.3 Defense Meteorological Satellite Program Special Sensor Microwave Imager (DMSP SSM/I) Data.* ..... *13*
*1.4.4 National Weather Service (NWS) stations.* ..... *13*
*1.4.5 Cooperative precipitation data.* ..... *13*
EXCURSUS: THE RELATIONSHIP BETWEEN VOLUMETRIC SOIL MOISTURE AND MEASURED DAILY EVAPOTRANSPIRATION. ..... 14

**SENSITIVITIES OF THE RGDA METHOD** ..... **19**

2.1 CHANGING THE DEPTH OF THE TOP SOIL LAYER ..... 19
2.2 FULL COLUMN FORCING ..... 20
2.3 RGDA METHOD WITH HALF THE ORIGINAL BATS VEGETATION. ..... 21
2.4 SAND VS. SANDY CLAY LOAM ..... 22
*2.4.1 Large scale observations* ..... *23*
*2.4.2 Small scale observations* ..... *23*

**CASE STUDY: 2 AUGUST 1991. MODERATELY WET SOIL AROUND A LAKE REGION.** ..... **32**

3.1 VALIDITY OF THE ASSIMILATED SOIL MOISTURE FIELD ..... 32
3.2 COMPARISON BETWEEN THE RGDA METHOD AND A HOMOGENEOUS SOIL MOISTURE RUN TO OBSERVATIONS ..... 34
3.3 USEFULNESS OF THE RGDA METHOD ..... 34
3.4 SUMMARY. ..... 36

**CASE STUDY: 6 AUGUST 1991. SOIL MOISTURE CONTRASTS IN AN AREA OF HETEROGENEOUS VEGETATION. ..... 47**

4.1 VALIDITY OF THE ASSIMILATED SOIL MOISTURE FIELD ..... 47
4.2 COMPARISON BETWEEN THE RGDA METHOD AND A HOMOGENEOUS SOIL MOISTURE RUN TO NWS OBSERVATIONS. ..... 48
4.3 USEFULNESS OF THE RGDA METHOD ..... 48
4.4 SENSITIVITY TO THE TIME PERIOD OF FORCING IN THE RGDA METHOD ..... 50
4.5 SUMMARY. ..... 52

**CASE STUDY: 11 SEPTEMBER 1991. SOIL MOISTURE CONTRASTS IN NEARLY HOMOGENEOUS VEGETATION ..... 65**

5.1 VALIDITY OF THE ASSIMILATED SOIL MOISTURE FIELD ..... 66
5.2 COMPARISON BETWEEN THE RGDA METHOD AND A HOMOGENEOUS SOIL MOISTURE RUN TO NWS OBSERVATIONS. ..... 67
5.3 USEFULNESS OF THE RGDA METHOD ..... 67
5.4 SUMMARY. ..... 69

**CONCLUSIONS ..... 80**

6.1 SUMMARY OF ALL CASE STUDIES ..... 80
6.2 ACCOMPLISHMENTS ..... 81
6.3 RESULTS ..... 82
6.3 IDEAS FOR FUTURE RESEARCH ..... 83

**BIBLIOGRAPHY ..... 85**

**APPENDIX: BASIC HYDROLOGY AND LAND-AIR INTERACTIONS SEEN USING THE RGDA METHOD. ..... 88**

A.1 BASIC HYDROLOGY IMPORTANT FOR STUDYING LAND-AIR INTERACTIONS ..... 88
*A.1.1 Interception* ..... *88*
*A.1.2 Infiltration* ..... *89*
*A.1.3 Evapotranspiration* ..... *89*
*A.1.4 Basic hydrology in the RGDA method* ..... *90*
A.2 SURFACE ENERGY BUDGET IN THE RGDA METHOD ..... 91
A.3 RGDA METHOD ANALYZED USING TIME SERIES PLOTS ..... 91
*A.3.1 Ground Temperature and Bare Soil Moisture* ..... *92*
*A.3.2 Effects of data assimilation method on surface latent and sensible heat fluxes* 93
*A.3.3 Surface air temperature and relative humidity.* ..... *94*
*A.3.4 Surface air temperature with respect to ground temperature.* ..... *94*
A.4 SUMMARY ..... 95

LIST OF TABLES

TABLE 1. 1 RAMS VERSION 3A OPTIONS FOR ALL RUNS IN THIS STUDY.....16
TABLE 1. 2 SOIL TYPES IN RAMS.....16
TABLE 1. 3 COMMON VEGETATION TYPES FOUND IN THE GREAT PLAINS AND THE PARAMETERS USED IN THIS STUDY.....16

TABLE 2. 1 SOIL COLUMN LAYERS FOR JONES RUN (3CM TOP LAYER) AND GUCH RUN (0.5CM TOP LAYER).....25

TABLE 3. 1 RAMS V3A CONFIGURATION FOR 2 AUGUST 1991.....38
TABLE 3. 2 RGDA METHOD, CONTROL RUN AND NWS SURFACE OBSERVATIONS FOR 18Z ON 2 AUGUST 1991 IN GRID 3.....38
TABLE 3. 3 SURFACE SENSIBLE HEAT FLUX FOR 18Z ON 2 AUGUST 1991 IN GRID 3.....38

TABLE 4 . 1 RAMS V3A CONFIGURATION FOR 6 AUGUST 1991.....53
TABLE 4 . 2 RGDA METHOD, CONTROL RUN AND NWS SURFACE OBSERVATIONS FOR 18Z ON 6 AUGUST 1991 IN GRID 3.....53
TABLE 4 . 3 SURFACE SENSIBLE HEAT FLUX FOR 18Z ON 6 AUGUST 1991 IN GRID 3.....53

TABLE 5. 1 RAMS V3A CONFIGURATION FOR 11 SEPTEMBER 1991.....70
TABLE 5. 2 RGDA METHOD, CONTROL RUN AND NWS SURFACE OBSERVATIONS FOR 18Z ON 11 SEPTEMBER 1991 IN GRID 3.....70
TABLE 5. 3 SURFACE SENSIBLE HEAT FLUX FOR 18Z ON 11 SEPTEMBER 1991 IN GRID 3....70

TABLE A.1 TYPICAL WET REGION REACTION TO THE RGDA METHOD.....97
TABLE A.2 TYPICAL DRY REGION REACTION TO RGDA METHOD.....97

LIST OF FIGURES

FIGURE 1. 1 GROUND SURFACE HEATING RATES DERIVED FROM CLOUD-CLEARED GOES-7 IR IMAGES BETWEEN 15:31Z AND 16:01Z FOR 8 AND 9 SEPTEMBER 1991. HIGH HEATING RATES ARE INDICATED BY THE LIGHTEST SHADES (1), LOW HEATING RATES BY THE DARKER SHADES(2), AND CLOUD CLEARED REGIONS IN BLACK (3).....17
FIGURE 1. 2 EXAMPLES OF ASSIMILATED SOIL MOISTURE MAP FOR 8 SEPTEMBER 1991. AREAS WITH ONLY A FEW CONTOURS ARE GENERALLY DRY REGIONS OR CLOUD-CLEARED REGIONS (AS SHOWN IN PREVIOUS FIGURE). AREAS WITH LOTS OF CONTOURS HAVE SOIL MOISTURE VALUES > 24%.....18

FIGURE 2. 1 REGIONS WHERE THE GROUND TEMPERATURES ARE GREATER THAN 303 K FOR THE JONES RUN (M048) AND THE GUCH RUN (M049) AT 16Z. M049 HAS A SMALLER TOP LAYER AND THUS WARMER GROUND TEMPERATURES. .....26
FIGURE 2. 2 REGIONS OF PERCENT BARE SOIL MOISTURE > 24% (WET SOIL) FOR THE JONES M048 RUN AND THE M049 RUN. .....26
FIGURE 2. 3 BARE SOIL MOISTURE PERCENT FOR TOP LAYER FORCING (M049) AND FULL COLUMN FORCING (M051), EACH WITH A .5 CM TOP SOIL LAYER. LAYER 11 REPRESENTS THE TOP LAYER OF SOIL AND LAYER 10 REPRESENTS THE LAYER JUST BENEATH THE TOP LAYER. COMPARE WITH FIGURE 1. 2.....27
FIGURE 2. 4 TEMPERATURES FOR A RUN WITH 50% BATS VEGETATION (M050) AND A RUN WITH 100% BATS VEGETATION FRACTIONS (M049). TEMPERATURES > 32 °C ARE SHADED.....28
FIGURE 2. 5 BARE SOIL MOISTURE > 24% (WET SOIL) FOR M050 AND M049 RUNS.....28
FIGURE 2. 6 REGIONS FOR TEMPERATURES > 303 K AT THE GROUND FOR THE SANDY RUN (M052) AND THE JONES RUN WITH SANDY CLAY LOAM (M048).....29
FIGURE 2. 7 BARE SOIL MOISTURE > 24% FOR 16Z AND 20Z FOR THE RUNS M052 (SANDY SOIL) AND M048 (SANDY CLAY LOAM SOIL). .....29
FIGURE 2. 8 BARE SOIL MOISTURE FOR SANDY RUN AT THE LAYER JUST BELOW THE SURFACE, LAYER 10.....30
FIGURE 2. 9 THE LATENT AND SENSIBLE HEAT FLUXES AT THE SURFACE FOR THE M052 CASE (SANDY SOIL, WET REGION).....30
FIGURE 2. 10 SURFACE TEMPERATURE (C) AND RELATIVE HUMIDITY VALUES FOR A WET REGION IN THE SANDY RUN (M052). .....31
FIGURE 2. 11 GROUND TEMPERATURES (K) AND BARE SOIL MOISTURE (%) FOR A DRY REGION IN THE M052 RUN WITH SANDY SOIL. COMPARE WITH FIGURE A.3.....31

FIGURE 3.1 AUGUST 2, 1991 HEATING RATES FROM 1501Z-1531Z. BRIGHTEST REGIONS ARE HEATING THE FASTEST. BLACK REGIONS ARE CLOUD-CLEARED AND NOT INCLUDED IN THE ASSIMILATION. CIRCLED REGION SHOWS CLOUD CONTAMINATION. 39
FIGURE 3.2 RAMS GRID FOR 2 AUGUST 1991 ..... 39
FIGURE 3.3 MICROWAVE EMISSIVITY MAP FOR CHANNEL 7 ON 3 AUGUST 1991, APPROXIMATELY 15:20Z. DARK AREAS INDICATE LOW EMISSIVITIES (PROBABLE WET AREAS) AND BLACK REGIONS ARE CLOUD-CLEARED OR MISSING DATA REGIONS. BOX INDICATES LOCATION OF GRID 3. ..... 40
FIGURE 3.4 VISIBLE IMAGE FOR 3 AUGUST 1991 AT 15:31Z. BOX INDICATES LOCATION OF GRID 3. ..... 40
FIGURE 3.5 WET REGIONS (BARE SOIL MOISTURE > 24%) FOR 2 AUGUST 1991 CASE STUDY. ..... 41
FIGURE 3. 6 TOTAL PRECIPITATION, INCHES, FOR 28 JULY 1991- 3 AUGUST 1991. BOX INDICATES GRID 3 FOR 2 AUGUST 1991 CASE ..... 41
FIGURE 3.7 LAKE REGIONS IN GRID 3 SUPERIMPOSED ON THE SURFACE SOIL MOISTURE AT 16:10Z FOR 2 AUGUST 1991. LAKES NUMBERED 1-8 ARE SURROUNDED BY WET (> 24%) SOIL AND LAKES NUMBERED 9-12 ARE SURROUNDED BY DRIER SOIL. ..... 42
FIGURE 3.8 SURFACE OBSERVATIONS FOR 18:00Z ON 2 AUGUST 1991. ..... 43
FIGURE 3. 9 VEGETATION FOR 2 AUGUST 1991 GRID 3. PROMINENT VEGETATION TYPES ARE 1-CROPLAND, 2-SHORT GRASS AND 5-TALL GRASS. ..... 43
FIGURE 3.10 WIND SPEED AT THE SURFACE FOR THE CONTROL RUN AND THE RGDA RUN AT 18:00Z. CONTOUR INTERVAL IS 0.5 °C. ..... 44
FIGURE 3.11 SURFACE LATENT HEAT FLUX (A), BARE SOIL MOISTURE(B) AND SURFACE SENSIBLE HEAT FLUX(C) AT THE SURFACE FOR A NORTH-SOUTH CROSS SECTION THROUGH THE LAKE REGION IN GRID 3 AT 18Z. ..... 45

FIGURE 4 . 1 MICROWAVE EMISSIVITY MAP FOR 6 AUGUST 1991, GRID 3. ..... 54
FIGURE 4 . 2 GRID 3 IR HEATING RATES BETWEEN 1531Z-1601Z ON 6 AUGUST 1991..... 54
FIGURE 4 . 3 RAMS GRID FOR 6 AUGUST 1991 CASE STUDY. ..... 55
FIGURE 4 . 4 CONTOURS OF WET REGIONS FOR 6 AUGUST 1991 CASE STUDY (BARE SOIL MOISTURE > 24%). CONTOUR INTERVAL IS 0.5%. ..... 55
FIGURE 4 . 5 VISIBLE IMAGE FOR 6 AUGUST 1991 AT 15:31Z. ..... 56
FIGURE 4 . 6 CO-OP 24-HR PRECIPITATION DATA FOR 5 AUGUST 1991 AND FOR BEFORE 16Z ON 6 AUGUST 1991. BOX INDICATES GRID 3. 6 AUGUST REPORTS ARE PLOTTED ABOVE 5 AUGUST REPORTS. ..... 56
FIGURE 4 . 8 SURFACE OBSERVATIONS AT 18:00Z FOR 6 AUGUST 1991 (NMC SURFACE ANALYSIS). ..... 57
FIGURE 4 . 9 LANDCOVER AND VEGETATION TYPE FROM BATS ON GRID 3. PREDOMINANT VEGETATION TYPES ARE (1) CROP/MIXED FARMING; (2) SHORT GRASS; AND (16) EVERGREEN SHRUB. THE SOLID NORTH-SOUTH LINE INDICATES 100Ø LONGITUDE. THE SOLID EAST-WEST LINE IS THE KS-OK BORDER ..... 57
FIGURE 4 . 10 LATENT HEAT FLUX (A), BARE SOIL MOISTURE (B), SENSIBLE HEAT FLUX (C), POTENTIAL TEMPERATURE (D) AND VERTICAL MOTION (E) FOR 18Z ON 6 AUGUST 1991. CROSS SECTION IS THE SAME AS IN THE PREVIOUS FIGURE. RISING MOTION IS IN SOLID CONTOURS AND SINKING MOTION IS IN THE DASHED CONTOURS FOR (E). ..... 59

FIGURE 4 . 11 NORTH-SOUTH CROSS SECTION FOR CONTROL AND RGDA RUNS FOR 6 AUGUST 1991 CASE STUDY AT 2130Z. SOUTHERLY WINDS (V) ARE CONTOURED BY .5 M/S IN A, VERTICAL MOTION (W) IS CONTOURED BY .04 M/S IN B.....60
FIGURE 4 . 12 WIND SPEED AT THE SURFACE FOR THE CONTROL RUN AND THE ASSIMILATION IN GRID 3 ON 6 AUGUST 1991 AT 2130Z. CONTOUR INTERVAL IS 0.5 M/S. DASHED LINE INDICATES CROSS SECTION USED IN THE PREVIOUS FIGURES. .....62
FIGURE 4 . 13 VISIBLE IMAGE FOR 00:01Z ON 7 AUGUST 1991, GRID 3 IS IN WHITE. .....63
FIGURE 4 . 14 CONTOURS OF WET REGIONS (> 24% VOLUMETRIC SOIL MOISTURE) FOR 6 AUGUST 1991 CASE STUDY. WITH THE ASSIMILATION OCCURRING BETWEEN 14Z AND 15Z INSTEAD OF 15Z TO 16Z. CONTOUR INTERVAL IS 0.5%. .....63
FIGURE 4 . 15 BARE SOIL MOISTURE > 24% FOR 6 AUGUST 1991, FORCING BETWEEN 16Z AND 17Z. .....64

FIGURE 5. 1 RAMS GRIDS FOR 11 SEPTEMBER 1991 CASE STUDY. .....71
FIGURE 5. 2 TIME RATE OF CHANGE FOR IR TEMPERATURES BETWEEN 1531Z AND 1601Z. DARK REGIONS HAVE THE LEAST TEMPERATURE CHANGE AND BRIGHT REGIONS HAVE THE HIGHEST TEMPERATURE CHANGE. CLOUDY AREAS ARE IN BLACK AND NOT INCLUDED IN CALCULATION. .....71
FIGURE 5. 3 CONTOURS OF WET REGIONS (BARE SOIL MOISTURE > 24%) FOR 9-11-91 IN THE RGDA METHOD. POSSIBLE CLOUD CONTAMINATION IN BOXES. .....72
FIGURE 5. 4 MICROWAVE EMISSIVITY MAP FOR CHANNEL 7 AT 15:35Z ON 9-11-91. BOX INDICATES APPROXIMATE AREA OF GRID 3. .....73
FIGURE 5. 5 VISIBLE IMAGE FOR 11 SEPTEMBER 1991 AT 15:31Z. WHITE BOX REPRESENTS GRID 3. .....74
FIGURE 5. 6 RADAR SUMMARY REPORTS FOR 2135Z AND 2235Z ON 10-SEPTEMBER-1991.74
FIGURE 5. 7 CO-OP 24 HOUR PRECIPITATION REPORTS FROM 10 SEPTEMBER 1991 AND FROM HOURS BEFORE 16Z ON 11 SEPTEMBER 1991 (PLOTTED ON TOP). BOX INDICATES GRID 3. .....75
FIGURE 5. 8 VEGETATION FOR GRID 3 IN 11 SEPTEMBER 1991 CASE STUDY. PROMINENT VEGETATION TYPES ARE: 1-CROP/MIXED FARMING, 2-SHORT GRASS, AND 7-TALL GRASS.....76
FIGURE 5. 10 NWS SURFACE OBSERVATIONS FOR 18Z ON 11 SEPTEMBER 1991.....76
FIGURE 5. 11 WET SOIL REGIONS > 24% BARE SOIL MOISTURE AT 1615Z FOR 11 SEPTEMBER 1991 IN THE RGDA RUN. BOX INDICATES REGION OF SOIL MOISTURE HETEROGENEITY WHICH APPEARS TO BE AFFECTING THE WINDS IN THE THIRD GRID IN THE RGDA RUN, DASHED LINE INDICATES APPROXIMATE POSITION OF CROSS SECTION FOR NEXT FIGURE. .....77
FIGURE 5. 12 VEGETATION FOR GRID 1 IN 11-SEPTEMBER 1991 CASE STUDY. GRID 2 IS INDICATED BY THE BLACK BOX AND THE CROSS SECTION IS INDICATED BY THE DASHED LINE. PROMINENT VEGETATION TYPES IN GRID 2 ARE: 1-CROP/MIXED FARMING, 2-SHORT GRASS, 5-DECIDUOUS BROADLEAF TREE, 7-TALL GRASS, 16-EVERGREEN SHRUB AND 18-MIXED WOODLAND. .....77
FIGURE 5. 13 TOTAL MIXING RATIO (G/KG), POTENTIAL TEMPERATURE (øK), VERTICAL WIND SPEED (M/S X 105, SOUTHERLY WIND SPEED (M/S) AND SURFACE SENSIBLE HEAT FLUX (W/M2) IN A NORTH-SOUTH CROSS SECTION FOR 11 SEPTEMBER 1991 CASE AT

18:00Z. BLACK LINE INDICATES VERY WET SOIL, GREY LINE INDICATES SLIGHTLY WET SOIL. ..... 79

FIGURE 6. 1 FLOWCHART EXAMINING MAJOR QUESTIONS STUDIED IN THIS THESIS. ..... 84

FIGURE A. 1 SURFACE ENERGY BUDGET TERMS FOR THE VEGETATION COMPONENT OF THE SURFACE, FROM JONES (1996) ..... 98
FIGURE A.2 CLOUD-CLEARED MICROWAVE EMISSIVITY MAP FOR CHANNEL 7, 8 SEPTEMBER 1991, 15:30Z. DARK AREAS ARE LOW EMISSIVITIES (PROBABLE WET AREAS), CLOUD CLEARED REGIONS ARE BLACK. ..... 99
FIGURE A.3 THE GROUND TEMPERATURE AND THE PERCENT BARE SOIL MOISTURE PLOTTED WITH RESPECT TO TIME FOR A MOIST REGION ON 8 SEPTEMBER 1991. APPROXIMATE PERIOD OF ASSIMILATION (10800S-14400S) IS UNDERLINED. ..... 99
FIGURE A.4 THE GROUND TEMPERATURE AND THE BARE SOIL MOISTURE PERCENT FOR A DRY AREA USING THE RGDA METHOD. ..... 100
FIGURE A.5 SURFACE LATENT AND SENSIBLE HEAT FLUXES WITH RESPECT TO TIME FOR A WET REGION IN THE RGDA METHOD ..... 100
FIGURE A.6 SURFACE LATENT AND SENSIBLE HEAT FLUXES FOR A DRY REGION USING THE RGDA METHOD. ..... 101
FIGURE A.7 TEMPERATURE AND RELATIVE HUMIDITY NEAR THE SURFACE FOR A WET REGION IN THE RGDA METHOD. ..... 101
FIGURE A.8 TEMPERATURE OF BARE SOIL AND TEMPERATURE OF THE AIR JUST ABOVE THE BARE SOIL FOR A WET REGION USING THE RGDA METHOD FOR THE 8 SEPTEMBER 1991 CASE. ..... 102
FIGURE A. 9 TEMPERATURE IN CELSIUS FOR A WET REGION USING THE RGDA METHOD BETWEEN 15 AND 16Z (NOT TO SCALE) ..... 102

Chapter 1

# Introduction

## *1.1 Outline of Research*

This research will focus on the latest techniques to infer surface boundary conditions from atmospheric models using information from polar and geostationary satellites. Satellites are an important tool because of their ability to monitor nearly all portions of the earth at much higher resolutions (in space and time) than *in-situ* measurements.

The first part of this thesis focuses on a new method to infer surface soil moisture developed by Jones (1996). This method is called the RAMS/GOES Data Assimilation and will be referred to as the RGDA, or simply the assimilation method. An explanation of the RGDA method and the equations used is given in this chapter. Chapter 2 studies the model run originally done by Jones (1996) and looks at sensitivities in the RGDA method by changing some of the initialization parameters.

The second part of this thesis focuses on three new case studies using the RGDA method to retrieve surface soil moisture amounts and study land-air interactions. Chapters 3, 4 and 5 describe each new case study in depth and chapter 6 attempts to draw general conclusions about the assimilation method as well as about land-air interactions. Appendix is provided for those who have no background knowledge of the RGDA method and would like a qualitative description of how it works.

There are five questions this thesis explores.

1. What are the sensitivities of the RGDA method? (Chapter 2)
2. Is the RGDA soil moisture field valid? (Chapter 3-5)
3. Is RAMS treating evapotranspiration and infiltration in a realistic manner? (Appendix, Chapters 2, 4)
4. Does the RGDA method improve upon a homogeneous soil moisture control run when comparing output to surface observations? (Chapters 3-5)
5. What circulations can heterogeneous soil moisture generate in RAMS? (Chapters 3-5).

In the future, answers to these questions will provide a basis for routinely remotely sensing soil moisture fields and using them in a numerical mesoscale model to study land-air interactions. The case studies presented here will also help atmospheric scientists predict which situations may require knowledge of soil moisture fields for successful numerical weather prediction. The assimilation can also be used to verify a numerical mesoscale model treatment of the ground surface (soil moisture, vegetation, lake features, evaporation and infiltration), because the observed satellite infrared (IR) heating rates are very close to ground truth surface heating rates.

Each case study was for an area in the central plains during the summer of 1991 because microwave emissivity maps were available (Jones, 1996). These maps help validate the soil moisture fields generated by the RGDA method. Furthermore, each case study had to have clear skies in the morning hours for the RGDA method to work (IR ground temperatures needed to be retrieved via satellite). The questions (1-5) were complicated enough to warrant more than one new case study. The three cases chosen were:

1. 2 August 1991, in order to study moderately wet soil around a lake region,
2. 6 August 1991, in order to study soil moisture contrasts in an area of heterogeneous vegetation and

3. 11 September 1991, in order to study soil moisture contrasts in an area of homogeneous vegetation.

These cases are meant to describe some typical land-air interactions which occur due to heterogeneous surface soil moisture fields.

### *1.2 Background*

A numerical weather model's frequent inability to properly place convective storms causes difficulty for modelers. As numerical weather models have become more sophisticated to study mesoscale events, there has been increasing concern about getting the model's lower boundary condition correct with respect to soil moisture and vegetation. Convection placement is very sensitive to soil moisture and vegetation parameterizations according to several dry line studies (Shaw, 1994 and Grasso, 1995).

Findings from Gannon (1978) and McCumber and Pielke (1981) show that moisture is the most important soil variable for the study of land-air interactions and that in most cases it overrides the effects of changing surface albedo and changing soil texture and type. Not only is it important to infer surface soil moisture accurately, but it has also been shown by McCumber and Pielke (1981) that numerical weather models are sensitive to soil moisture profile as well.

Segal and Avissar (1988) studied the generation of thermally-induced flows between vegetation and bare soil. They found that some circulations which developed were on the same order as a sea breeze when the synoptic flow was specified as calm in the model. They called these "nonclassical mesoscale circulations" (NCMC's). Segal et al. (1989) combined satellite, observational and modeling approaches to study circulations between irrigated areas and dry land regions in northeast Colorado. For three case studies they found that NCMC's were very weak due to significant terrain-forced and synoptic flow (0-5 m/s). This work is similar, but will focus on the effect of horizontal variability in soil moisture during non-negligible synoptic flows

(generally 5-10 m/s) with very weak terrain-forced flow. Emphasis is placed upon modeling these flows because observations do not have high enough spatial resolution to confirm the existence of NCMC's for the periods being studied.

There are several indices based on satellite data to infer surface soil moisture [e.g. Soil Wetness Index (SWI) from the National Oceanic and Atmospheric Administration (NOAA), described by Achutuni et al., (1994) and the Soil Moisture Index described by McFarland and Neale (1991)] and vegetation type [e.g. the Normalized Difference Vegetation Index (NDVI)]. There have also been techniques developed to map microwave surface emissivities using microwave and infrared satellite data (Jones, 1996). Some microwave channels (e.g. 19.35 GHz) on polar orbiting satellites are able to infer soil moisture several inches below the surface. However, these channels have low horizontal resolution (69 x 43 km), and this low resolution has led investigations to the possibility of using visible and IR data to infer soil moisture. McNider et al. (1994) uses a technique that infers soil moisture terms by using observed IR temperature changes and placing them into the surface energy budget equation. Gillies and Carlson (1995) have developed a method that uses a "universal" triangle to derive surface moisture availability using the NDVI along with satellite data from the Advanced Very High Resolution Radiometer (AVHRR).

Methods which don't use satellite data to specify soil moisture are popular because they are easy to implement. The Antecedent Precipitation Index (API) is frequently used to initialize RAMS. This index takes into account the amount of rain which falls in the domain but does not include irrigation effects or distinguish between vegetation or soil types. Also, the API underestimates precipitation if rain or snow occurs where there are no surface observations. There is also the Weekly Crop Index available for use, but this is dependent on the types of crops being planted in the area.

### 1.2.1 The McNider et al. Method

This method is described by McNider et al. (1994). A short summary is provided here, and the RGDA method will be summarized in the next section.

The technique uses the surface energy equation (Blackadar, 1979):

$$C_b \frac{\partial T}{\partial t} = R_n + E + H + G \qquad (1.1)$$

where $C_b$ is the ground surface heat resistance (J/(K m$^2$), $T$ is the temperature (K), $R_n$ is the net radiation at the surface (W/ m$^2$), $E$ is the latent heat flux (W/ m$^2$), $H$ is the sensible heat flux (W/ m$^2$), and $G$ is the soil heat flux (W/ m$^2$). The latent heat flux term in the surface energy budget is assumed to be most difficult to quantify. The technique assimilates IR satellite-observed surface skin temperature tendencies into the model's surface energy budget (equation 1.1). The predicted rate of temperature change from the model is altered so that it conforms more closely to observed rate of temperature change from satellite while being energetically consistent. This is done by analytically solving Monin-Obukov similarity expressions (Stull, 1988) to get a soil moisture value that gives correct temperature change in the surface energy budget.

There are several assumptions and conditions that must be satisfied. One must be doing short-term prediction or diagnostic modeling where frequent external adjustment is allowed. Cloud-free views of the surface must be frequent for the time period being modeled. The largest error in the surface energy budget must be the availability of surface moisture. This means that errors in specifying parameters such as wind speed, surface roughness and ground surface heat resistance must be small compared to the errors in the surface moisture terms.

The benefit of this technique is that one avoids having to specify many parameterizations of vegetation and soil processes. Absolute calibration of the satellite sensor is not needed because it only deals with rate of change of surface skin temperature and not absolute surface

skin temperature. Use of geostationary satellites will avoid some problems involving viewing angle dependence which are found using polar orbiting satellites.

The main drawback with this method is that ground surface heat resistance and thermal inertia values are difficult to quantify. This topic is explored in Carlson et al. (1981), the TELL-US model described by Rosema et al. (1978), the Apparent Thermal Inertia quantity described by Pohn et al. (1978), and Price (1982). McNider et al. used the inverted form of equation 1.1 to solve for ground surface heat resistance using observations for the net energy fluxes and change of skin temperature measured in FIFE [the First ISLSCP (International Satellite Land Surface Climatology Project) Field Experiment] for a Kansas prairie site. The quantity varied wildly between -50,000 J/(K $m^2$) and +50,000 J/(K $m^2$) due to very small rates of change in skin temperature as well as variations in energy fluxes.

### 1.2.2 A quantitative description of the RGDA method.

This method is more detailed than the McNider et al. method because satellite forcing is partitioned between bare soil, shaded soil, water and vegetation. Each grid cell in RAMS is evaluated using United States Geologic Survey (USGS) datasets which include NDVI based vegetation fractions. The satellite-observed change in temperature with respect to time is assumed to be the correct ground surface heating rate and the model error in this value is assumed to be caused by the latent heat flux term in the surface energy budget.

The model is then forced by satellite data to obtain the correct heating rate by moistening or drying out bare and shaded soil (the forcing is proportional to the percentage of bare and shaded soil coverage in the grid cell) as well as altering the vegetation moisture profile. Because wet soil heats slower than dry soil, a grid cell that heats too quickly is corrected by increasing soil moisture. In extreme cases a grid cell may flood to produce the correct heating rate. If the model is heating up too slowly, the soil is assumed to be overly moist and the model is forced to dry it

out. In principle, this should work for times of both heating and cooling during the day. However, the method tends to become unstable during times of cooling because the latent heat term can no longer be assumed to be the most unknown term in the surface energy budget (Jones, 1996).

A convenient part of the method is that one need not find the ground surface heat resistance, as parameterizations in the model for thermal inertia for water, bare soil, shaded soil and eighteen different vegetation types are already in RAMS. The percentage of vegetation, water, and bare soil must be known fairly accurately for each area being modeled. The equation for the RAMS heating rate is shown below.

$$\left(\frac{\partial T}{\partial t}\right)_m = f_L\left(\frac{\partial T_L}{\partial t}\right)_m + f_V\left(\frac{\partial T_V}{\partial t}\right)_m + f_W\left(\frac{\partial T_W}{\partial t}\right)_m \qquad (1.2)$$

The subscripts $L$, $V$ and $W$ represent land, vegetation and water. The $f$ denotes the fraction of the grid cell occupied by the subscript term. The subscript $m$ denotes that the terms are from the model, not the satellite. The assimilation assumes

$$\left(\frac{\partial T_W}{\partial t}\right) = 0 \qquad (1.3)$$

and that all fractional terms are correct. The time rate of change for land temperature and vegetation temperature are adjusted by changing latent heat flux in the surface energy budget, particularly the ground surface friction humidity term.

$$Q_{top\ soil\ layer,adjusted} = Q_{top\ soil\ layer,unadjusted} + \Delta E \qquad (1.4\ a)$$

$$\Delta E = L_V \rho_a u_{*L} \Delta q_{*L} \qquad (1.4\ b)$$

Here $Q$ represents net flux at the surface, $E$ represents latent heat flux at the surface, $L_V$ represents the latent heat of vaporization, $\rho_a$ is the density of air, $u$ is the wind speed just above the surface, and $q$ is the ground surface humidity. An asterisk indicates a friction quantity (Jones,

1996). The assimilation must change heating rates while keeping relative magnitudes of different heating rate components the same, i.e.

$$\frac{\left(\frac{\partial T_L}{\partial t}\right)_{adjusted}}{\left(\frac{\partial T_V}{\partial t}\right)_{adjusted}} = \frac{\left(\frac{\partial T_L}{\partial t}\right)_{unadjusted}}{\left(\frac{\partial T_V}{\partial t}\right)_{unadjusted}} \qquad (1.5)$$

The governing equation for updating the time rate of temperature change for land becomes:

$$\left(\frac{\partial T_L}{\partial t}\right)_{m'} = \left[\frac{\left(\frac{\partial T}{\partial t}\right)_s}{f_L + f_V\left(\frac{\partial T_V}{\partial t}\right)_m\left(\frac{\partial T_L}{\partial t}\right)_m^{-1}}\right] \qquad (1.6)$$

A solution for a new surface soil moisture value (Jones, 1996) is iteratively found using Newton's method. When surface soil moisture values converge, the time rate of temperature change for land stops being updated. The value for time rate of temperature change for vegetation is a function of $\left(\frac{\partial T_L}{\partial t}\right)_{adjusted}$ and $\left(\frac{\partial T}{\partial t}\right)_s$ and a corresponding vegetation moisture content is then calculated for the vegetation profile.

The volumetric soil moisture amounts measured in the field are generally representative of bare soil moisture. Because of this, bare soil moisture is analyzed here rather than shaded soil moisture or moisture in the vegetation column. Jones (1996) found that bare soil moisture was fairly representative of shaded soil moisture and vegetation moisture, although bare soil moisture evaporated faster.

The assimilation of satellite data was done using PORTAL (Polar Orbiter Remapping and Transformation Application Library) files (Jones, 1995) to grid the data into the RAMS projection space. The IR data was first processed to generate cloud-free files using a threshold

technique classifying everything cooler than 280 K in the 11 μm IR channel to be a cloud. Surface heating rate files were generated for the RAMS projection space and converted to ASCII format to use in the model. Each assimilation period was one hour long. Each model run was twelve hours long (12z to 00z).

As shown in the equations, soil moisture maps derived from the RGDA method are obtained directly from change in temperature as seen from the IR channel of GOES-7. Figure 1. 1 shows ground surface heating rates derived from IR satellite data at 15:31z and 16:01z. The brightest shades represent the largest heating rates (a 3 K increase during the half hour period, for areas not contaminated by clouds). Cloud-cleared areas are in black. The darkest shades of grey represent the lowest heating rates (0-1 K increase during the half hour period). The lowest heating rates should correspond to the wettest and/or most vegetated regions. The RAMS model is needed to derive soil moisture values from the satellite data because it has a database of vegetation types. RAMS also is initialized with the morning's weather and should have some estimates as to how much of the ground surface heating rate is due to temperature advection (i.e. perhaps very cold air is moving over dry soil, lowering the heating rate).

One can see in Figure 1. 1 that the lowest heating rates are in the eastern central plains and that higher heating rates are in the western central plains. This pattern also occurs in soil moisture maps produced after the assimilation in the 8 September case, as shown in Figure 1. 2. The soil moisture for 9 September is similar, but more cloud-contaminated, and so is not shown here. Percent soil moisture refers to volumetric soil moisture (kg water/kg water at saturation). There are three different cases shown in Figure 1. 1 and Figure 1. 2. The region labeled "1" is a dry region heating about 5 K/hr. The region labeled "2" is a wet region heating between 0 and 1 K/hr. The region labeled "3" has been cloud-cleared. Cloud-cleared regions will have a soil moisture amount which is a function of the specified initialization of volumetric soil moisture. This is the same value that RAMS would generate if there were no assimilation, and is almost

always the same or drier than regions using the RGDA method (see Appendix). Both the 8 and 9 September 1991 cases have significantly large cloudy regions affecting the assimilation's retrieval of soil moisture. These are seen as the black regions in the time rate of temperature change maps. The high heating rates (up to 13 K/hr) are not due to land heating up at that rate; instead they are due to a moving cloud which was not eliminated. These regions are generally on the border of cloud-cleared regions and can be avoided by choosing a domain to study that lies several kilometers away from cloud-cleared regions.

## *1.3 RAMS*

### 1.3.1 Lower Boundary Conditions as currently used in RAMS version 3a

The prognostic soil model and vegetation model that RAMS uses is described by McCumber and Pielke (1981) and Tremback (1990). Initializing RAMS consists of databases which include topography, sea surface temperature, land percentage, vegetation distribution and soil type. RAMS is normally run with homogeneous soil type distribution and surface soil moisture content set at a constant value. Unfortunately, soil type and moisture distribution is nearly always heterogeneous over moderately sized domains. Vegetation parameterizations are derived using the Biosphere-Atmosphere Transfer Scheme (BATS is described by Dickinson et al., 1993) where there are 18 land types specified and from which the Leaf Area Index (LAI) and fractional vegetation amounts can be estimated. Because the model runs were for summertime periods in the central plains, the LAI was limited to a value of 3 (following Shaw, 1995).

RAMS is fairly flexible about allowing user input of different types of surface boundary conditions in the model. The Antecedent Precipitation Index (API) has been used (Shaw, 1995 and Copeland, 1995) as have improved vegetation and soil type distributions (Copeland, 1995). However, the initialization which is easiest and most frequently used is a constant surface soil

moisture content and the BATS vegetation description. This is what will be used for all control runs.

### 1.3.2 RAMS Initialization and Configuration

Initialization information (soundings, surface observations and National Meteorological Center pressure data) was provided by the mass storage system at the National Center for Atmospheric Research (NCAR). Table 1. 1 describes the RAMS options chosen for all the runs.

Only very basic microphysics has been used in the model. Water vapor is allowed to condense to cloud water wherever supersaturation is attained, but no other forms of liquid or ice water are used. The vertical equation of motion includes the positive buoyancy effect of water vapor and the liquid water loading of cloud water. Rain, pristine ice, snow, aggregates and hail are not activated microphysical parameters in the model runs. The reason for these simplifications is to focus on more direct effects of land-air interactions (wind speed just above the surface, surface air temperatures and surface relative humidities) rather than indirect effects such as cloud microphysics or the amount of rain or hail generated by a particular storm. Obviously, with this microphysics, RAMS is not allowed to add soil moisture to the domain by raining. These studies focus on how RAMS reacts to soil moisture variations which have been derived from satellite data.

Soil type is important when analyzing land-air interactions. RAMS has twelve different soils to choose from; all (except peat) are based on the USDA soil classification pyramid. Four parameters are particularly important to consider when choosing a ground surface type. The dry soil thermal diffusivity gives a value for how quickly heat can transfer through soil layers. The saturation soil hydraulic conductivity governs how easily water can move through the soil column. The dry soil volumetric heat capacity controls how much energy is needed to heat the soil. The saturation volumetric moisture content gives a number for the maximum amount of

water the ground can absorb. Table 1. 2 shows the values for these parameters as a function of RAMS ground cover type. This work follows Shaw's 1995 work in the central plains and uses sandy clay loam as the soil type.

Vegetation type is also important, particularly its albedo, fractional vegetation amount and LAI. The most important vegetation types in the central plains and parameters associated with them are shown in Table 1. 3. The higher the albedo the more solar radiation that is reflected away. The vegetation fraction indicates the percent of each grid cell covered with the specified plant type. The leaf area index roughly corresponds to how much the specified plant type transpires due to the amount of leaves it has.

### *1.4 Instruments and station observations used in case studies.*

#### 1.4.1 Archived data used to initialize the RAMS model

All model runs used in this study were initialized at 12:00z with archived data prepared by the Data Support Section in the Scientific Computing Division at the National Center for Atmospheric Research. The data consisted of NMC surface analyses, NMC upper air observations and NMC global analyses of 2.5 degree gridded pressure.

#### 1.4.2 GOES-7 Data

The visible and IR data for all case studies are from the Visible-Infrared Spin Scan Radiometer (VISSR) sensor on the GOES-7 satellite. The sensor was operating in the multispectral imaging (MSI) mode and provided infrared imagery at 11.2 μm (channel 8) with 4 km x 8 km nominal resolution. Visible imagery had 1 km x 1 km nominal resolution. Because satellite data used in the RGDA method involves rate of temperature change, absolute calibration of GOES-7 datasets is not required.

### 1.4.3 Defense Meteorological Satellite Program Special Sensor Microwave Imager (DMSP SSM/I) Data.

The datasets used to generate microwave surface emittance maps were from the GOES-7 VISSR sensor and from the DMSP SSM/I sensors. All emittance maps were processed by Jones (1996).

The SSM/I used was from the DMSP F-8 and F-10 sun-synchronous satellites. The emissivity maps shown are from channel 7 on the SSM/I. Channel 7 has a frequency of 85.5 GHz, horizontal polarization and an effective field of view of 15 x 13 km. The datasets were sampled at 12.5 km intervals with 128 scan-line elements (Jones et al., 1995).

### 1.4.4 National Weather Service (NWS) stations.

Each NWS station takes surface observations every hour. These surface observations are used to create NMC surface analysis every three hours. Surface observation accuracy varies greatly depending on instrument placement, instrument quality, and the instrument operators. The spatial resolution of the NWS stations probably is not enough to diagnose mesoscale breezes. However, the stations provide some ground truth which can tell whether or not the models are on the right track.

### 1.4.5 Cooperative precipitation data.

The cooperative precipitation datasets were obtained from the data support section of NCAR. This dataset provided a summary of the day from many stations across the country. Each station takes precipitation measurements once a day using a rain gauge. The quality of the measurements are not as high as the measurements from NWS due to low temporal resolution. However, spatial resolution of the data is higher than for NWS stations. For this reason co-op

precipitation data was useful for understanding surface soil moisture amounts and finding out if wet soil regions were due to rain events.

***Excursus: The relationship between volumetric soil moisture and measured daily evapotranspiration.***

The agricultural community frequently measures daily evapotranspiration. The RGDA method alters volumetric soil moisture. Relating these two quantities is therefore important. Suppose one has 20% volumetric soil moisture (averaging bare and shaded soil components) in the top layer of sandy clay loam soil before the RGDA method and 30% volumetric soil moisture after the RGDA method. How much more water has been added?

At 20% volumetric soil moisture one can use the saturation volumetric moisture for sandy clay loam in Table 1. 2 to find the actual amount of water in the soil.

$$0.20 \times \frac{0.420 m^3 water}{m^3 soil} = 0.084 \frac{m^3 water}{m^3 soil} \qquad (1.7).$$

However, this is only true for the top layer of soil. Perhaps the top layer is 3 cm deep. Now,

$$0.03m \times \frac{0.084 m^3 water}{m^3 soil} = \frac{0.00252 m^3 water}{m^2 soil} \qquad (1.8)$$

If all the water evaporates out during the day, 0.00252 m of water will evaporate from each square meter of land. This is the same as a daily evaporation value of 0.00252m or about 0.10 inches.

At 30% volumetric soil moisture one has

$$0.30 \times \frac{0.420 m^3 water}{m^3 soil} \times 0.03 m = \frac{0.00378 m^3 water}{m^2 soil} \qquad (1.9).$$

In this case the daily evaporation value would be about 0.15 inches. The actual value of evapotranspiration (which includes the effects of transpiring vegetation) would be higher. The net change in daily evapotranspiration due to soil moisture using the RGDA method would be about .05 inches. With such a small change in the net daily evapotranspiration, one might wonder if the RGDA method is working within the noise of the system. The importance of the RGDA method is not just in the daily moisture flux; it is also important for the partitioning of latent and sensible heat flux at the surface. In the absence of temperature advection, air over wet land will not heat up as quickly as air over dry land. Jones (1996) has done sensitivity tests which show that the RGDA method is not significantly affected by random noise in the satellite data. There is a clear signal of soil moisture when using the RGDA method and it is not within the noise of the system to be looking at evapotranspiration and analyzing surface heat fluxes surface due to assimilated soil moisture.

**Table 1. 1 RAMS version 3A options for all runs in this study.**

| *Category* | *RAMS option* |
|---|---|
| initialization | variable |
| radiation | Mahrer and Pielke (1977) |
| lateral boundary condition | Klemp/Willhelmson (1978) |
| top boundary condition | wall on top |
| continuity equation | nonhydrostatic |
| advection | second order |
| timestep | 30 sec |
| time differencing scheme | forward timestep/leapfrog timestep hybrid |
| top soil layer depth | 3 cm |
| soil type | sandy clay loam |
| Vegetation fraction | 50% BATS fractions (see p.21) |
| Satellite forcing in RGDA method | top layer only |

**Table 1. 2 Soil types in RAMS.**

| | Dry soil thermal diffusivity $m^2/sec$ | Saturation soil hydraulic conductivity m/s | Dry soil volumetric heat capacity $J/m^3$ K | Saturation volumetric moisture content $m^3/m^3$ |
|---|---|---|---|---|
| sand | 2.40E-7 | 1.76E-3 | 1.47E+6 | 3.95E-1 |
| loamy sand | 2.37E-7 | 1.56E-4 | 1.41E+6 | 4.10E-1 |
| sandy loam | 2.34E-7 | 3.47E-5 | 1.34E+6 | 4.35E-1 |
| silt loam | 2.29E-7 | 7.20E-6 | 1.27E+6 | 4.85E-1 |
| loam | 2.24E-7 | 6.95E-6 | 1.21E+6 | 4.52E-1 |
| sandy clay loam | 2.15E-7 | 6.30E-6 | 1.18E+6 | 4.20E-1 |
| silty clay loam | 2.09E-7 | 1.70E-6 | 1.32E+6 | 4.77E-1 |
| clay loam | 2.09E-7 | 2.45E-6 | 1.23E+6 | 4.76E-1 |
| sandy clay | 2.00E-7 | 2.17E-6 | 1.18E+6 | 4.26E-1 |
| silty clay | 1.94E-7 | 1.03E-6 | 1.15E+6 | 4.92E-1 |
| peat | 1.00E-7 | 8.00E-6 | 8.74E+5 | 3.63E-1 |

**Table 1. 3 Common vegetation types found in the great plains and the parameters used in this study.**

| | *albedo* | *vegetation fraction* | *leaf area index* |
|---|---|---|---|
| crop/mixed farming | 20 | 43 | 3 |
| short grass | 26 | 40 | 2 |
| tall grass | 16 | 40 | 3 |
| evergreen shrub | 10 | 40 | 3 |

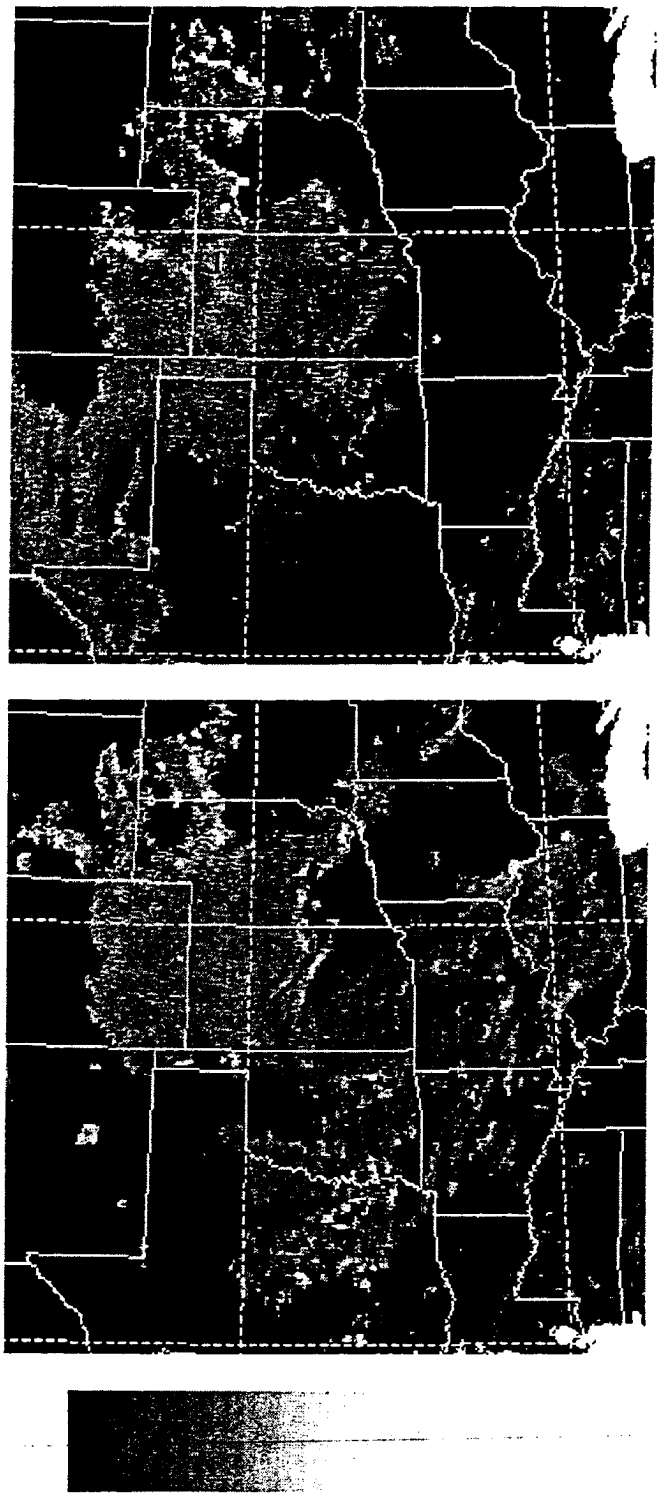


**Figure 1. 1 Ground surface heating rates derived from cloud-cleared GOES-7 IR images between 15:31z and 16:01z for 8 and 9 September 1991. High heating rates are indicated by the lightest shades (1), low heating rates by the darker shades(2), and cloud cleared regions in black (3).**

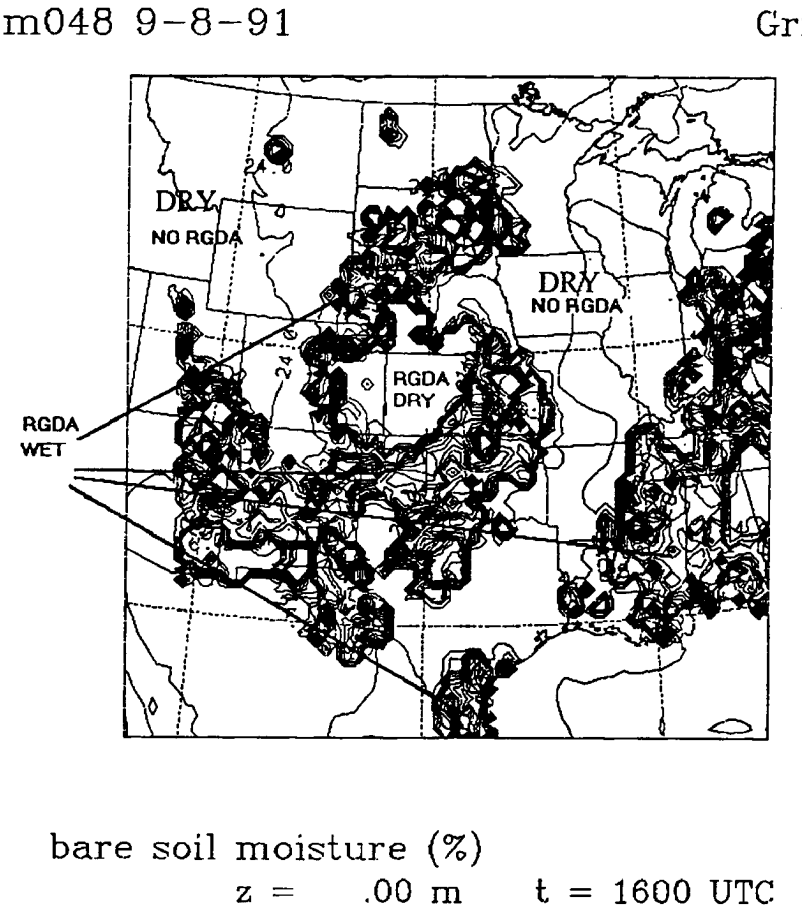


**Figure 1. 2 Examples of assimilated soil moisture map for 8 September 1991. Areas with only a few contours are generally dry regions or cloud-cleared regions (as shown in previous figure). Areas with lots of contours have soil moisture values > 24%.**

Chapter 2

## Sensitivities of the RGDA method

There are four initialization parameters that must be specified to use the RGDA method but for which there are very few *in-situ* observations. These are the top layer soil depth, the moisture in the deep levels of soil, the fractional amount of vegetation and the homogeneous soil type. It is likely that one or more of these parameters will be specified incorrectly by the RGDA method user and so sensitivity tests must be done to see how important each one is. In this section, values for each of the parameters which are just or almost as reasonable as the values chosen by Jones, 1996 will be used to initialize the 8 September 1991 case.

### *2.1 Changing the depth of the top soil layer*

In RAMS there are 11 soil layers (layer 11 is at the surface). The assimilation matches the heating rate of layer 11 to the IR heating rate viewed by the satellite. It is very difficult to know how deep this top soil layer should be. This top layer should have homogeneous properties (how compact it is, how much moisture it contains and its temperature) throughout. Most importantly in the RGDA method, this layer should reflect what the IR channel of the satellite is sensing. Jones (1996) assumed this layer to be 3cm deep, which is a typical value used in RAMS. However, it is reasonable to think that this layer might be thinner, particularly because

the satellite is really only sensing ground skin temperature. Hence, a run which was the same as Jones' run except with a slightly different soil layer profile (see Table 2. 1) was done.

The results of this run showed that ground temperatures were 1.0 °C warmer at 1600z for the smaller top layer. Figure 2. 1 shows the regions where bare soil temperatures are warmer than 303 K at the ground. The Present run has warmer bare soil temperatures. However, because the surface layer is smaller the soil moisture maps look slightly different between runs (Figure 2. 2). A thinner surface layer will not need as much forcing by adding soil moisture in the assimilation as a larger surface layer because it has less thermal inertia.

Because the soil moisture map was drier in the new run and the ground layer thinner, the soil moisture evaporated faster than it did in the Jones run. The lack of *in-situ* measurements for the soil top layer depth is a problem which can cause errors when predicting surface temperatures using RAMS. This parameter also governs the speed at which the RGDA method's soil moisture map evaporates and so is important when calculating latent and sensible heat fluxes throughout the day. However, problems associated with the specification of the top layer depth are not as significant when looking at general patterns of surface soil moisture.

### *2.2 Full Column Forcing*

The IR sensor on a satellite can only sense skin temperature. Because of this, only the top layer is forced with satellite data in the RGDA method. The moisture at the surface layer is therefore physically based. The other ten layers are more difficult to specify without *in-situ* measurements. Sometimes the top layer of soil is more wet than the bottom ten layers and sometimes it is more dry. Jones (1996) initialized the bottom ten layers of soil to be 25% volumetric soil moisture because this value is typical in RAMS. What if one instead decided to make the assumption that the bottom ten layers had the same volumetric soil moisture as the top layer of soil?

An attempt was made to force the entire column of soil rather than just the top layer. This was done by having the RGDA method calculate the new soil moisture amount for the top layer and then set the bottom ten layers to have the same soil moisture content as the top layer. The top layer was set at 0.5 cm deep. The hypothesis was that soil moisture gradients would be maintained for a longer period of time with full column forcing because moisture would infiltrate up to the top layer as the top layer was evaporating. However, this did not appear to happen. Instead, the run was almost exactly the same as the top-layer only forcing run. Figure 2. 3 shows that full column forcing did not change the behavior of the top layer of soil (layer 11), but did change the behavior of the lower layers (i.e. layer 10). In effect the lower layers were not coupled to the top layer of soil. They remained moist while the top layer evaporated out all of its moisture. Because the atmosphere is only altered when the top layer of soils behavior is altered, the run with full column forcing was the same atmospherically as the run with only top layer forcing.

This run used sandy clay loam soil. Future research may involve trying full column forcing with sandier soil which may be able to diffuse moisture up to the top layer from the bottom layer. A sandy run was attempted (see section 2.4) in this research, but with only top layer forcing. The most common soil types in the great plains region are loam and sandy clay loam soil (Soil map of the world, 1975).

### *2.3 RGDA method with half the original BATS vegetation.*

A suggestion by Jones (1996) was that the vegetation fractions specified for the plains in September by the BATS scheme in RAMS were too high. The reason for this is because in September the fields in the plains have been harvested and the vegetation fraction should be lower. A 100% vegetation fraction in the RGDA method implies that the heating rate in the area is independent of bare soil moisture and so only the moisture of the vegetation component is

altered. A 0% vegetation fraction in the assimilation implies that the heating rate is not dependent on vegetation at all and is highly dependent on soil moisture. A typical value for vegetation fraction in a grid cell is about 80% and Jones has suggested that it may be more like half that after harvesting. Hence, the next run was with a 0.5 cm top layer and all the BATS specified vegetation fractions divided by two

The air temperatures in the 50% vegetation run were between 0.5 and 1 degree warmer than the air temperatures in a comparable run with 100% BATS specified vegetation fraction (M049) at 20z (Figure 2. 4).

The bare soil moisture map is more wet in the 50% vegetation run (Figure 2. 5). This is because ground surface heating rates are much more dependent on bare soil. These results demonstrate that the RGDA method is sensitive to vegetation fraction, although the method still generates similar soil moisture patterns overall.

### *2.4 Sand vs. Sandy Clay Loam*

From section 2.2 it is clear that surface bare soil moisture was evaporating in the 8 September case faster than it was allowed to infiltrate into the soil. Jones (1996) suggests that this may be due to high winds in the area of forcing. However, it could also be due to diffusion coefficients characteristic to sandy clay loam soil. As there are many different soil types in the satellite forcing region and they are of different textures and compactness types, it could be that a different soil type would be chosen for the RAMS run. Shaw (1995) and Grasso (1996) both used sandy clay loam for the central plains region with good modeling results. However, sand allows more infiltration of water than sandy clay loam soil and so should provide some interesting comparisons. This run is exactly like the Jones run (3 cm top layer, top layer forcing, and 100% BATS vegetation) but with sand specified for the soil. The sand is still initialized with 25% bare soil moisture to be consistent with the sandy clay loam run. McCumber and Pielke (1981) suggest

that a realistic surface soil moisture value for sand is about 7% soil moisture in the south Florida region, so it is expected that the sandy run will be too wet overall.

### 2.4.1 Large scale observations

At 16z the sand run has much cooler bare soil temperatures. Only a small portion of the domain is greater than 303 K at the ground (Figure 2. 6). Sand that is 25% wet stays cooler than sandy clay loam which is 25% wet, in part because the albedo of wet sand is higher than the albedo of wet sandy clay loam. The top layer in the sandy run is not initially as moist as the top layer in the sandy clay loam run because water is infiltrating to deeper levels. One can see from the 16z and 20z soil moisture maps that sand is better at maintaining soil moisture gradients than sandy clay loam (Figure 2. 7). This is due to the fact that water is better able to diffuse between layers in sand than in sandy clay loam. Moisture may go deeper into the sandy layers during the assimilation, but it is also able to come back up to the top layer as the top layer evaporates. The cooler temperatures of the sand also limit some evaporation.

We can see the infiltration of the water into deeper soil layers by looking at the layer just below the top layer (layer 10) in Figure 2. 8. Recall from Figure 2. 3 that at 20z there is no horizontal soil moisture gradient in layer 10 for sandy clay loam.

### 2.4.2 Small scale observations

The latent and sensible heat fluxes are shown in Figure 2. 9. One can see the effect of the maintenance of the soil moisture on partitioning between latent and sensible heat. The latent heat and sensible heat follow a pattern where the diurnal cycle controls their magnitudes more than the amount of soil moisture left in the top layer. This was not the case for sandy clay loam soil (see Appendix).

The large values for latent heat imply that there is a lot of evaporative cooling. We can see this in the temperature and humidity time series for a wet region. The surface air temperatures are low compared to the sandy clay loam run (Appendix). One can see that sand is not releasing sensible heat into the air as effectively as sandy clay loam. This is illustrated in Figure 2. 10 and in Appendix. The relative humidity is much higher for the sandy run than the sandy clay loam run, showing that moisture is being released into the air from wet sand.

In dry sandy regions the sand heats up very slowly before the assimilation. After the assimilation takes place the heating rate is significantly higher than it was before the assimilation. The assimilation is able to raise the natural heating rate of sand but was not able to do this with sandy clay loam (see Figure 2. 11 and Appendix).

Although sand does not appear to be the best soil choice for the central plains it looks as if the RGDA method may have the most influence and work better in sandy regions.

**Table 2. 1 Soil column layers for Jones run (3cm top layer) and Guch run (0.5cm top layer).**

| *Soil Level* | *Jones run* | *Guch run* |
|---|---|---|
| 11 | 0-3cm | 0-0.5 cm |
| 10 | 3-6 cm | 0.5-1.5 cm |
| 9 | 6-9 cm | 1.5-3 cm |
| 8 | 9-12 cm | 3-6 cm |
| 7 | 12-16 cm | 6-9 cm |
| 6 | 16-20 cm | 9-12 cm |
| 5 | 20-25 cm | 12-16cm |
| 4 | 25-30 cm | 16-20 cm |
| 3 | 30-40 cm | 20-30 cm |
| 2 | 40-50 cm | 30-50 cm |
| 1 | 50-100 cm | 50-100 cm |

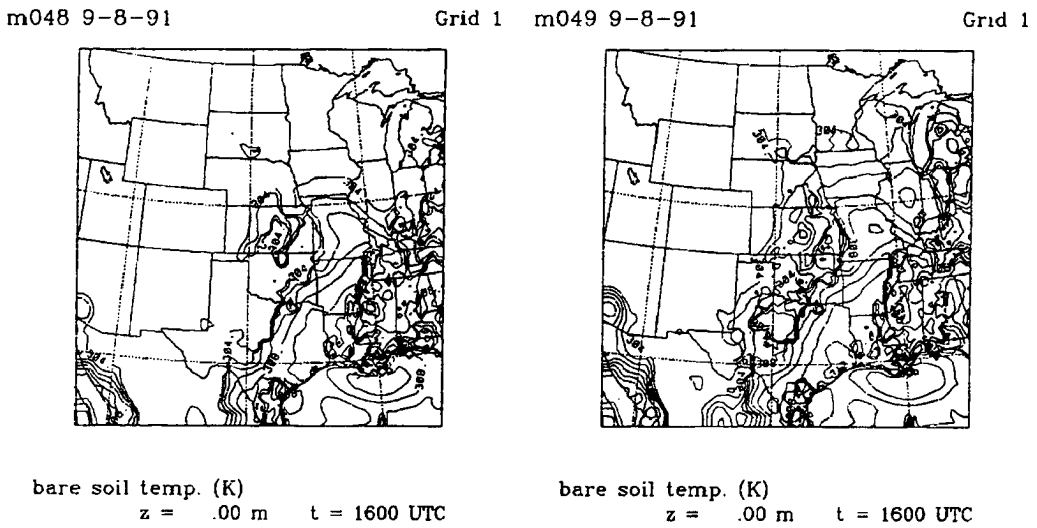


**Figure 2. 1 Regions for bare soil temperatures > 303 K for the Jones run (m048) and the Guch run (m049) at 16z. M049 has a smaller top layer and thus warmer ground temperatures.**

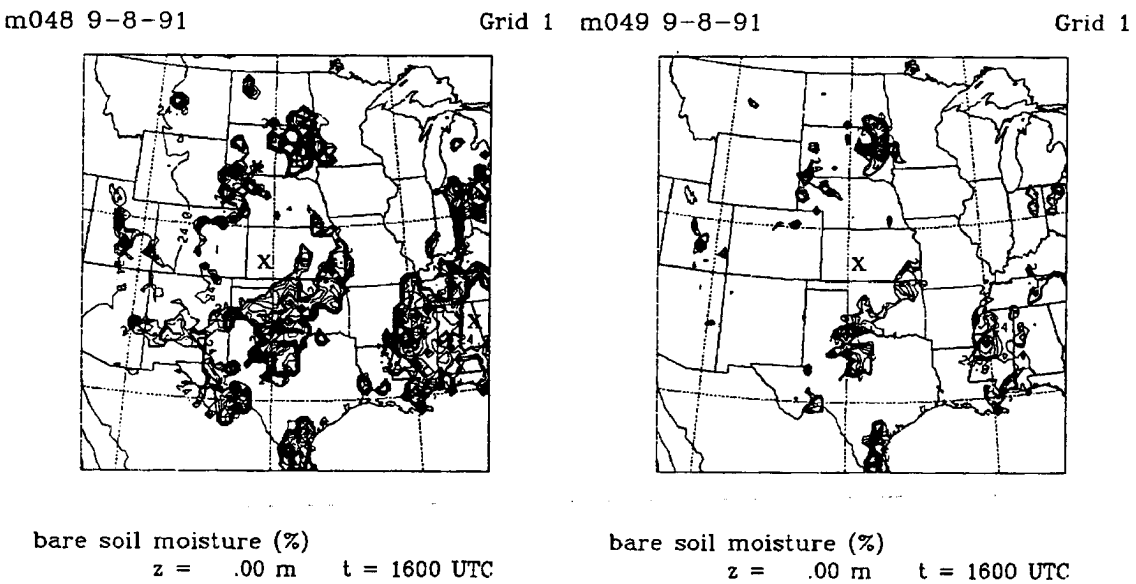


**Figure 2. 2 Regions of percent bare soil moisture > 24% (wet soil) for the top layer=3.0 cm (m048) run and the top layer =0.5 cm (m049) run. Maximum soil moisture is 63% for both cases. Areas marked with "x" are dry.**

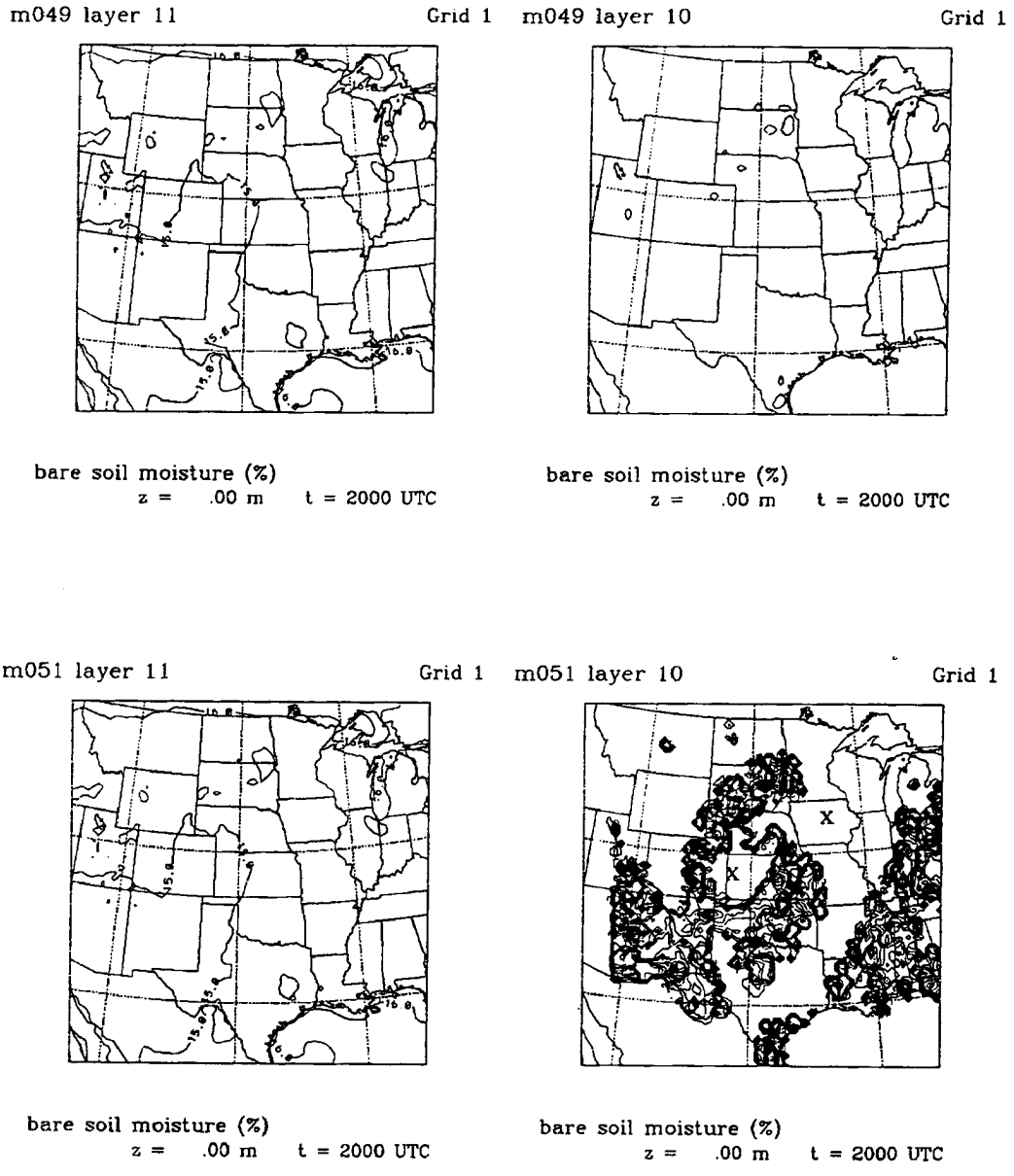


**Figure 2. 3 Bare soil moisture percent for top layer forcing (m049) and full column forcing (m051), each with a 0.5 cm top soil layer. Layer 11 represents the top layer of soil and layer 10 represents the layer just beneath the top layer. Compare wet soil regions to those in Figure 1. 2.**

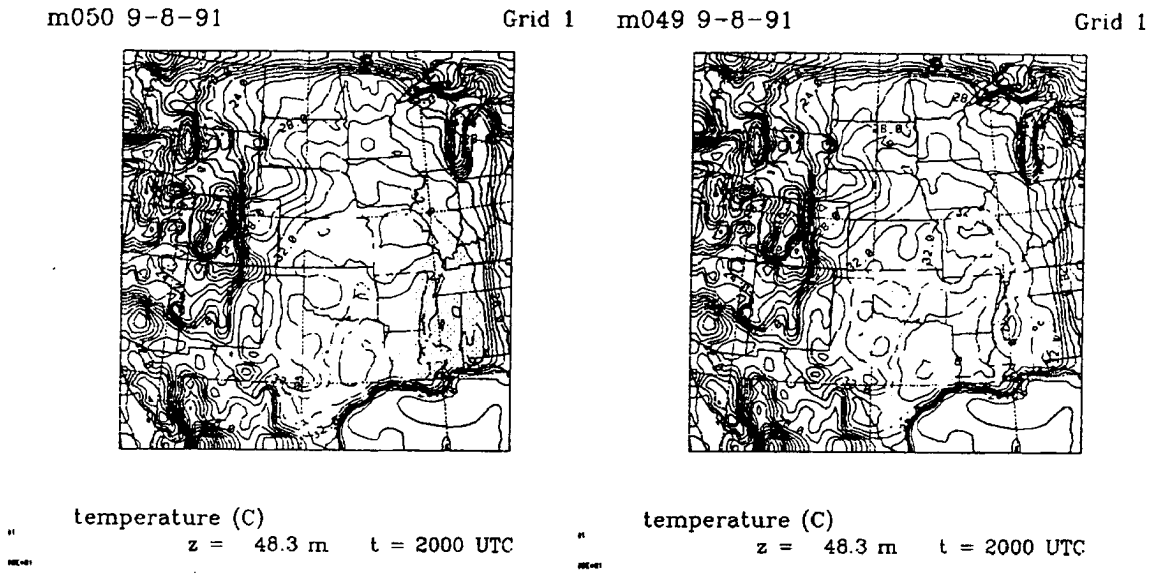


**Figure 2. 4 Temperatures for a run with 50% BATS vegetation (m050) and a run with 100% BATS vegetation fractions (m049). The contour interval is 1 ° C and temperatures > 32 ° C are shaded.**

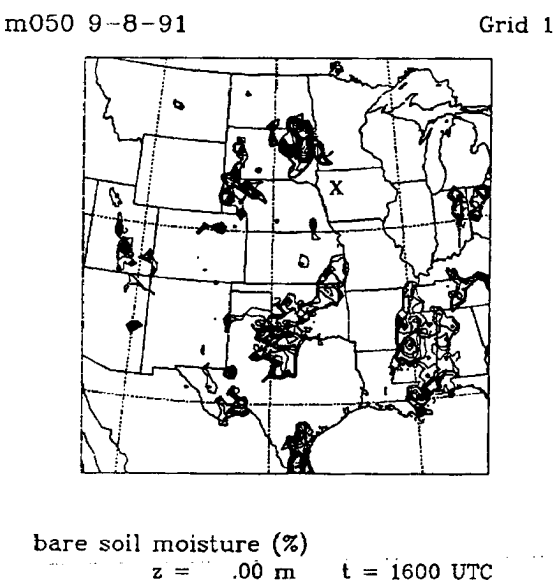


**Figure 2. 5 Bare soil moisture > 24% (wet soil) for 50% vegetation and 0.5 cm top layer run. Compare with Figure 2. 2.**

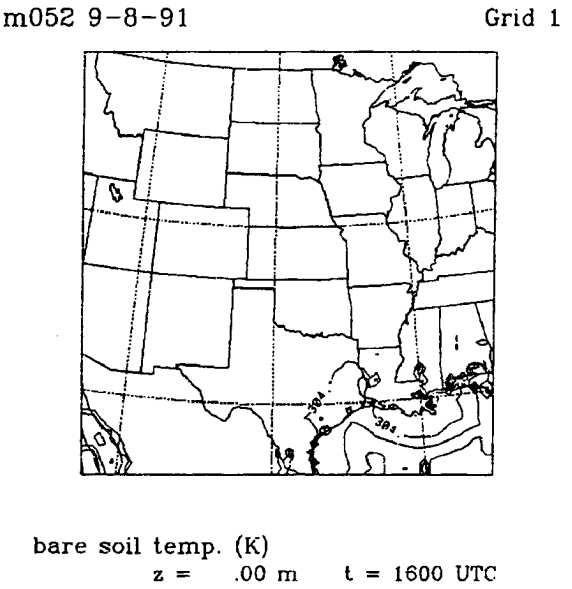


**Figure 2. 6 Regions for temperatures > 303 K at the ground for the sandy run (m052), 3.0 cm top layer. Compare with the sandy clay loam run in Figure 2. 1.**

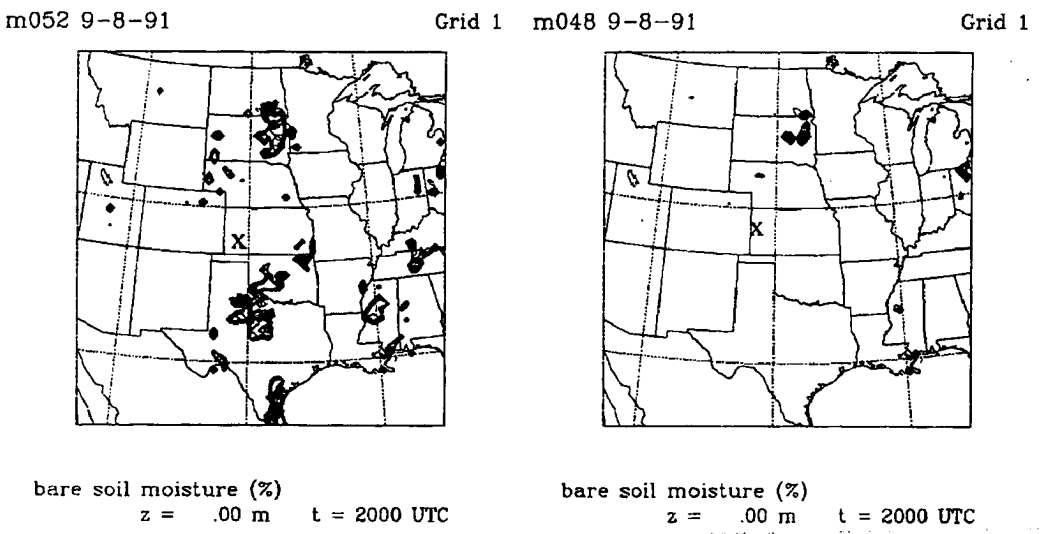


**Figure 2. 7 Bare soil moisture > 24% for 20z for the runs m052 (sandy soil, 3.0 cm top layer) and m048 (sandy clay loam soil, 3.0 cm top layer).**

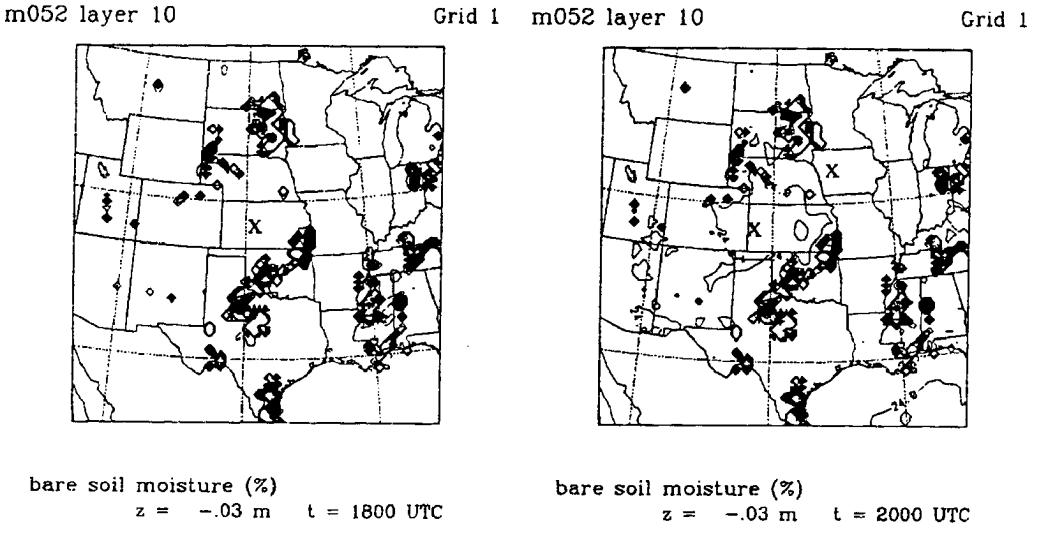


**Figure 2. 8 Bare soil moisture > 24% for sandy run at the layer just below the surface, layer 10.**

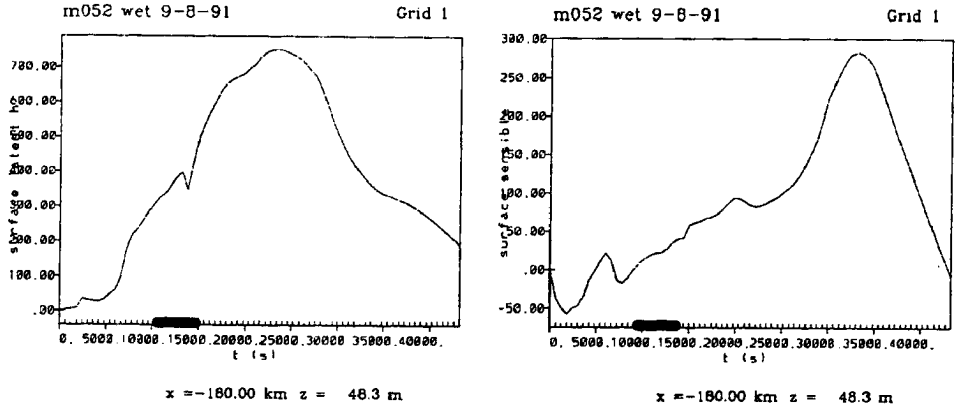


**Figure 2. 9 The latent and sensible heat fluxes at the surface for the m052 case (sandy soil, wet region).**

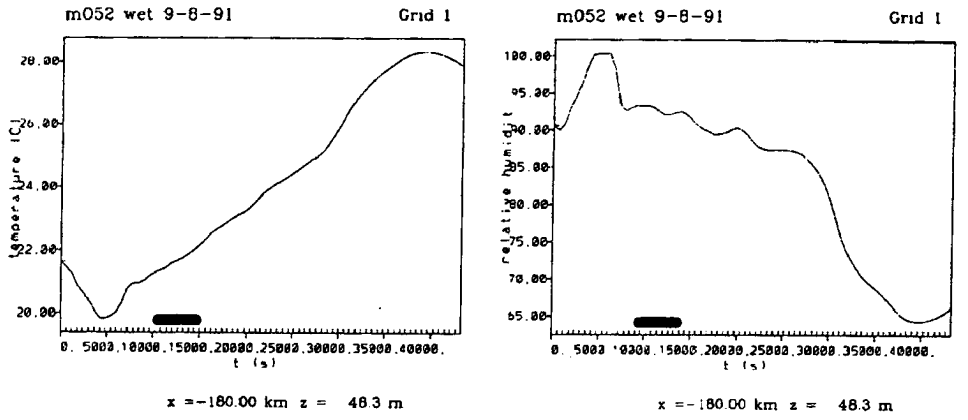


**Figure 2. 10 Surface temperature (C) and relative humidity values for a wet region in the sandy run (m052).**

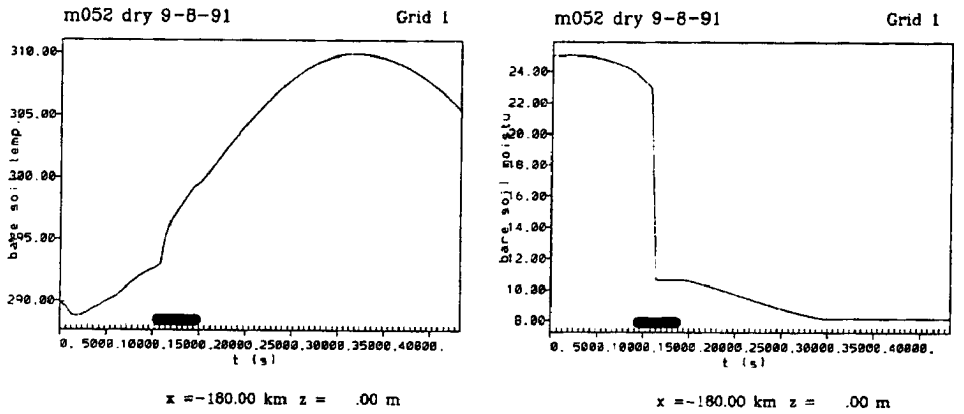


**Figure 2. 11 Ground temperatures (K) and bare soil moisture (%) for a dry region in the m052 run with sandy soil. Compare with Figure A.4.**

Chapter 3

**Case Study: 2 August 1991. Moderately wet soil around a lake region.**

This case study is for a very hot and sunny day over the plains. The grids for this case were chosen to maximize the availability of IR data at the ground surface in the third (highest spatial resolution) grid. Figure 3.1 shows the rate of temperature change for the period between 15:01-15:31z which is used to develop the soil moisture map. Based on this, Figure 3.2 and Table 3. 1 describe the model grids used for this run.

### *3.1 Validity of the assimilated soil moisture field*

Failures of the cloud clearing scheme are the most likely cause of errors in the satellite-derived soil moisture field. The smallest grid (5 km spacing) for this case contains very little contamination by clouds (Figure 3.2). However, it is difficult to find an area completely sunny and Figure 3.1 shows cloud contamination near the third grid between 15:01z and 15:31z in the dashed circle. The white spot in the region represents a very high heating rate and the dark spot represents very low heating. This is a small, warm cloud which was not detected during the cloud clearing scheme. It was at the white spot at 15:01z and moved to the dark spot at 15:31z. An improved cloud clearing scheme would improve the assimilation technique. As it is now, the dark region falsely corresponds to wet soil.

Heterogeneous soil moisture was not the main factor in picking this case study; instead it is discussed as an example of a typical summer day in the great plains. The microwave emissivity map in Figure 3.3 (3 August 1991 is shown) suggests some moisture variations in the small grid area, many of which are small lakes. Looking at the visible image in Figure 3.4, one can see some cloudy areas in low emissivity regions on the west side of grid 3. These low emissivity regions are probably due to clouds and not to high soil moisture.

The general pattern of the soil moisture values is that the northeast part of grid 3 is the most wet (Figure 3.5). The reports of total precipitation for 28 July 1991-3 August 1991 (Figure 3. 6) suggest that a pattern of surface wetness similar to the one modeled using the assimilation in grid 3 could exist. No significant rain fell in grid 3 on 3 August 1991. The microwave emissivity map for 3 August 1991 also has a pattern similar to the weekly precipitation amount, except in the western portion of grid 3 where the emissivity map was contaminated by clouds.

One application of the RGDA method is to evaluate the accuracy of the model's positioning of lake features. A lake which is too small in the RAMS initialization will generate wet soil regions surrounding it after the assimilation. A lake which is too large in the RAMS initialization will generate dry soil regions surrounding it. Figure 3.7 shows the bare soil moisture mapping generated one time-step after the assimilation with prominent lakes labeled. Two-thirds of the lakes are surrounded by wet soil and one third are surrounded by dry soil. However, one case study is not enough to figure out if this is due to actual soil moisture conditions or errors in the model initialization of the lake features.

Usually more important than the last ten days of precipitation for the soil moisture map are the last 10 hours. Radar reports and cooperative precipitation data are not shown for this case because there was no rain reported in grid 3 on either 1 August 1991 or the hours before 16z on 2 August 1991. Soil moisture variations in this case are probably more indicative of the seasonal rain patterns than short term rain events. One can infer this by the relatively low values of soil

moisture, comparing the maximum in the 8 September case (Figure 2. 2) of near 63% to the maximum in the 2 August case of near 26%.

### *3.2 Comparison between the RGDA method and a homogeneous soil moisture run to observations.*

Comparing the RGDA method to the control run is only interesting in the first hours of the run for this case, as the two runs become very similar as time goes on and the assimilated soil moisture becomes more homogeneous. The time 18:00z was chosen to compare the two as this is just two hours after the assimilation and there are still some soil moisture gradients in the area. Also, the surface observations for 18:00z are readily available (see Figure 3.8). There is a trough northwest of grid 3. The winds in grid 3 are southerly, coming from the gulf stream region. High temperatures are between 91 and 94 ° F. Dew point temperatures are between 56 and 72 ° F in grid 3. The vegetation, predominantly cropland, for grid 3 is shown in Figure 3. 9.

Table 3. 2 presents the range for the RGDA method, the control and the observations for wind speed, relative humidity and temperature in grid 3. Because figures for the control and the RGDA method are very similar and rather uninteresting, they are not presented here.

In general, use of the RGDA method did not improve temperature or wind speed over the control run. The relative humidity field is improved over the control run, with a larger range of relative humidities in the domain and a more realistic maximum as compared to NWS observations.

### *3.3 Usefulness of the RGDA method.*

Two hours after the RGDA method was used to generate a realistic pattern of soil moisture, the differences between it and the control run were minor. Why should one bother using satellite data to initialize soil moisture? As it turns out, there were some interesting

interactions between Lake Texoma and the wet soil moisture field that are not apparent when simply looking at the ranges given in Table 3. 2. The gradient over Lake Texoma in wind speed is larger for the control run than for the RGDA method. This is shown in Figure 3.10. The wind speed on the south edge of Lake Texoma is 3.0 m/s for both model runs. The wind speed on the north edge of Lake Texoma is 4.5 m/s in the control run and just 4.0 m/s in the RGDA method. This is a significant change considering that Lake Texoma is not a large body of water. The RGDA method could be used to diagnose the severity of lake breezes. An example of this type of work is the cross section in Figure 3.11. The lake is a minimum for both latent and sensible heat release. Moderately wet soil releases more latent heat than a lake region. This is due to the large specific heat of water (about twice that of wet soil) and due to the fact that the diurnal variation of wet soil only effects the top few layers of soil (at most half a meter), whereas for a lake the penetration of radiation can be several meters. Water tends to store solar radiation it receives and land tends to return it to the atmosphere in the form of both latent (if the soil is wet) and sensible heat. This results in a small sensible heat gradient between a lake region and a wet soil region. Ultimately, the lake has a smaller impact on surface air temperature and relative humidity patterns than if the surrounding soil were dry.

To understand the sensible heat flux in terms of air temperatures in the mixed layer, one can do a simplified analysis and assume a balance exists between the time rate of change of static energy, the net radiation at the surface and the surface sensible heat flux (Wallace and Hobbs, 1977). One can approximate the density, the specific heat of air and the time rate of change of temperature to be independent of height throughout the mixed layer. For this case,

$$\rho c_p \frac{\partial T}{\partial t} \int_{0m}^{top} dz = R_n + H \qquad (3.1).$$

The time rate of change of temperature can be found using the density to be 1.25 kg/ $m^3$, the specific heat to be 1004 J/(Kg K) and the net vertical flux of radiation at the surface to be a typical morning value of 300 W/$m^2$ (Appendix). The height of the boundary layer is about 1.0 km. Using this analysis, the RGDA method has air above land heating approximately 0.5 K/hr more than air above the lake. In the control, air above land is heating approximately 0.6 K/hr more than air above the lake (Table 3. 3). These small differences are the reason there is slightly more circulation around the lake in the control run than in the RGDA method run. It should be noted, however, that RAMS uses a much more sophisticated manner of relating surface sensible heat flux to the temperature of the boundary layer. Therefore, the numbers presented are only approximations of the numbers which RAMS uses.

The cross section in Figure 3.11 is also interesting because one can see how the bare soil moisture field in (B) changes the surface latent heat flux in (A). The soil moisture from the RGDA method appears to be superimposed onto the surface latent heat flux generated in the control. A fluctuation of 0.5% soil moisture corresponds to a fluctuation of about 20 W/$m^2$ in the surface latent heat flux. Also, in (C), the 0.5% soil moisture fluctuation corresponds to a negative fluctuation of about 20 W/$m^2$ in the surface sensible heat flux, as expected from the surface energy balance. These fluxes are from the top layer of soil, which is 3.0 cm deep.

### *3.4 Summary.*

The RGDA method produced a very plausible soil moisture map for 2 August 1991 in the eastern portion of grid 3. The western part of grid 3 appears to have been contaminated by a cloud moving out of grid 3 in the early part of the assimilation, making it artificially dry. The pattern of relative humidity generated in the data assimilation was better than the control run. The temperatures in both the control run and the assimilation run were between 1 and 3 ° C too cool, the control run being warmer by about 0.5 ° C. Wind patterns were very similar between the

observations, the control and the assimilation. Overall the best result of the assimilation appears to be the more realistic relative humidity field at the surface in the morning hours. This model run also demonstrated how lake-effects may be reduced when the lake is near regions of wet soil rather than dry soil.

**Table 3. 1 RAMS v3a configuration for 2 August 1991**

| *Grid Option* | *Value in 2 August 1991 case study for grids 1, 2 and 3* |
|---|---|
| x spacing | 60 km, 20 km, 5 km |
| y spacing | 60 km, 20 km, 5 km |
| number of x grid points | 40, 50, 66 |
| number of y grid points | 40, 50, 66 |
| center latitude | 36.4, 34.4, 34.4 |
| center longitude | -97.8, -97.4, -97.4 |

**Table 3. 2 RGDA method, control run and NWS surface observations for 18z on 2 August 1991 in grid 3.**

| *18z* | *wind speed* | *relative humidity* | *temperature* |
|---|---|---|---|
| RGDA | 2-6.5 m/s | 36-50% | 30.5-31.5 °C |
| control | 2-6.5 m/S | 36-45% | 31.0-32.5 °C |
| NWS observations | 2.5-5 M/S | 28-51% | 33-34 °C |

**Table 3. 3 Surface sensible heat flux for 18z on 2 August 1991 in grid 3.**

| | *Value* | *Surface type* | *Mixed layer heating* |
|---|---|---|---|
| RGDA $H_{min}$ | 230 $W/m^2$ | lake | 1.5 K/hr |
| RGDA $H_{max}$ | 380 $W/m^2$ | wet crops | 2.0 K/hr |
| Control $H_{min}$ | 230 $W/m^2$ | lake | 1.5 K/hr |
| Control $H_{max}$ | 430 $W/m^2$ | crops | 2.1 K/hr |

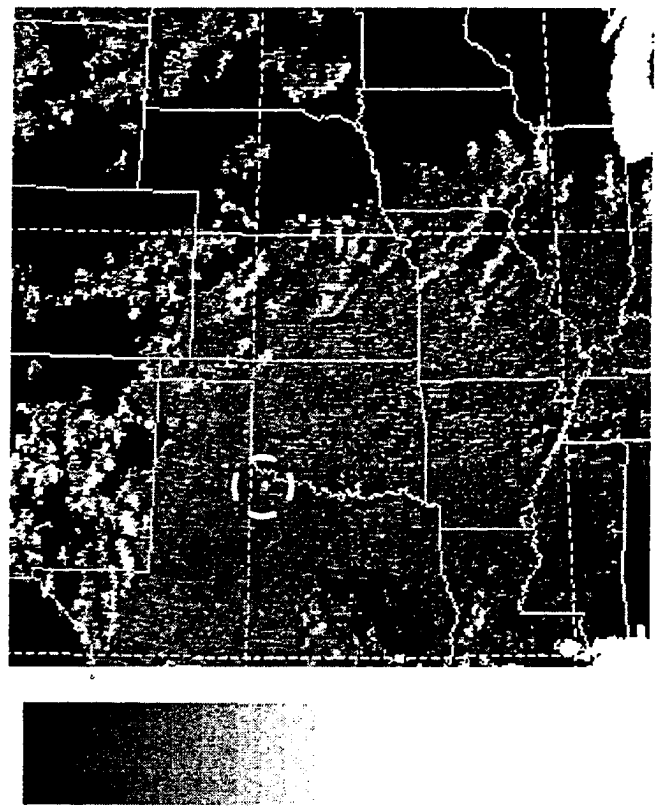


**Figure 3.1 August 2, 1991 heating rates from 1501z-1531z. Brightest regions are heating the fastest. Black regions are cloud-cleared and not included in the assimilation. Circled region shows cloud contamination.**

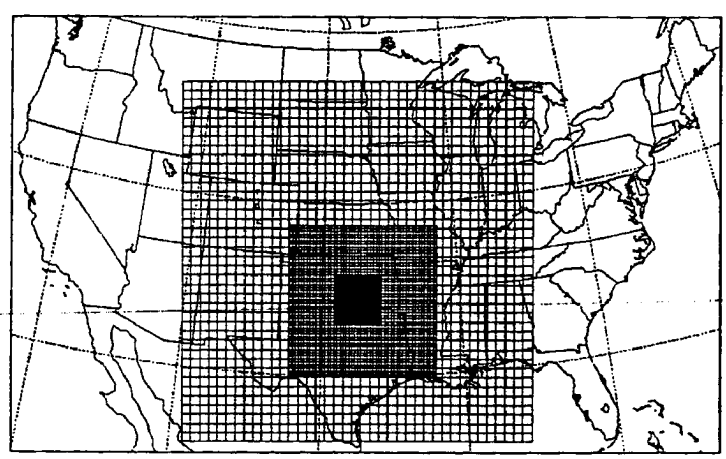

**Figure 3.2 RAMS grid for 2 August 1991**


**Figure 3.3 Microwave emissivity map for channel 7 on 3 August 1991, approximately 15:20z. Dark areas indicate low emissivities (probable wet areas) and black regions are cloud-cleared or missing data regions. Box indicates location of grid 3.**

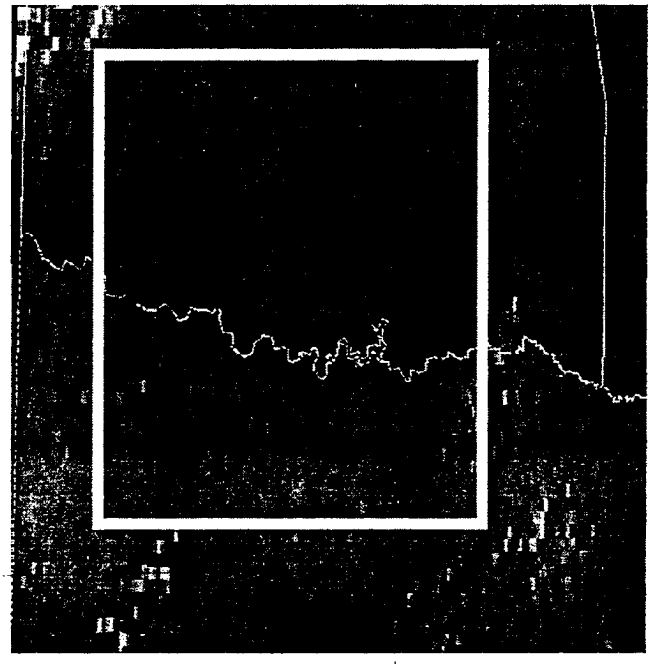

**Figure 3.4 Visible image for 3 August 1991 at 15:31z. Box indicates location of grid 3.**

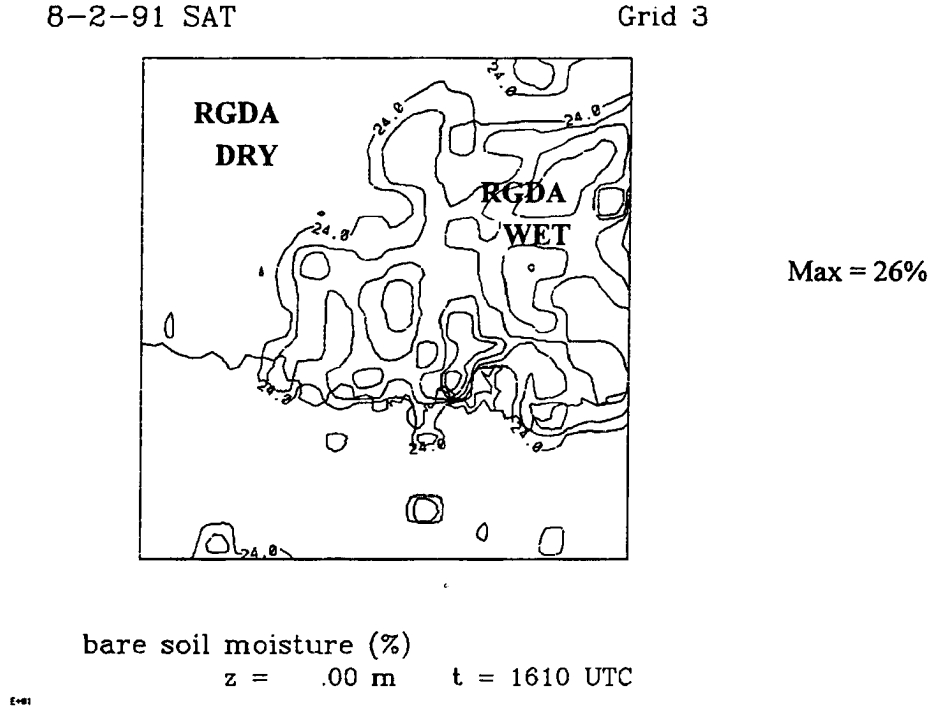


**Figure 3.5 Wet regions (bare soil moisture > 24%) for 2 August 1991 case study.**

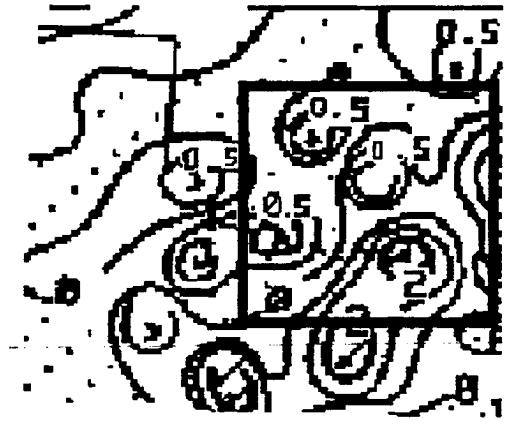


**Figure 3. 6 Total precipitation, inches, for 28 July 1991- 3 August 1991. Box indicates grid 3 for 2 August 1991 case.**

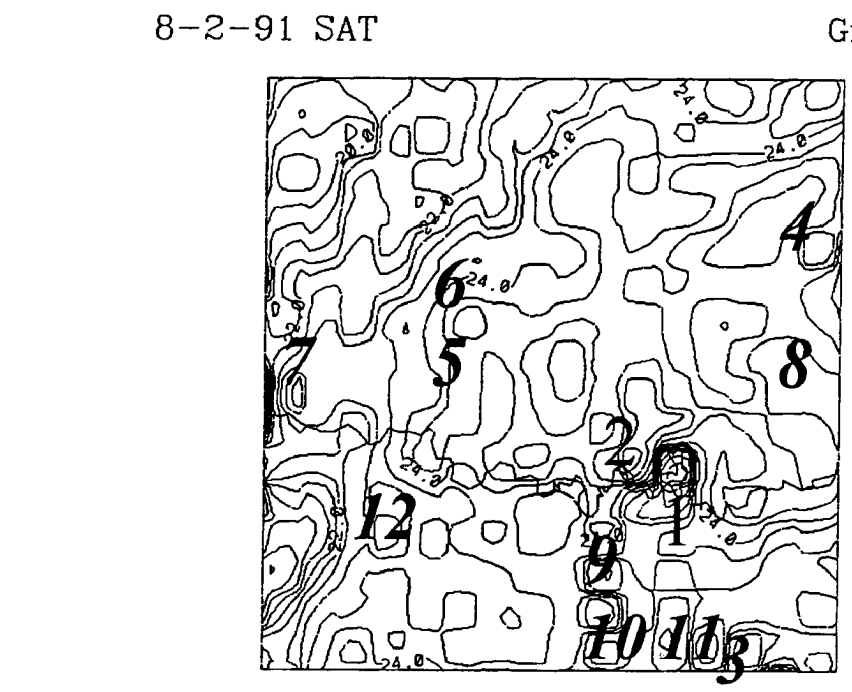


1.Lake Texoma
2.Arbuckle Reservoir
3.Lake Quitman
5.Waurika Lake
6.Ft. Cobb Lake
7.Tom Steed Lake
9.Lake Denton
10.Lake Dallas
11.Lake Tawakoni

**Figure 3.7 Lake regions in grid 3 superimposed on the surface soil moisture at 16:10z for 2 August 1991. Lakes numbered 1-8 are surrounded by wet (> 24%) soil and lakes numbered 9-12 are surrounded by drier soil.**

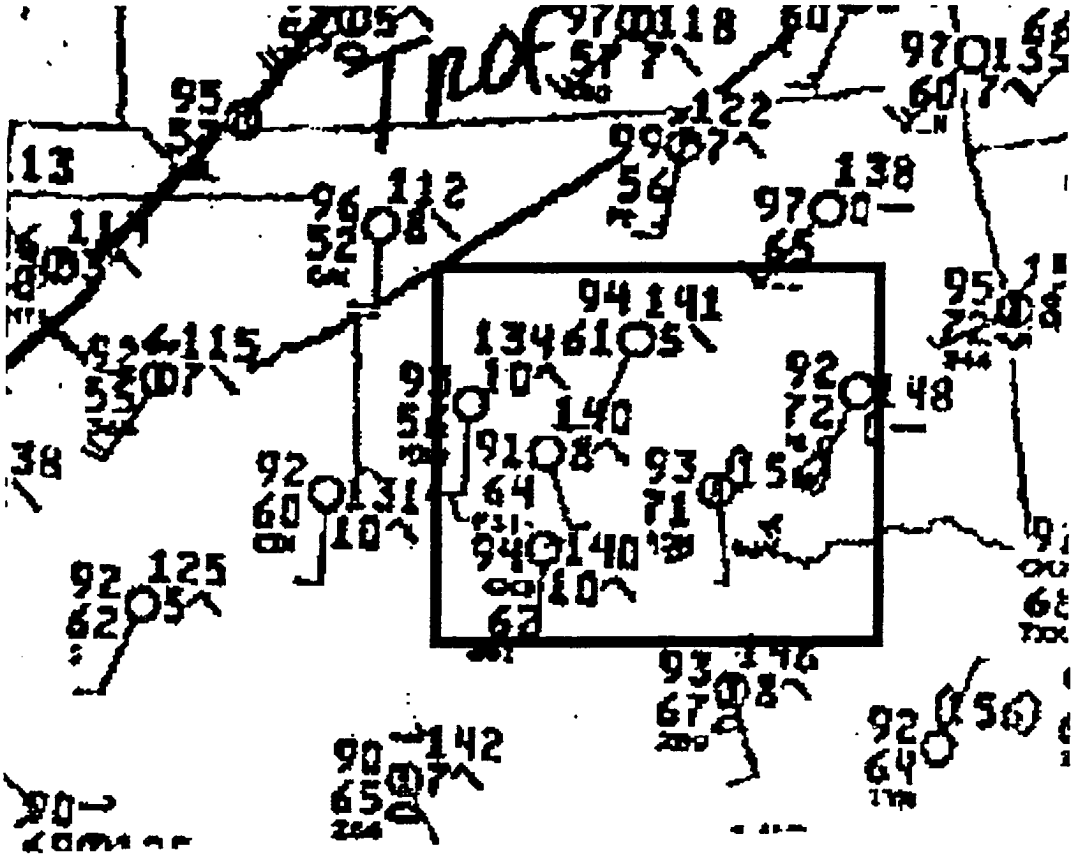

Figure 3.8 Surface observations for 18:00z on 2 August 1991.

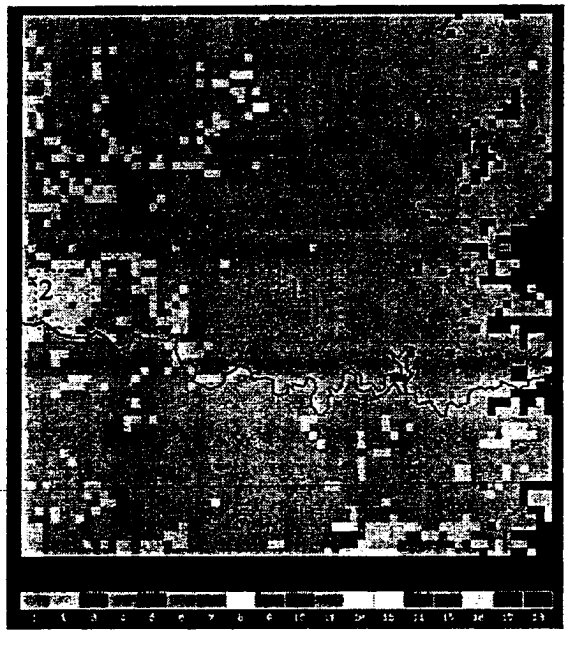

Figure 3. 9 BATS vegetation for 2 August 1991 grid 3. Prominent vegetation types are 1-cropland, 2-short grass and 5-tall grass.

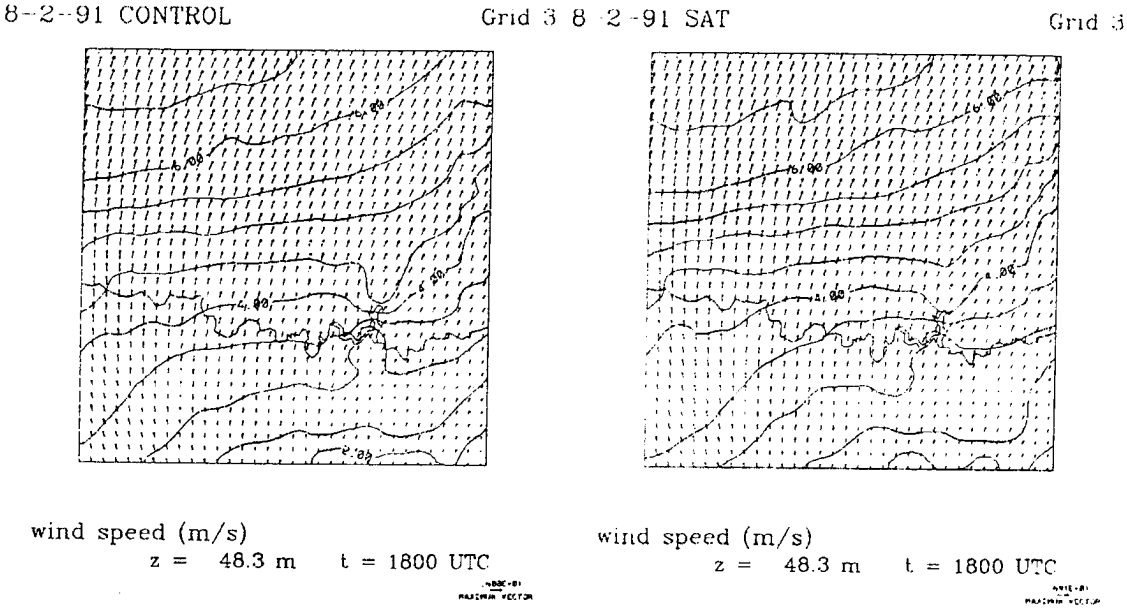


**Figure 3.10 Wind speed at the surface for the control run and the RGDA run at 18:00z. Contour interval is 0.5 m/s.**

A

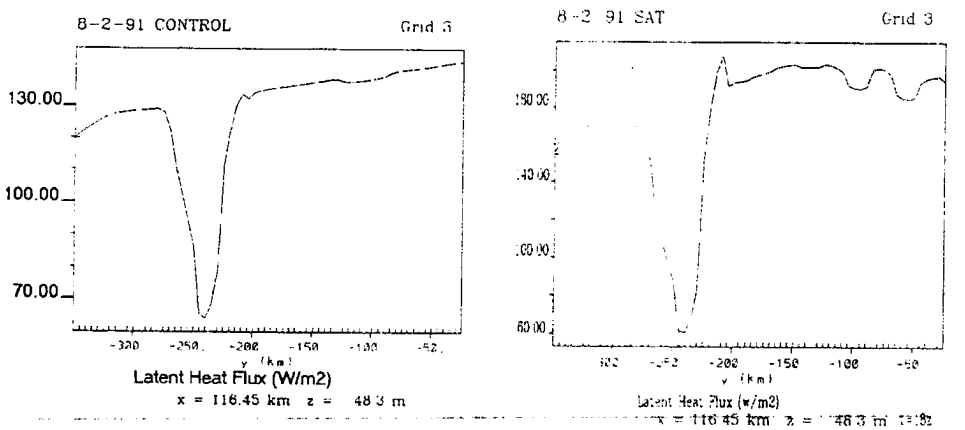

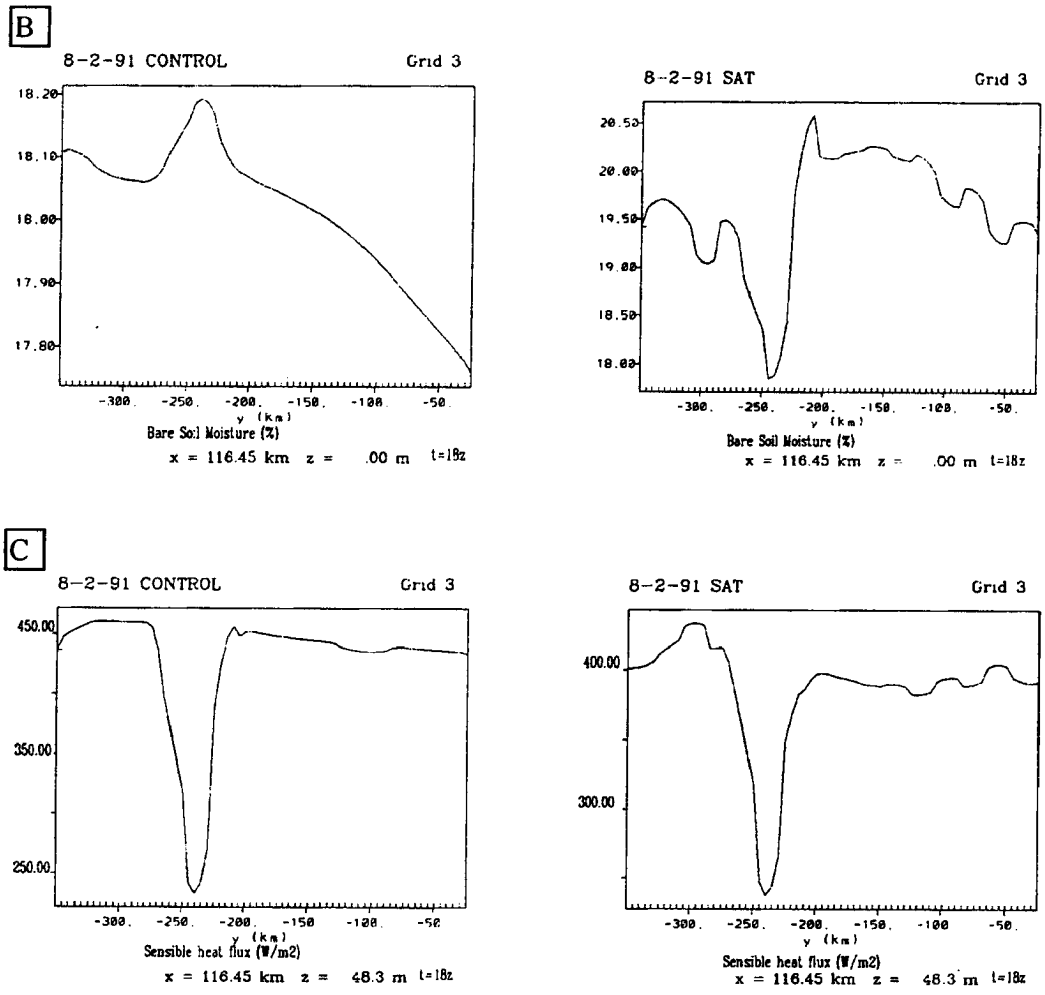


**Figure 3.11 Surface latent heat flux (A), bare soil moisture(B) and surface sensible heat flux(C) at the surface for a north-south cross section through the lake region in grid 3 at 18z.**

Figure 4 . 5. Recall that small clouds in the visible image are areas where the microwave emissivity map may be contaminated. The southern portion of grid 3 is slightly contaminated by clouds. Also, the western edge of grid 3 in the assimilation appears to be caused by cloud contamination (see IR heating rate map for that region in Figure 4 . 2).

Cooperative 24-hr precipitation data for measurements taken on 5 August and before 16z on 6 August are shown in Figure 4 . 6. The precipitation fell in the western portion of grid 3 on 5 August and in the eastern portion on 6 August. The areas where rain fell are frequently the same areas the RGDA method finds wet. This indicates that the RGDA method is detecting real soil moisture caused by recent rain events.

### *4.2 Comparison between the RGDA method and a homogeneous soil moisture run to NWS observations.*

In Table 4 . 2, wind speed, relative humidity and temperature ranges for grid 3 are listed with observations from NWS. Again wind speed and temperature fields did not improve using the RGDA method, but the maximum relative humidity value was closer to NWS observations. The observations from NWS are shown in Figure 4 . 7. There is a weak trough on the northwest edge of grid 3.

### *4.3 Usefulness of the RGDA method.*

In this case there are significant heterogeneities in vegetation type as well as the soil moisture field. This is shown in Figure 4 . 8. The most prominent vegetation types are cropland, short grass and evergreen shrub. Comparing Figure 4 . 8 to the soil moisture map in Figure 4.4 one can see that the evergreen shrub and grassland regions are more dry than cropland regions. This is an ideal case to use to study heterogeneous soil moisture fields within heterogeneous

vegetation fields. The north-south cross sections of surface latent heat flux, bare soil moisture and surface sensible heat flux are shown in Figure 4 . 9 A, B, and C. Fluctuations of 1.0% soil moisture are causing latent and sensible heat fluctuations at the surface of approximately 25 $W/m^2$. This is slightly smaller than what happened in the 2 August case (where a 1% soil moisture fluctuation corresponded to an approximately 40 $W/m^2$ fluctuation in sensible heat flux at the surface). The reason the numbers are different is that the increase in soil moisture is an increase in volumetric soil moisture. Adding 1% volumetric soil moisture will cause more significant changes in surface heat fluxes if the soil is dry (perhaps 18%) than if the soil is already quite wet (26%).

Surface sensible heat flux has a much stronger gradient in the cross section for the assimilation than for the control run. The control run has surface sensible heat flux from the top layer (3.0 cm) of cropland to be about 400 $W/m^2$ and surface sensible heat flux from the top layer of grass and shrub regions to be about 470 $W/m^2$. Using the simplified technique described in equation 3.1, Table 4 . 3 was calculated. In the control, air above grass and shrubs is heating up approximately 0.1 K/hr more than air above the cropland. Using the RGDA method, surface sensible heat flux from cropland is near 250 $W/ m^2$ and surface sensible heat flux from grass and shrubs is 500 $W/ m^2$. Air above grass and shrubs is now heating approximately 0.7 K/hr faster than air above cropland.

Potential temperature and vertical motion are shown in D and E of Figure 4 . 9. Areas with wet soil (cropland) are associated with lower potential temperatures. A parcel of air conserving potential temperature would sink in these areas. Sinking in wet region is observed in the vertical motion field (dashed contours). Conversely, rising motion is enhanced in dry regions (solid contours). Circulation developing in the control is enhanced by the RGDA method's soil moisture field.

Circulation is relatively minor at 18z (maximum updraft of 3 cm/s in the RGDA method), but as the day continues it becomes more important. At 2130z, the disturbance has propagated north (due to ambient southerly winds of about 10 m/s) and is much stronger. Maximum updraft for the RGDA method is now 53 cm/s. Maximum updraft for the control run is about half that, at 24 cm/s. These figures for the same cross section as before are shown in Figure 4 . 10. The cause of the updrafts can be seen more easily in Figure 4 . 11. Wind speed in the first layer above the surface is shown. Wind speed in the control run is between 4.0 and 10.0 m/s. Wind speed in the RGDA method run is between 2.0 and 12.0 m/s. The tightly contoured region corresponds to where there is convergence at the surface (areas of soil and vegetation heterogeneities) and therefore updrafts seen in the cross sections before. The regions of convergence correspond well to satellite images from the afternoon of the case day. Figure 4 . 12 shows the visible image for 00:01z on 7 August. Cloudy areas are appearing over areas of modeled convergence. Small amounts of cloud liquid water in the convergence regions were modeled in the RGDA method, but no cloud liquid water was modeled in the control run for the third grid.

### *4.4 Sensitivity to the time period of forcing in the RGDA method.*

The previous version of the RGDA method had forcing between 15:00z and 16:00z. Because such heterogeneity was found in the soil moisture map it was decided that 6 August was the best case study to test the RGDA method's sensitivity to the time period of forcing and to check the speed of evaporation in the RAMS model.

An RGDA run was done with forcing between 14:00z and 15:00z. The soil moisture map that this run produces at 15:15z should be wetter than the soil moisture map in Figure 4 . 4 because it is earlier in the day and less soil moisture has evaporated. However, if the data assimilation and the RAMS model are working correctly one would assume that both assimilation

runs would have similar soil moisture maps for 16:15z. Figure 4 . 13 shows the results from the new assimilation (assimilation "B") at 15:15z and 16:15z. Assimilation B at 15:15z has a similar pattern and slightly wetter regions than assimilation A retrieved for 16:15z as expected. However, assimilation B's soil moisture mapping at 16:15z is much drier than the original assimilation. This indicates one of two things:

1) The assimilation's wet soil regions are caused by something other than wet soil (i.e. problems with the vegetation code in RAMS) or
2) The RAMS model is evaporating the soil moisture too quickly.

The problem appears to be caused by the latter. From the time series plots shown in Appendix it was evident that moisture was evaporating fast. Also, assimilation B at 15:15z has a soil moisture map very similar to the co-op precipitation data from Figure 4 . 6. This implies that there is not a problem with the vegetation.

It is important to note that because the data assimilation occurred earlier in the day, soil moisture evaporated sooner and the data assimilation run became very similar to the control run, with less convergence and no moist convection produced. Therefore, the RGDA run was sensitive to the time period being forced.

A third run for this case was done with forcing between 16z and 17z. The soil moisture field produced from this case is shown in Figure 4 . 14. The western portion of grid 3 is still shown as wet, but the rest of the grid is dry by this time. This picture is fairly consistent with the pattern derived from the other forcing periods, assuming that evaporation is occurring throughout the morning. Again, this hints that RAMS is evaporating the RGDA moisture too quickly because with earlier forcing periods there was no significantly wet soil left at 17z. It should be

emphasized that although the RAMS model evaporates the assimilated soil moisture too early in the day, the total amount of water that evaporates from the soil is realistic over the twelve hour run. Soil which is not shaded by vegetation is very dry by the afternoon hours for a sunny summer day. Therefore, the afternoon hours of the run have reasonable (low) values for surface latent heat flux when compared to typical observations.

### *4.5 Summary.*

This study emphasized that soil moisture heterogeneities are likely to occur near vegetation heterogeneities because different vegetation types transpire at different rates. In this case soil moisture heterogeneities enhanced breezes, caused originally by vegetation differences and a trough moving in, and generated stronger convection than a homogeneous soil moisture run was able to. Convection can be seen in that area from satellite pictures at 00:01z, while the RGDA method had it occur near 21:30z. Both the assimilation and the control appeared to move the trough into grid 3 too quickly, causing cooler temperatures and higher relative humidities than observations.

It was also found that this case day was sensitive to the time period of forcing in the RGDA method. An earlier time period (14z and 15z) produced a drier soil moisture mapping for 16z than the normal time period of forcing (15z and 16z), indicating that the model is probably evaporating soil moisture too quickly and has high values of surface latent heat flux for the morning hours of the run.

**Table 4 . 1 RAMS v3a configuration for 6 August 1991.**

| *Grid Option* | *Value in 6 August 1991 case study for grids 1, 2 and 3* |
|---|---|
| x spacing | 60 km, 20 km, 5 km |
| y spacing | 60 km, 20 km, 5 km |
| number of x grid points | 40, 50, 86 |
| number of y grid points | 40, 50, 54 |
| center latitude | 38.0, 38.0, 37.7 |
| center longitude | -98.8, -98.8, -99.2 |

**Table 4 . 2 RGDA method, control run and NWS surface observations for 18z on 6 August 1991 in grid 3.**

| *18z* | *Wind Speed* | *Relative Humidity* | *Temperature* |
|---|---|---|---|
| RGDA | 2.5-5.5 m/s | 38-47% | 27.5-32.5 °C |
| Control | 2.5-5.5 m/s | 38-43% | 28-33 °C |
| NWS observations | 5-10 m/s | 32-53% | 28-37 °C |

**Table 4 . 3 Surface sensible heat flux for 18z on 6 August 1991 in grid 3.**

| | *Value* | *Surface type* | *Mixed layer heating* |
|---|---|---|---|
| RGDA $H_{min}$ | 250 $W/m^2$ | wet cropland | 1.6 K/hr |
| RGDA $H_{max}$ | 500 $W/m^2$ | dry shrubs/grass | 2.3 K/hr |
| Control $H_{min}$ | 420 $W/m^2$ | crops | 2.1 K/hr |
| Control $H_{max}$ | 470 $W/m^2$ | shrubs/grass | 2.2 K/hr |

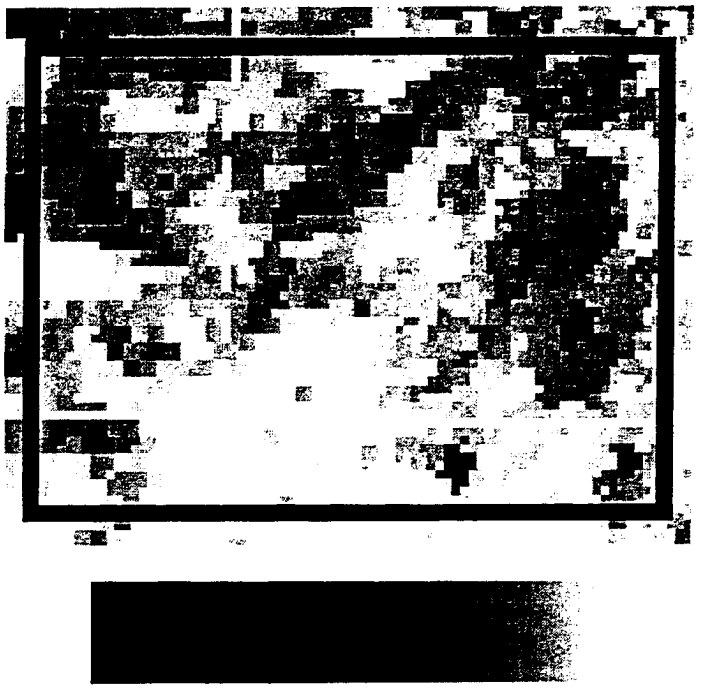

0.75 0.98

**Figure 4 . 1 Microwave emissivity map for 6 August 1991, grid 3.**

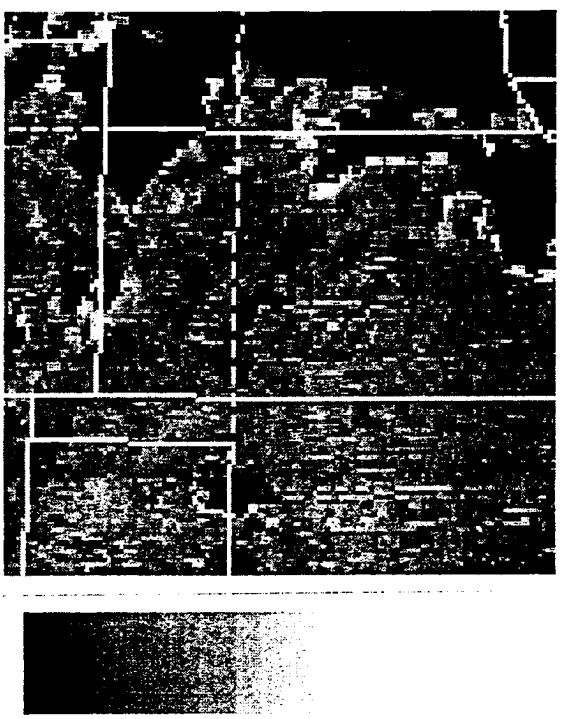

0 K/hr 13 K/hr

**Figure 4 . 2 Grid 3 IR heating rates between 1531z-1601z on 6 August 1991.**

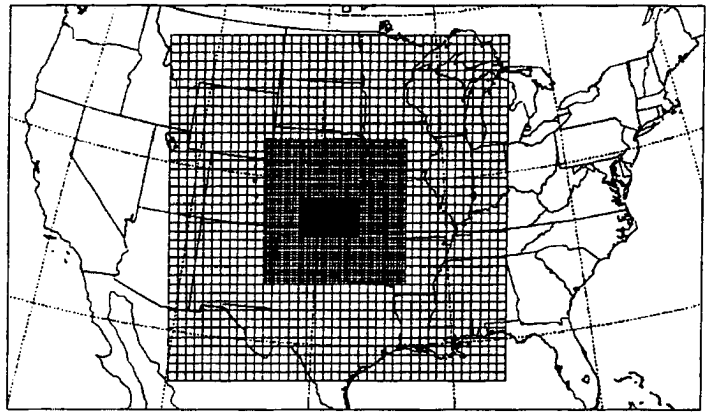

**Figure 4 . 3 RAMS grid for 6 August 1991 case study.**

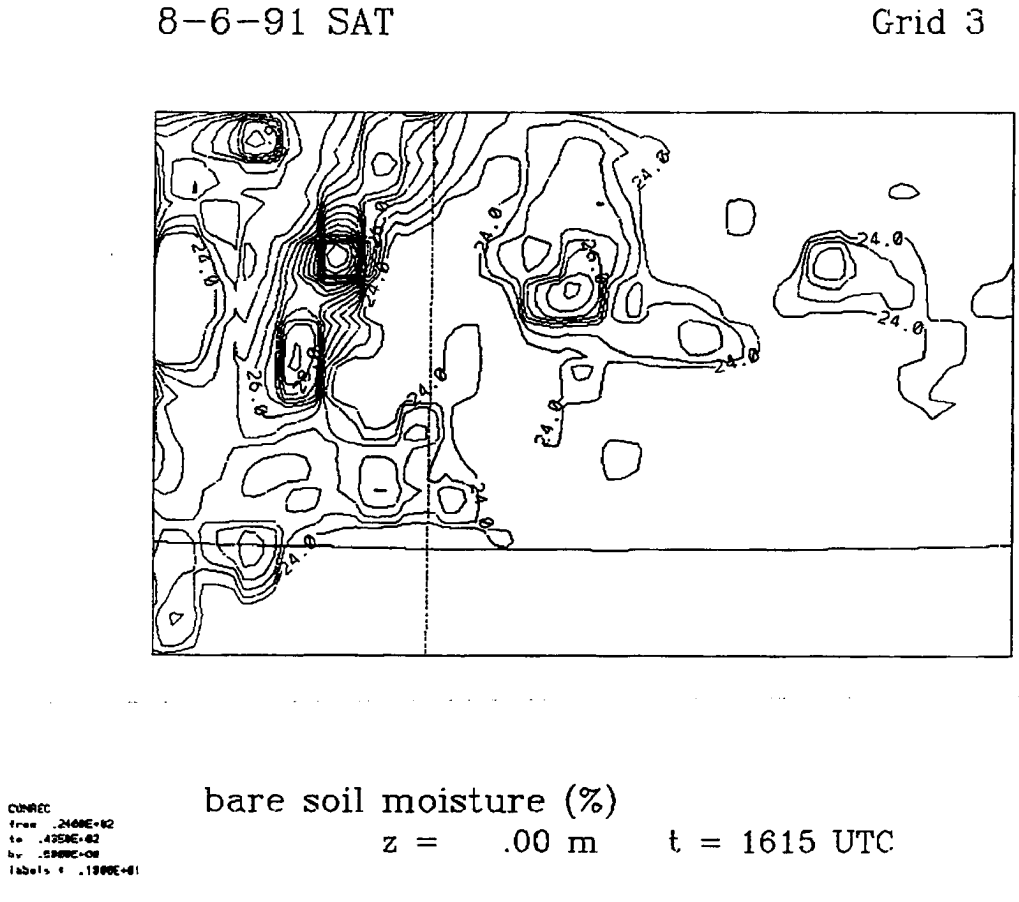


**Figure 4 . 4 Wet regions for 6 August 1991 (bare soil moisture > 24%).**

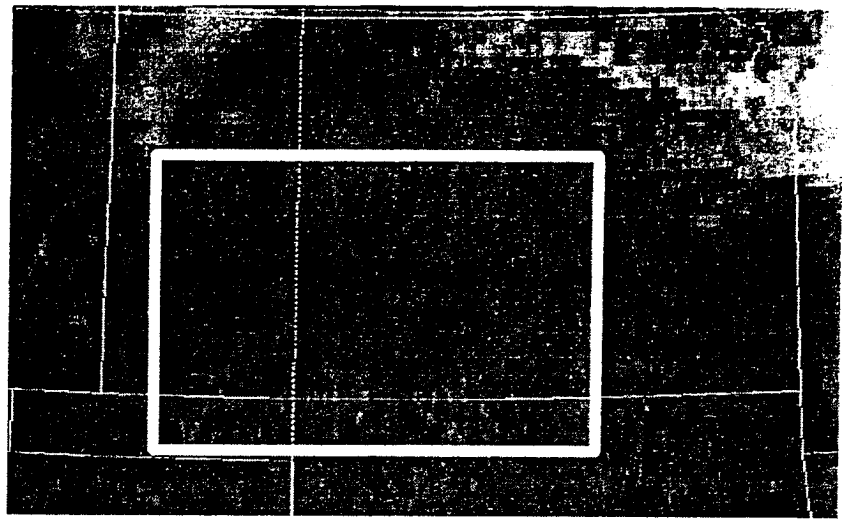

**Figure 4 . 5 Visible image for 6 August 1991 at 15:31z.**

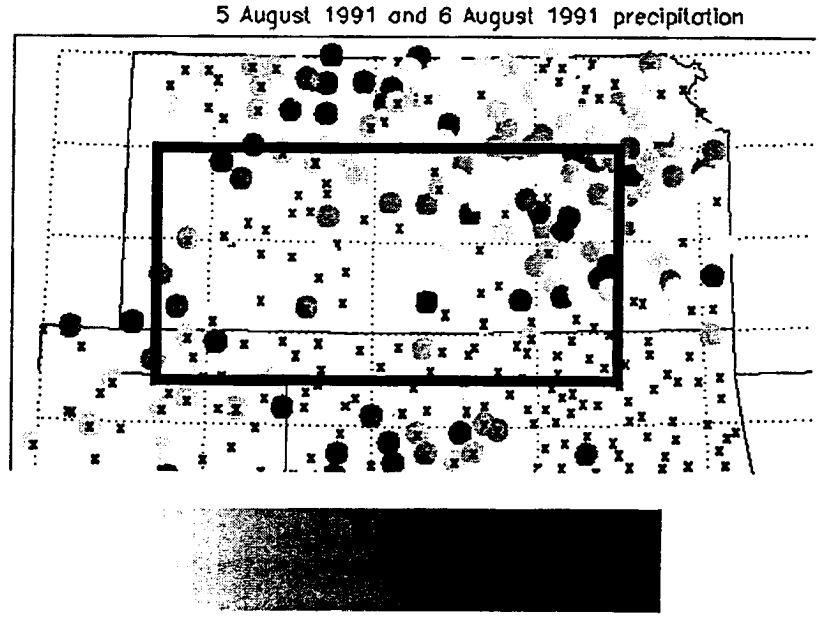


**Figure 4 . 6 Co-op 24-hr precipitation data for 5 August 1991 and for before 16z on 6 August 1991. Box indicates grid 3. 6 August reports are plotted above 5 August reports.**

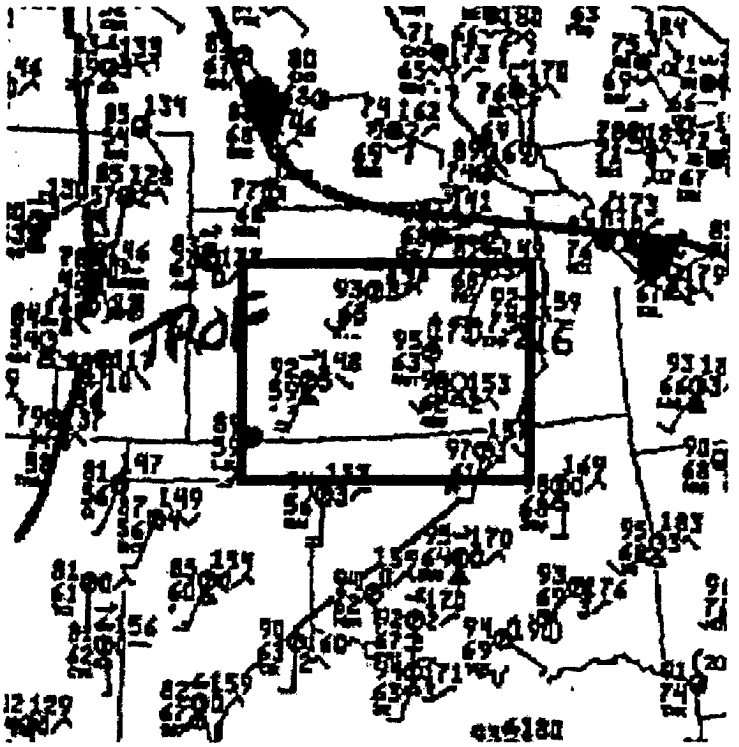

Figure 4 . 7 Surface observations at 18:00z for 6 August 1991 (NMC surface analysis).

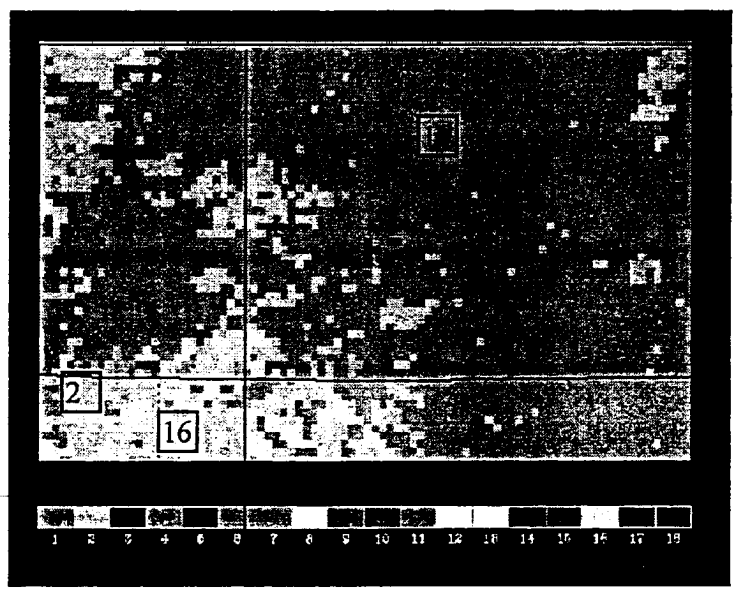


Figure 4 . 8 Landcover and vegetation type from BATS on grid 3. Predominant vegetation types are (1) crop/mixed farming; (2) short grass; and (16) evergreen shrub. The solid north-south line indicates 100ø longitude. The solid east-west line is the KS-OK border.

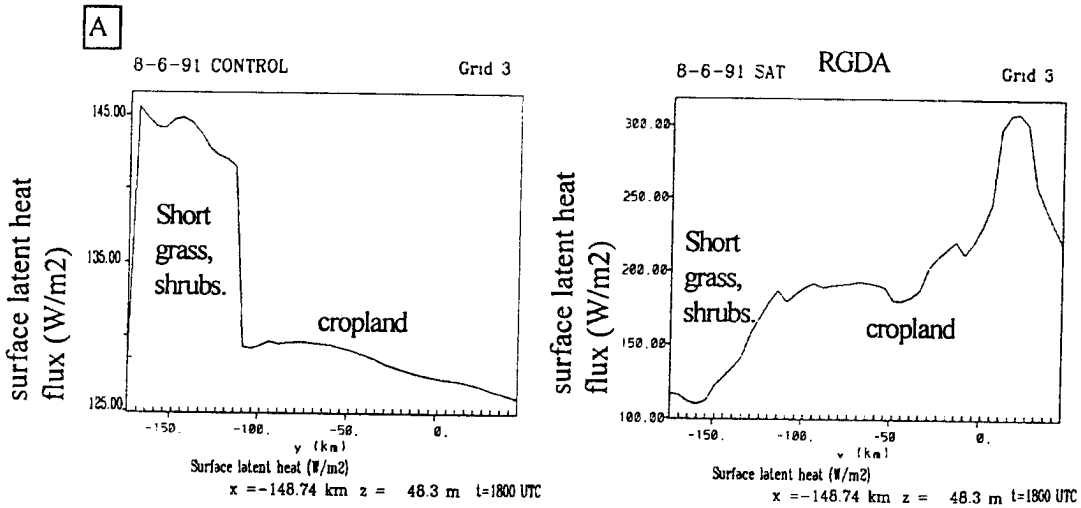
A
8-6-91 CONTROL
Grid 3
surface latent heat flux (W/m2)
Short grass, shrubs.
cropland
Surface latent heat (W/m2)
x =-148.74 km z = 48.3 m t=1800 UTC
8-6-91 SAT RGDA
Grid 3
surface latent heat flux (W/m2)
Short grass, shrubs.
cropland
Surface latent heat (W/m2)
x =-148.74 km z = 48.3 m t=1800 UTC

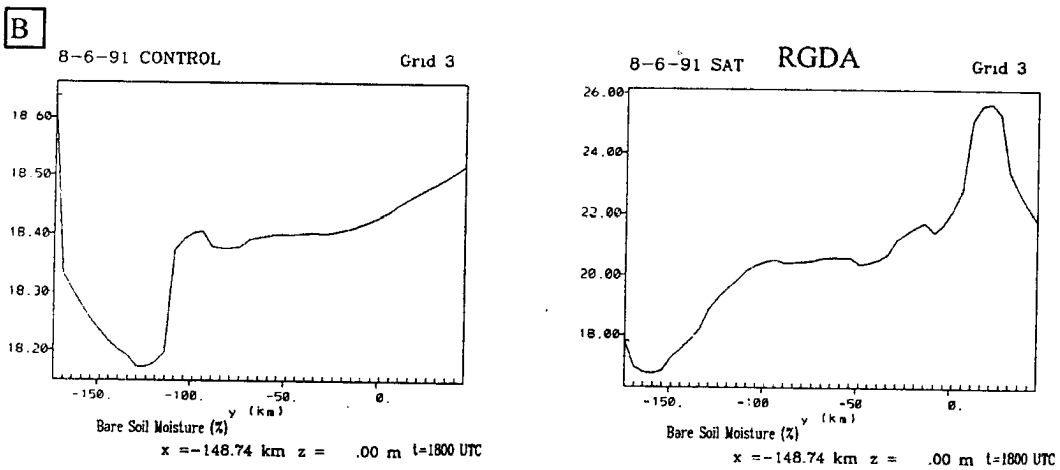
B
8-6-91 CONTROL
Grid 3
Bare Soil Moisture (%)
x =-148.74 km z = .00 m t=1800 UTC
8-6-91 SAT RGDA
Grid 3
Bare Soil Moisture (%)
x =-148.74 km z = .00 m t=1800 UTC

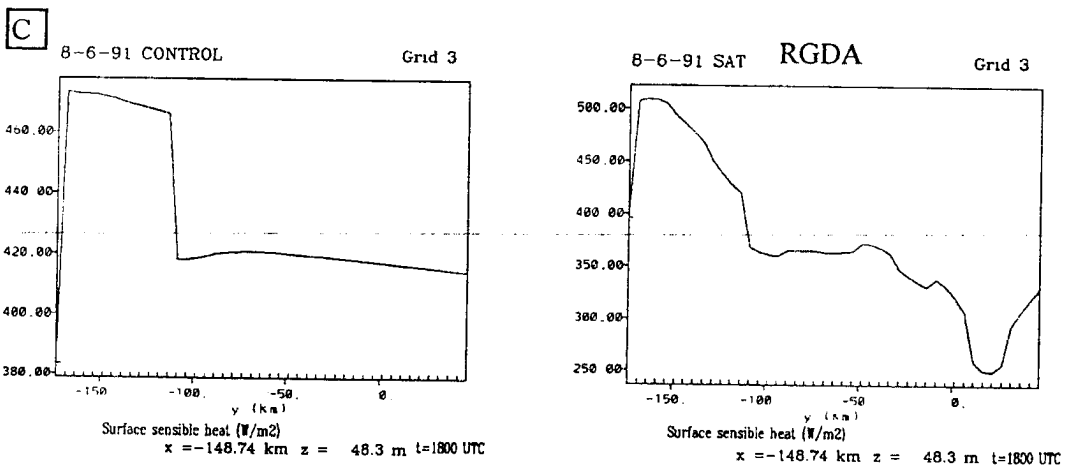
C
8-6-91 CONTROL
Grid 3
Surface sensible heat (W/m2)
x =-148.74 km z = 48.3 m t=1800 UTC
8-6-91 SAT RGDA
Grid 3
Surface sensible heat (W/m2)
x =-148.74 km z = 48.3 m t=1800 UTC

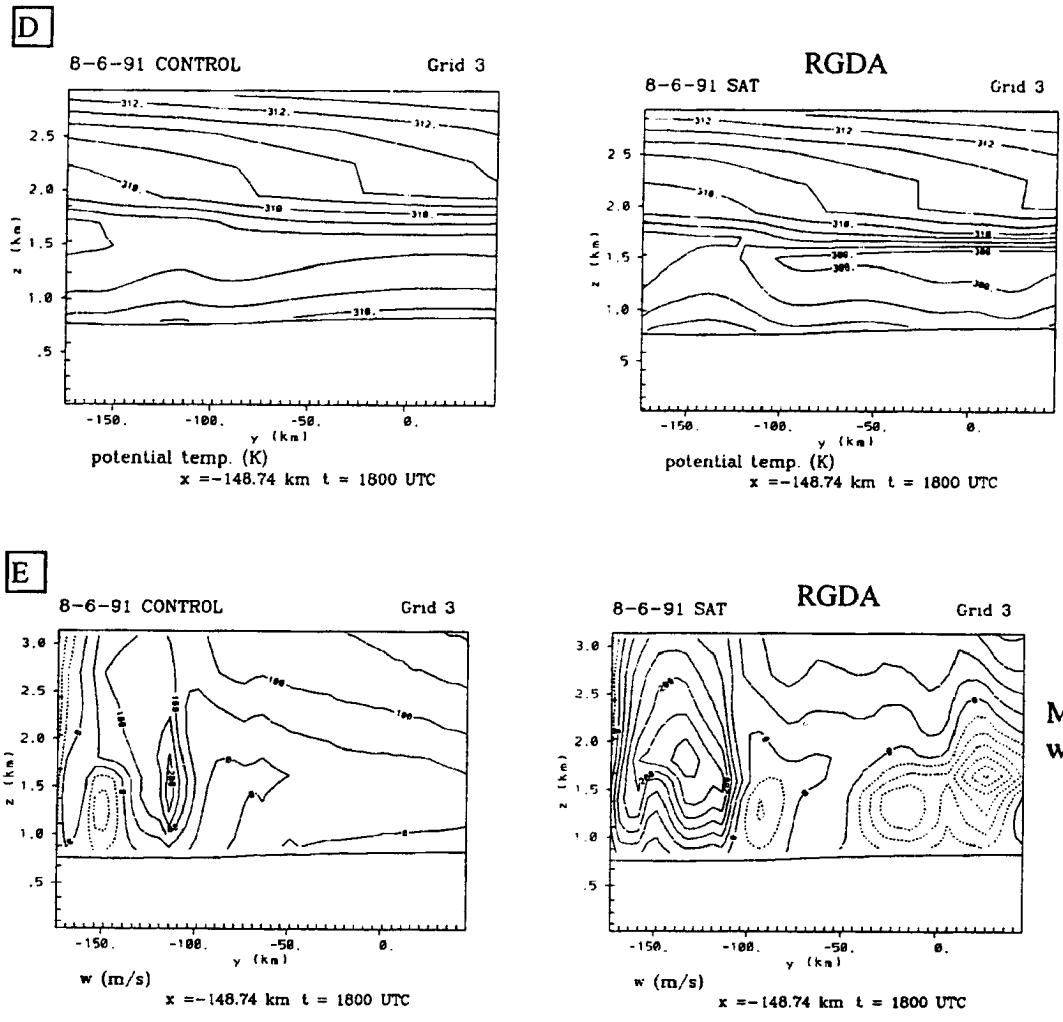


**Figure 4 . 9 Latent heat flux (A), bare soil moisture (B), sensible heat flux (C), potential temperature (D) and vertical motion (E) for 18z on 6 August 1991. Cross section is the same as in the previous figure. Rising motion is in solid contours and sinking motion is in dashed contours for (E).**

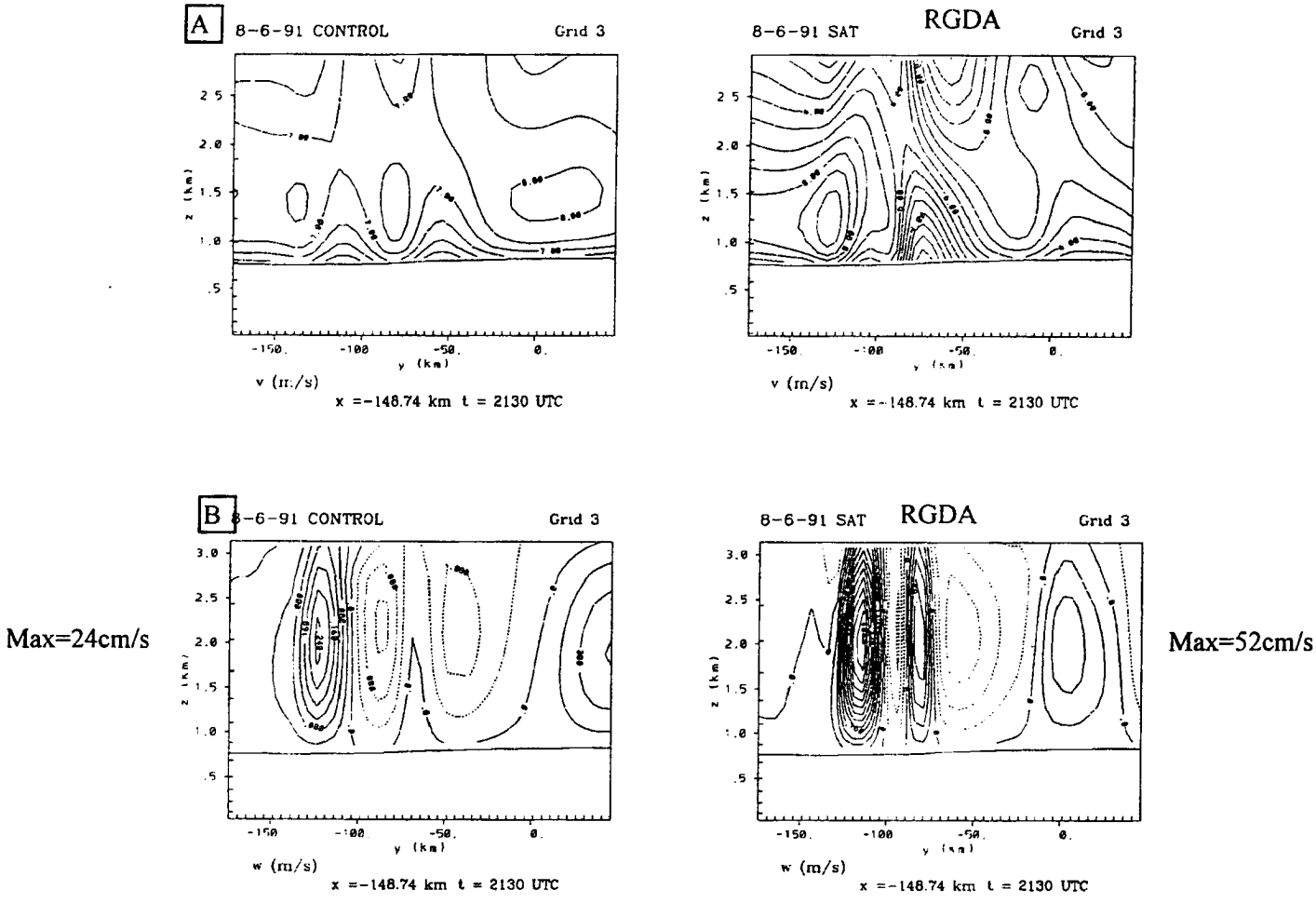


**Figure 4 . 10 North-South cross section for control and RGDA runs for 6 August 1991 case study at 2130z. Southerly winds (v) are contoured by 0.5 m/s in A, vertical motion (w) is contoured by .04 m/s in B. Solid contours indicate upward motion.**

8-6-91 control Grid 3

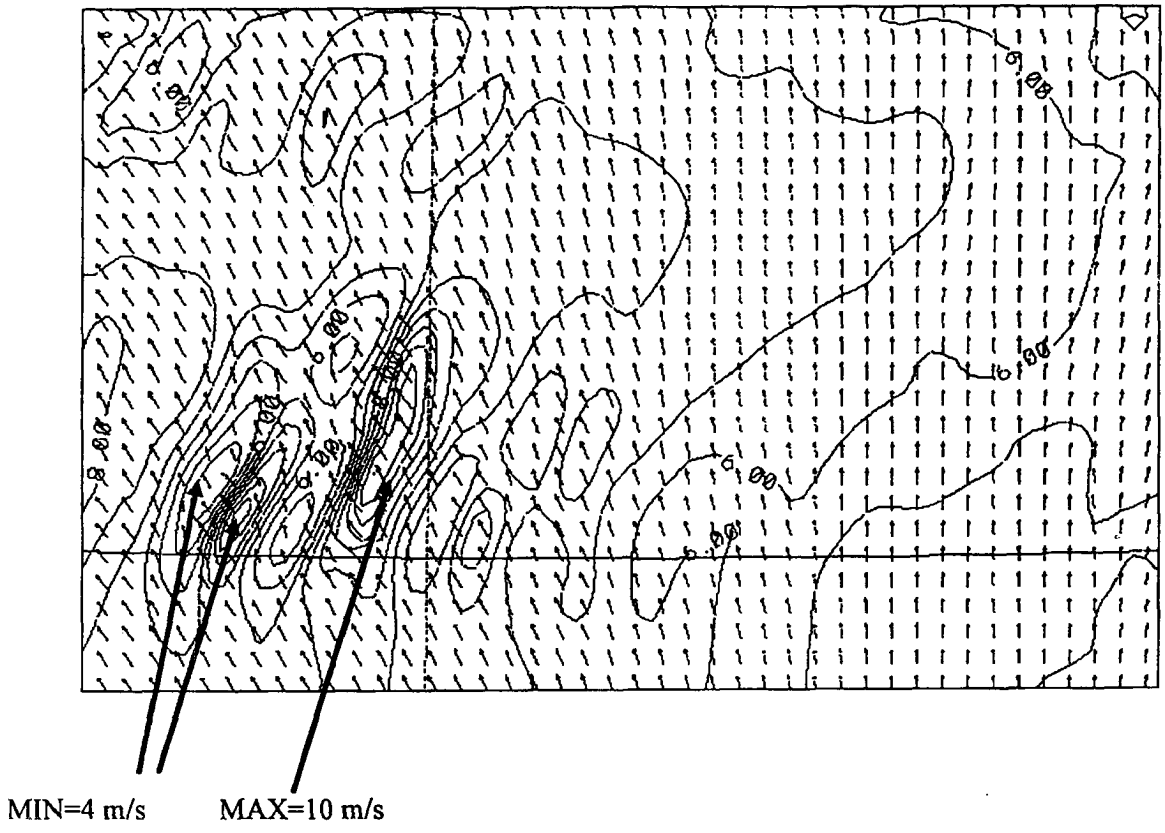


wind speed (m/s)

z = 48.3 m t = 2130 UTC

01

.982E+01
MAXIMUM VECTOR

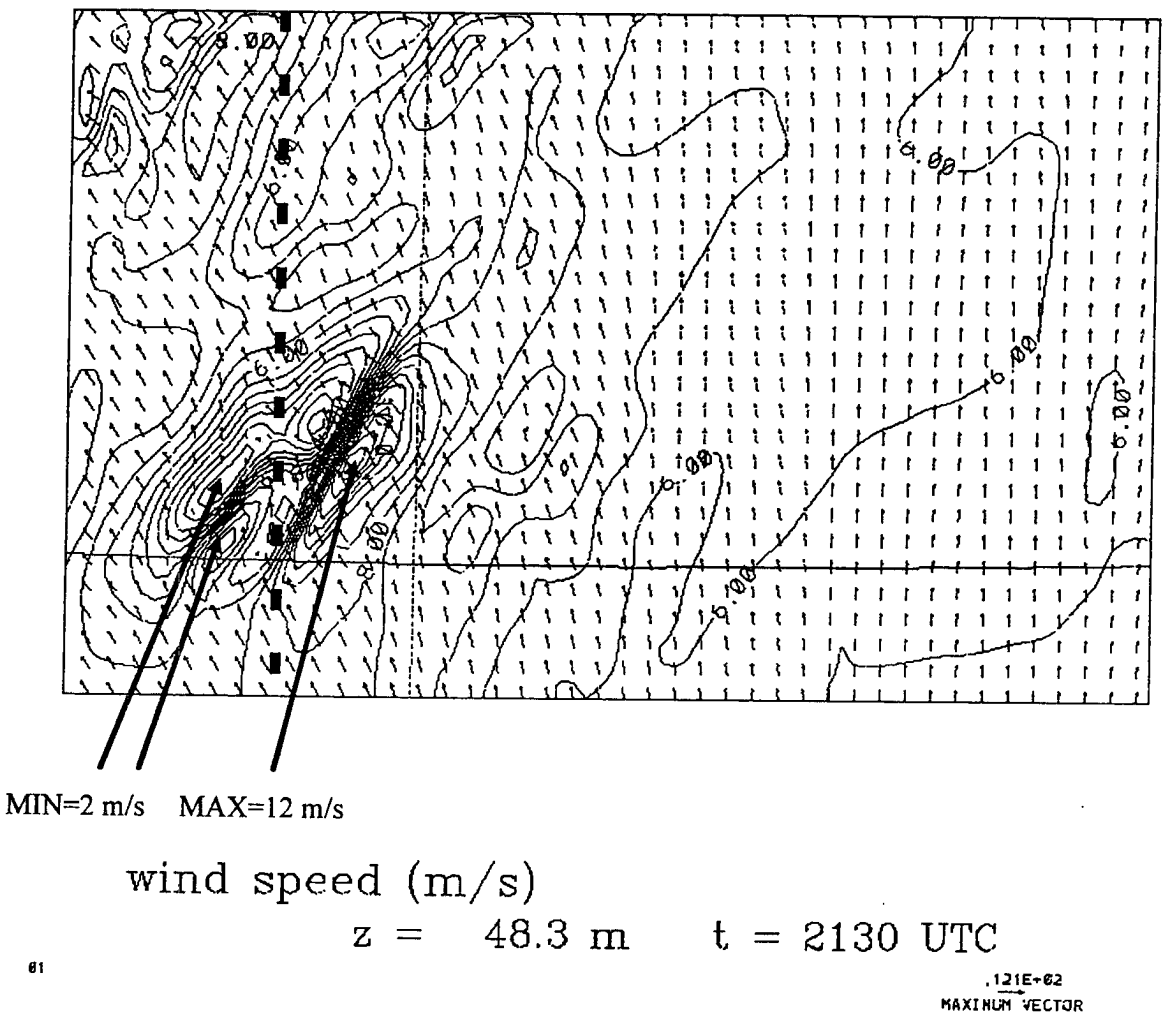


**Figure 4 . 11 Wind speed at the surface for the control run and the assimilation in grid 3 on 6 August 1991 at 2130z. Contour interval is 0.5 m/s. Dashed line indicates cross section used in the previous figures.**

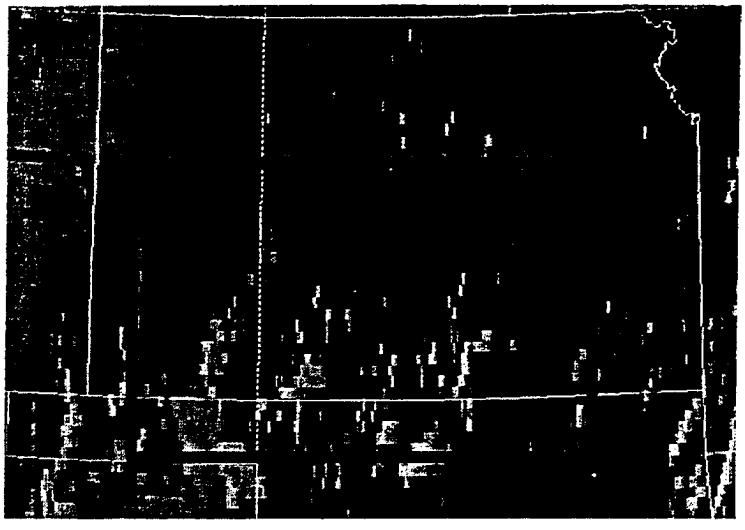

**Figure 4 . 12 Visible image for 00:01z on 7 August 1991, grid 3 is in white.**

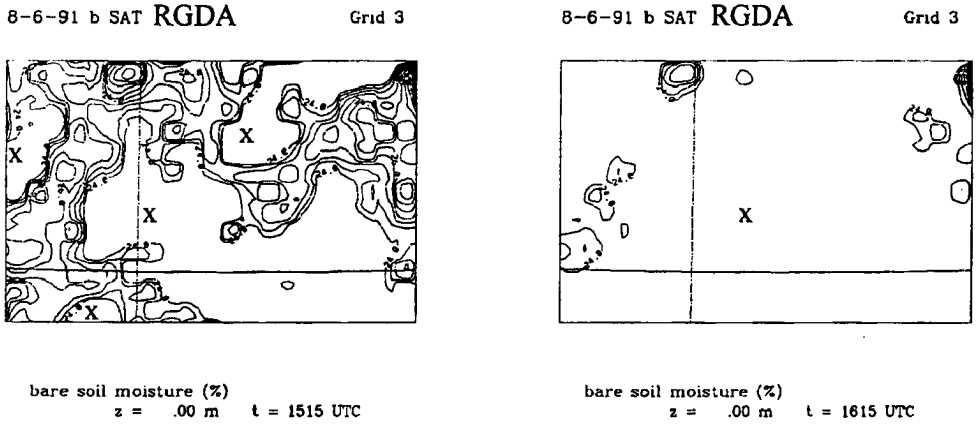


**Figure 4 . 13 Wet regions (> 24% volumetric soil moisture) for 6 August 1991 case study with the assimilation occurring between 14z and 15z instead of 15z to 16z. Regions marked with "x" are dry.**

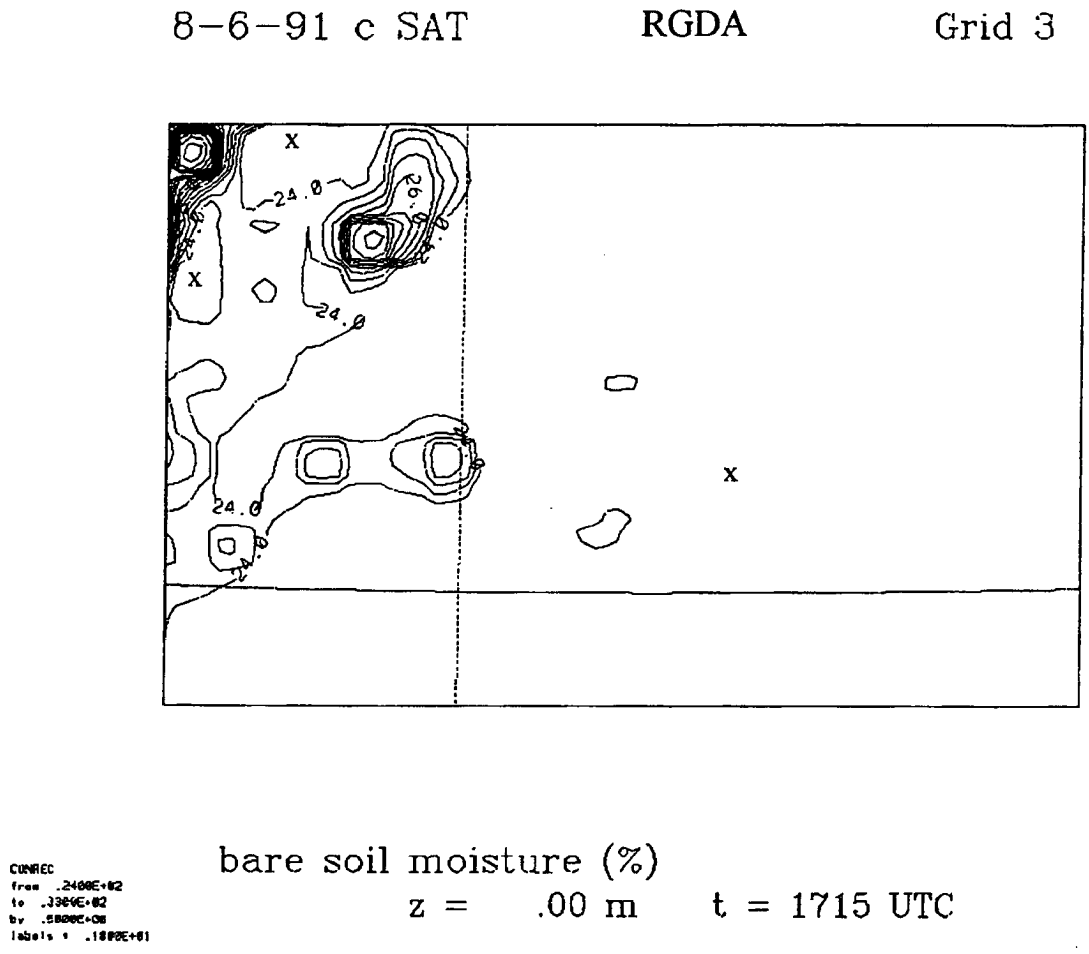


**Figure 4 . 14 Bare soil moisture > 24% for 6 August 1991, forcing between 16z and 17z.**

# Chapter 5

## Case Study: 11 September 1991. Soil moisture contrasts in nearly homogeneous vegetation.

One more case study was needed to reasonably assess the usefulness of the RGDA method and the validity of the soil moisture field created. This final case study is for the first fairly sunny morning after the 8 September case study. The grids chosen were based on the amount of cloud free regions available, with grid 3 having the fewest clouds. In Figure 5. 1 the three grids in RAMS are shown and shows the values of each grid's parameters. The western portion of grid 3 is mostly cropland, so this case can show the impact of heterogeneous soil moisture in regions of homogeneous vegetation. Figure 5. 2 shows the IR heating rate map derived from IR temperatures at 1531z and 1601z. Because the case study had quite a few low clouds, the cloud-clearing scheme had two steps:

1) All areas with IR channel 8 temperature < 280 K were assumed to be clouds (as before).
2) All areas where the time rate of change (between either 15:01z and 15:31z or 15:31z and 16:01z ) of temperature was less than or equal to 0 K were assumed to be clouds (the reason being that land regions should generally be heating up after sunrise).

### *5.1 Validity of the assimilated soil moisture field.*

Figure 5. 3 shows the resulting wet soil moisture map for 11 September 1991 after the data assimilation had run between 15:00z and 16:00z. In general, the pattern that the data assimilation picks up is very similar to the pattern that the microwave emissivity map shows. The microwave emissivity map for 11 September 1991 in Figure 5. 4 shows that there are probably some wet regions in the middle and southwest portions of grid 3. Figure 5. 5 is the corresponding visible image from which one can see some cloud contamination problems in the eastern portion of grid 3. Problem areas in the assimilation due to insufficient cloud-clearing are indicated by boxes in Figure 5. 3.

The recent radar maps are shown in Figure 5. 6 and the last 24 hours of precipitation as reported from cooperative stations for 10 September and before 16z on 11 September are shown in Figure 5. 7. The radar suggests that the central portion of grid 3 could be wet due to rain events less than 24 hours before. However, the cooperative stations only report a small amount of rain for the central region. This region also has a significant amount of irrigation (USGS Seasonal Landcover Regions, 1993) which could be causing the wet signal. The vegetation in grid 3 is such that there is tall grass in the eastern portion of the grid, with cropland dominating the rest (Figure 5. 8). The microwave emissivity maps cannot sense the ground in heavy vegetation. The tall grass area may therefore be wet and not well-represented by the microwave emissivity map. It is likely that the RGDA method generated a realistic soil moisture map considering that the microwave emissivity map has a similar pattern except for the tall grass regions. Also, there was a rain event over tall grass which could have generated the eastern portion of grid 3's wet soil.

### *5.2 Comparison between the RGDA method and a homogeneous soil moisture run to NWS observations.*

Table 5. 2 compares the wind speed, relative humidity and temperature for grid 3 at 18z between the control, the RGDA method and NWS observations. Again, air temperatures are cooler and relative humidities are higher in the assimilation than in the control. Wind speeds are 0.5 m/s higher in the RGDA method. The reason for this is studied in the next section.

The surface observations for 18:00z on 11 September 1991 are in Figure 5. 9. Both the RGDA run and the control run had very similar temperatures. At 18:00z temperatures in the modeled runs were about 2 °C cooler than observations at 18:00z in grid 3. This is typical at all time periods, and follows the trend of the 8 September case study as well as the 2 and 6 August case studies.

The relative humidity magnitudes of both the control and the RGDA simulations were too high at 18:00z to match most NWS observations. Winds for both runs approximate observations fairly well in magnitude and direction.

### *5.3 Usefulness of the RGDA method.*

The wind speeds at 18z match observations somewhat better than the control (Table 5. 2). The RGDA method may help understand some of the faster wind speeds reported better than a homogeneous soil moisture run. It appears that there is convergence in the RGDA method run due to wet soil north of grid 3. The wet soil moisture field for grid 1 must be analyzed to capture convergence. This field is shown in Figure 5. 10.

A north-south cross section through the approximate center of the box shown in Figure 5. 10 was taken to illustrate the wet-soil/dry-soil circulation more clearly. Vegetation for grid 1 is shown in Figure 5. 11. Notice that the cross section is through fairly homogeneous cropland, unlike the case for 6 August 1991. Figure 5. 12 (A) shows the total mixing ratio for the cross

section. The winds are southerly (coming from the left side of the figure). The wet soil regions are shown by dark lines through the y-axis. These regions exhibit the highest mixing ratio values for the data assimilation run. Figure 5. 12 (B) shows the potential temperature field for the cross section. There is a bulge in the potential temperature field just above the dry-soil region. This bulge is enhanced by the data assimilation because the wet soil regions correspond to minimums in potential temperature on both sides of the dry region, creating a modified heat island effect. The air temperature is warmer here due to lack of moisture and warmer ground temperatures for dry soil than for wet soil. The model has rising motion occurring over dry land and sinking motion over minimum potential temperatures associated with wet regions as seen in Figure 5. 12 (C). Figure 5. 12 (D) shows southerly wind speeds and it appears that convergence over the wet soil causes wind speeds south of it to increase by about 0.5 m/s. This corresponds to the faster grid 3 wind speeds for the RGDA method.

The surface sensible heat flux for this cross section is shown in Figure 5. 12 (E). For the control run the horizontal gradient is small, about 20 $W/m^2$ difference. Using equation 3.1, this leads to air above the higher sensible heat flux region heating about 0.1 K/hr faster than air above the low sensible heat flux regions. The satellite run has a more significant horizontal gradient. Caution must be used when determining the sensible heat flux gradient for this case because the grid spacing is 40 km and the minimum value is a $2\Delta X$ feature. For determining approximate air mass heating rates, a value of 250 $W/m^2$ will be used for the minimum surface sensible heat flux. Using this the horizontal gradient in sensible heat flux is about 100 $W/m^2$. This corresponds to a heating rate gradient of 0.3 K/hr, which is three times larger than the control run and appears to be the cause of the overall difference between the two runs. Values for sensible heat fluxes in each case are shown in Table 5. 2.

*5.4 Summary.*

A realistic soil moisture map was created using the RGDA method. Winds were slightly better approximated in the assimilation, with a modified heat island effect occurring due to dry soil next to wet soil both upwind and downwind. Relative humidity values were too high in the control. Because the RGDA method has relatively little effect in dry areas for sandy clay loam (see Appendix), it was unable to improve upon this and forced the humidity values higher than the control. This is consistent with the hypothesis that the model is evaporating soil moisture too quickly and a more reasonable soil type needs to be found to use in the central plains for homogeneous soil moisture.

**Table 5. 1 RAMS v3a configuration for 11 September 1991.**

| | *Grid 1* | *Grid 2* | *Grid 3* |
|---|---|---|---|
| number of x gridpoints | 70 | 90 | 60 |
| number of y gridpoints | 50 | 98 | 60 |
| delta x | 40 km | 10 km | 5 km |
| delta y | 40 km | 10 km | 5 km |
| center latitude | 35.4 | 35.4 | 37.7 |
| center longitude | -97.8 | -97.4 | -97.4 |

**Table 5. 2 RGDA method, control run and NWS surface observations for 18z on 11 September 1991 in grid 3.**

| *18z* | *Wind Speed* | *Relative Humidity* | *Temperature* |
|---|---|---|---|
| RGDA | 5.5-8.0 M/S | 52-58% | 28.5-30.0 °C |
| Control | 5.0-7.5 M/S | 51-53% | 28.5-30.5 °C |
| NWS observations | 5-10 M/S | 36-56% | 30.0-32.0 °C |

**Table 5. 3 Surface sensible heat flux for 18z on 11 September 1991 in grid 3.**

| | *Value* | *Surface type* | *Mixed layer heating* |
|---|---|---|---|
| RGDA $H_{min}$ | 250 $W/m^2$ | wet crops | 1.6 K/hr |
| RGDA $H_{max}$ | 350 $W/m^2$ | dry crops | 1.9 K/hr |
| Control $H_{min}$ | 350 $W/m^2$ | crops | 1.9 K/hr |
| Control $H_{max}$ | 368 $W/m^2$ | crops | 2.0 K/hr |

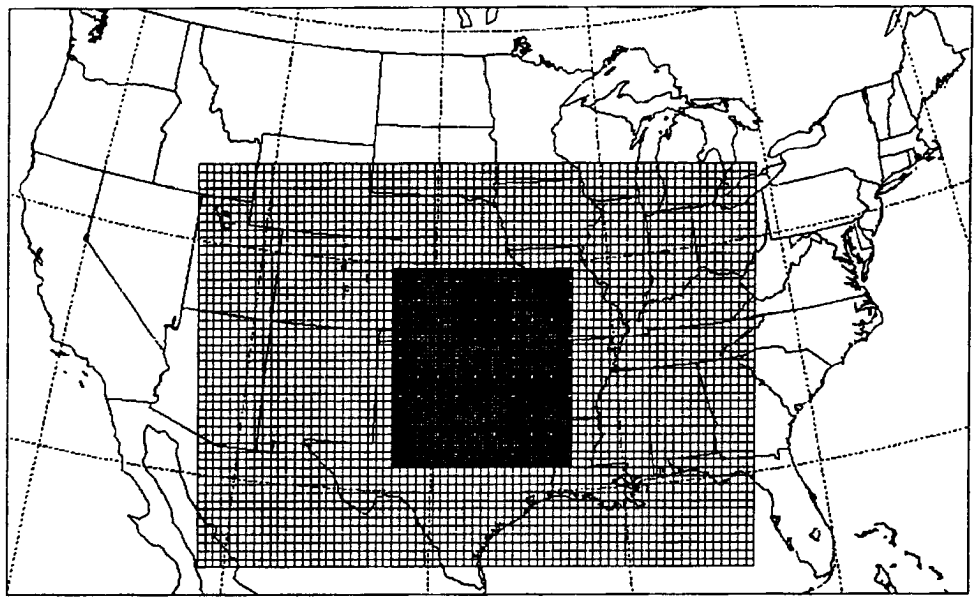

**Figure 5. 1 RAMS grids for 11 September 1991 case study.**

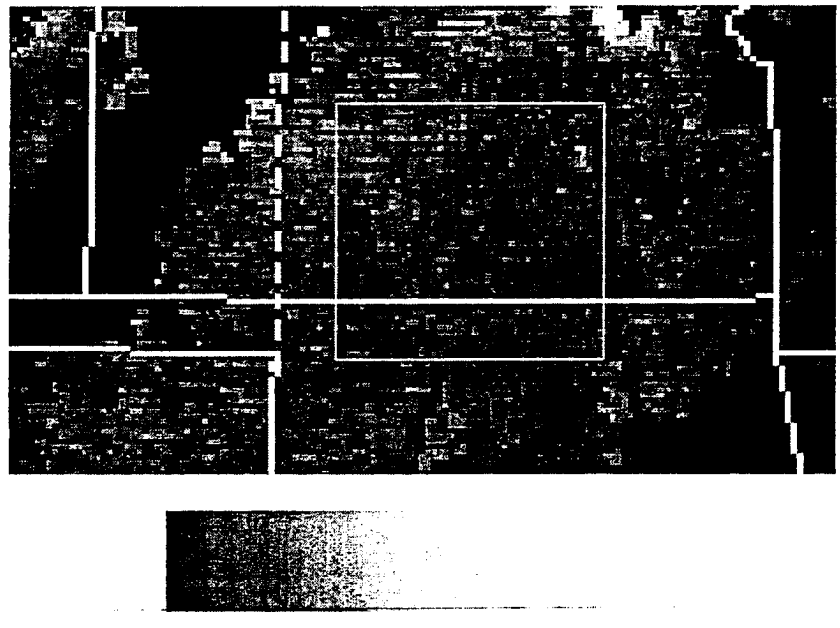


**Figure 5. 2 Time rate of change for IR temperatures between 1531z and 1601z. Dark regions have the least temperature change and bright regions have the highest temperature change. Cloudy areas are in black and not included in calculation.**

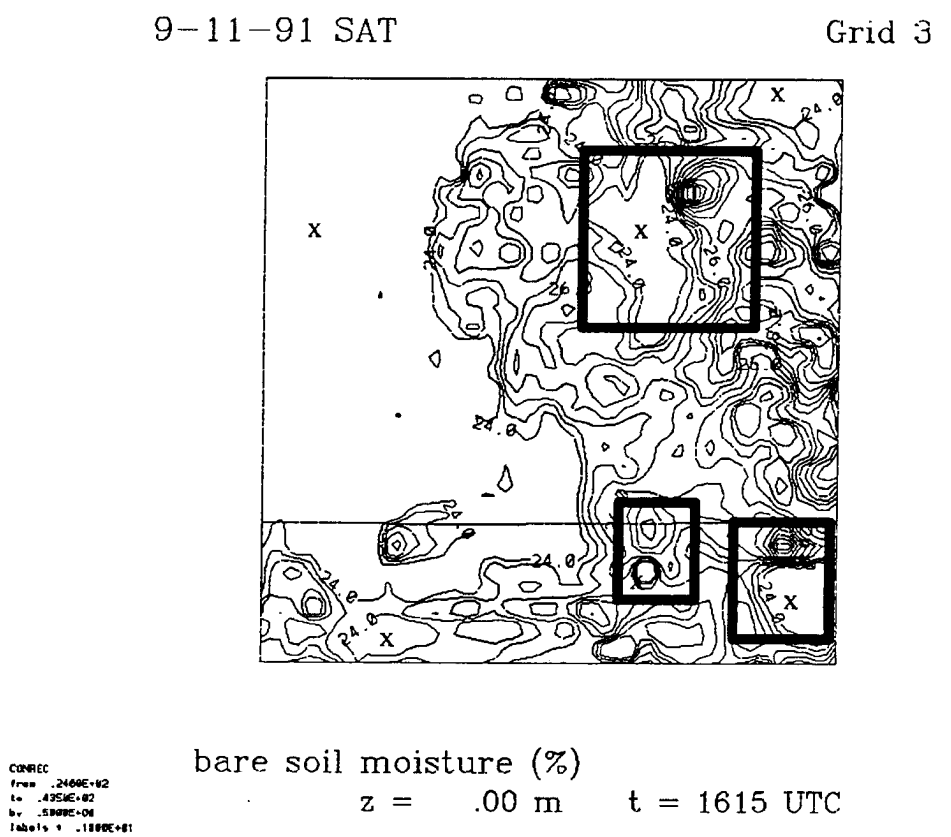


**Figure 5. 3 Contours of wet regions (bare soil moisture > 24%) for 9-11-91 in the RGDA method. Possible cloud contamination in boxes. Regions marked with "x" are dry.**

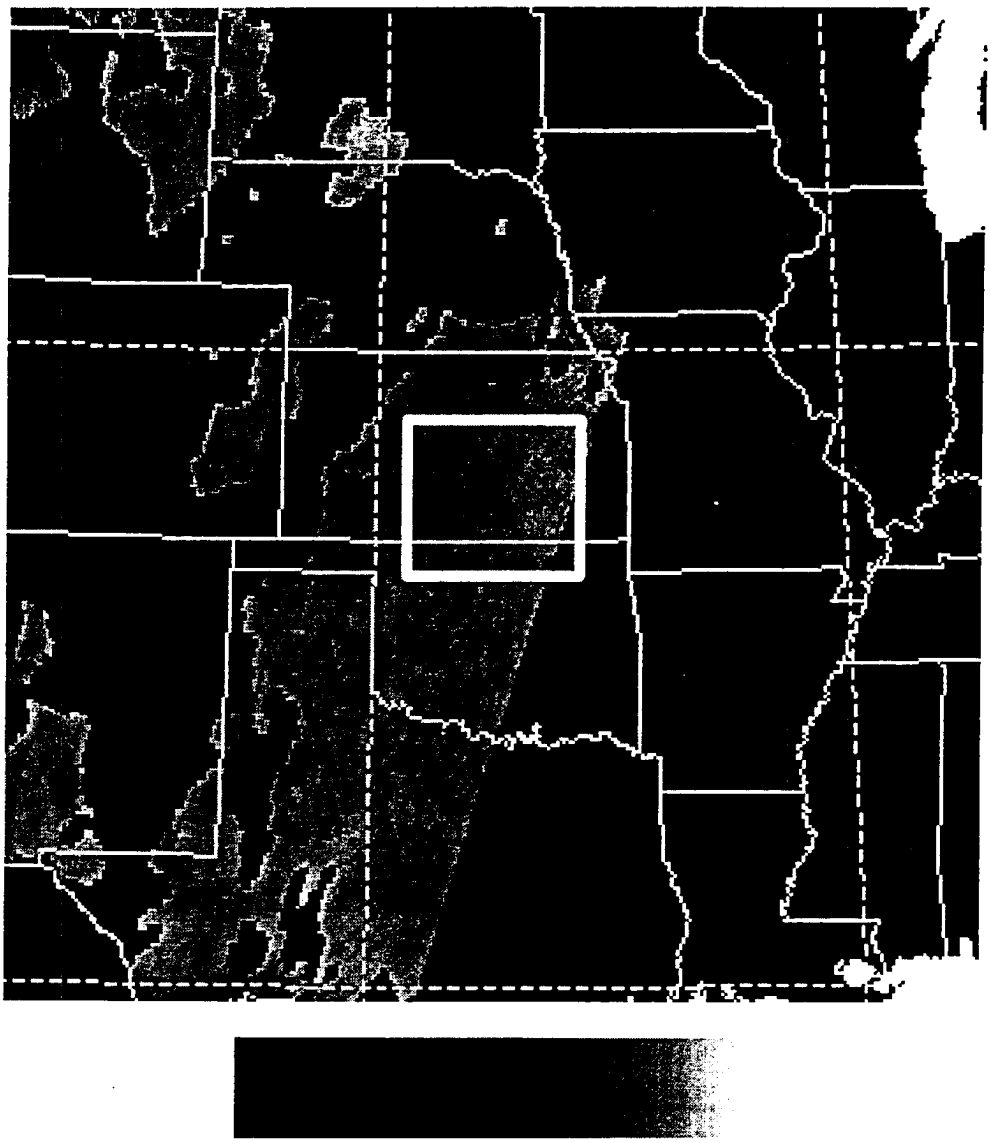


**Figure 5. 4 Microwave emissivity map for channel 7 at 15:35z on 9-11-91. Box indicates approximate area of grid 3.**

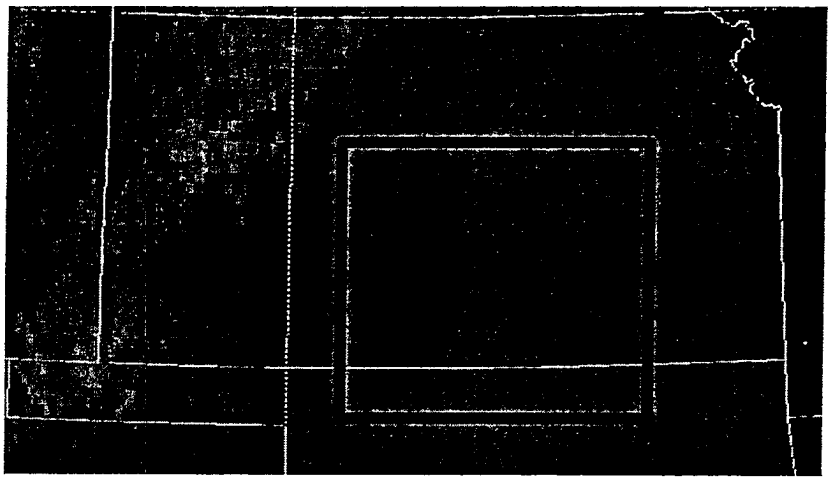

**Figure 5. 5 Visible image for 11 September 1991 at 15:31z. Box represents grid 3.**

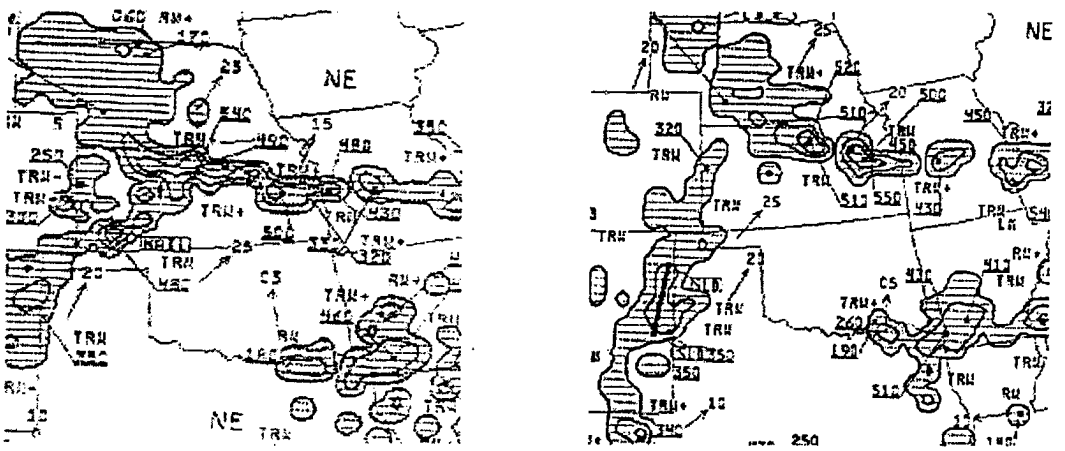


**Figure 5. 6 Radar summary reports for 2135z and 2235z on 10-September-1991.**

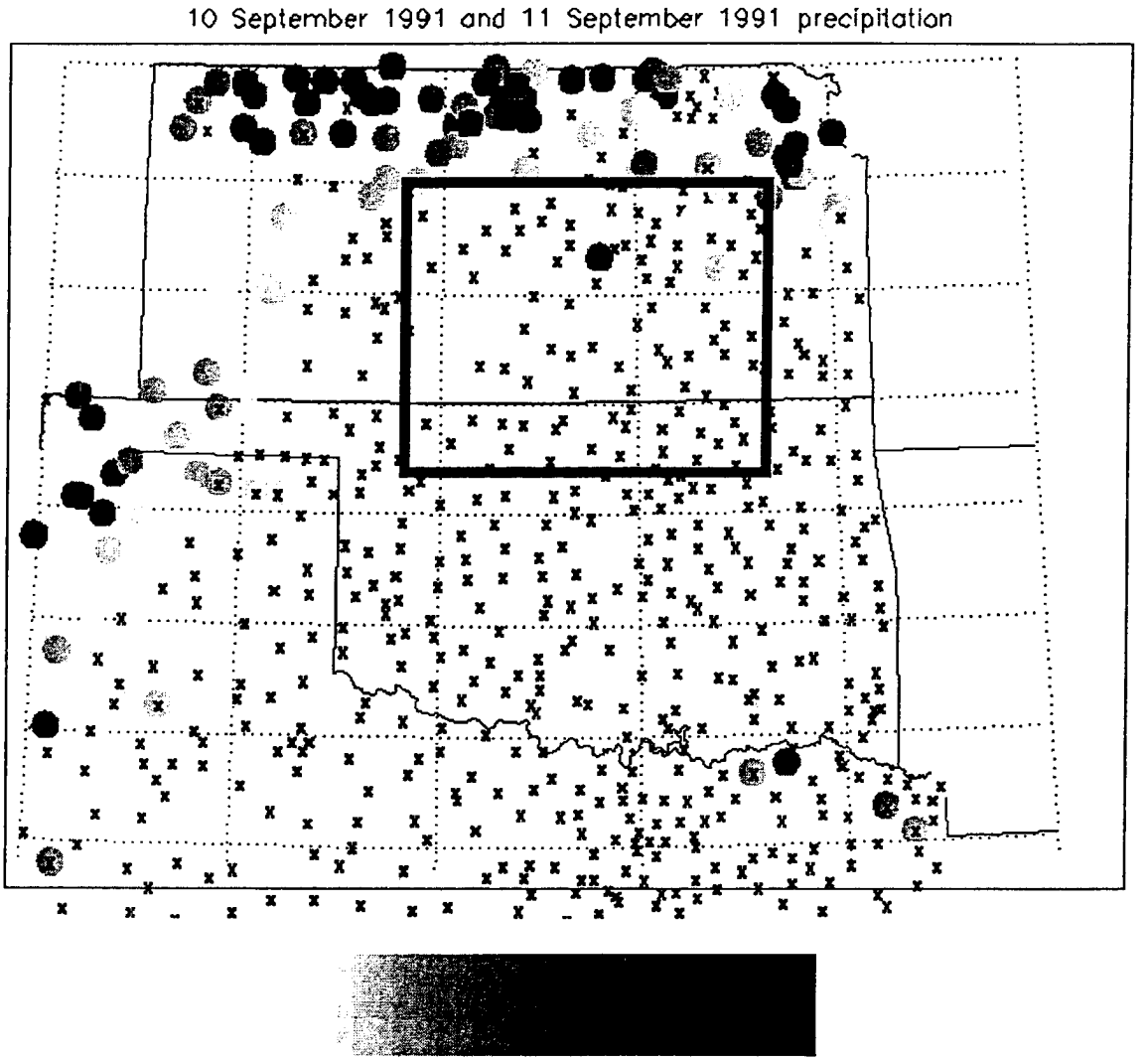


**Figure 5. 7 Co-op 24 hour precipitation reports from 10 September 1991 and from hours before 16z on 11 September 1991 (plotted on top). Box indicates grid 3.**

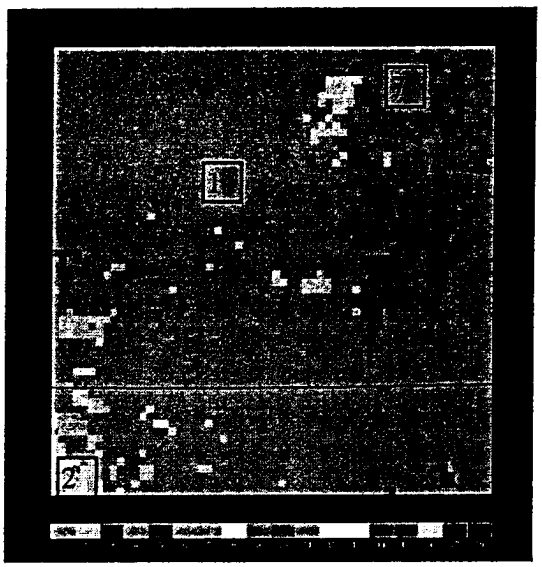

**Figure 5. 8 Vegetation for grid 3 in 11 September 1991 case study. Prominent vegetation types are: 1-Crop/mixed farming, 2-Short grass, and 7-Tall grass.**

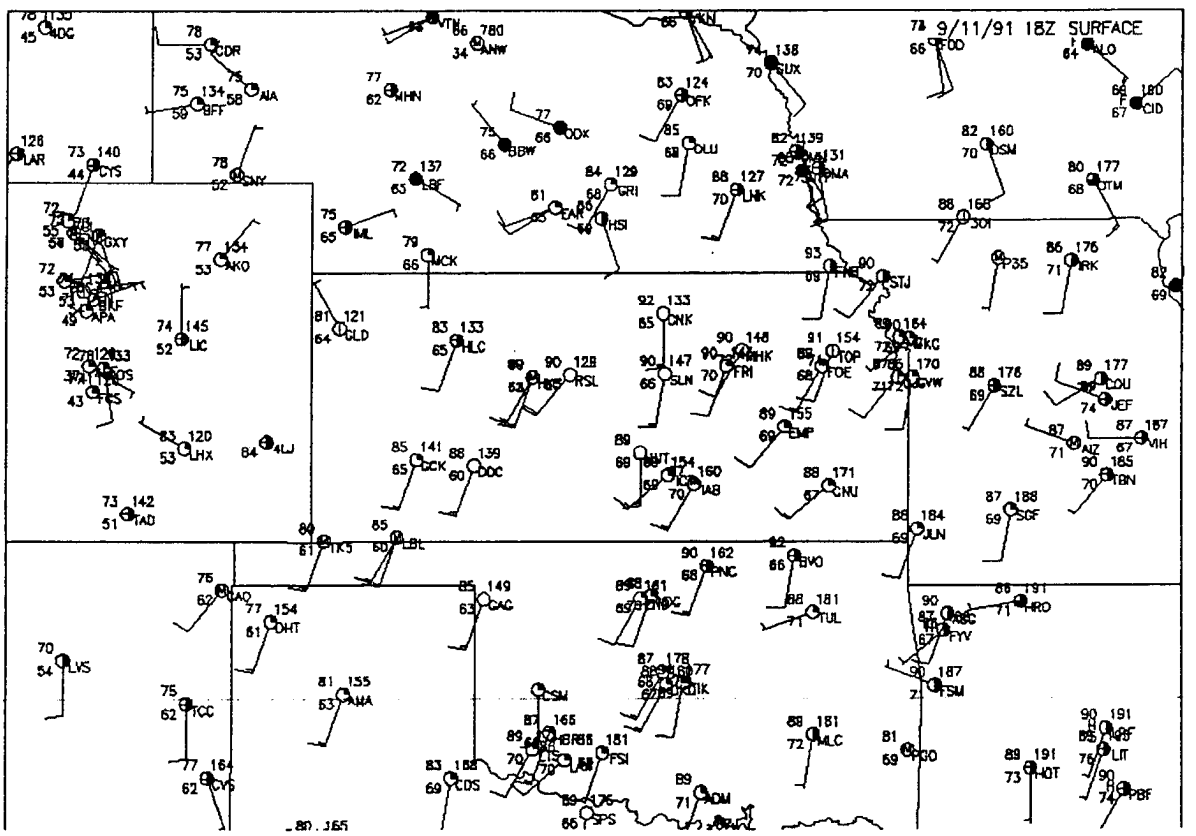


**Figure 5. 9 NWS surface observations for 18z on 11 September 1991.**

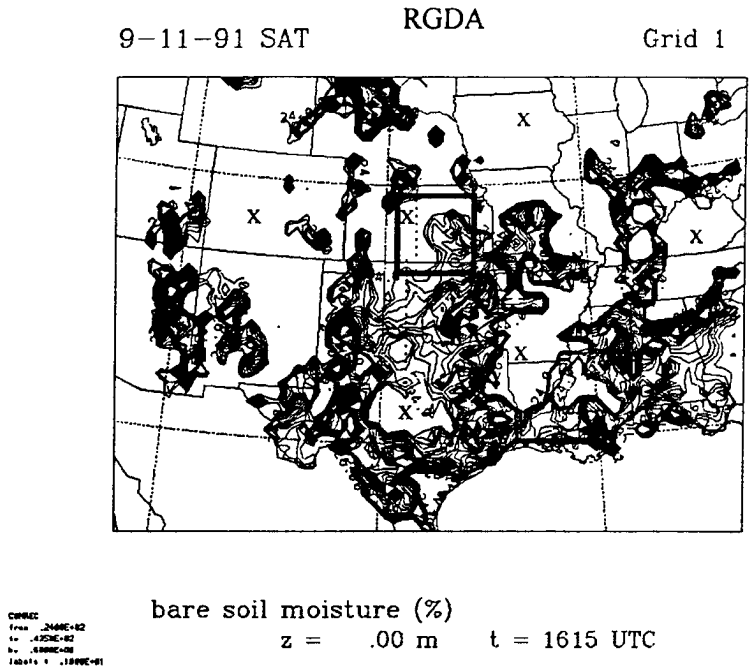


**Figure 5. 10 Wet soil regions > 24% bare soil moisture at 1615z for 11 September 1991 in the RGDA run. Box indicates region of soil moisture heterogeneity which appears to be affecting the winds in the third grid in the RGDA run, dashed line indicates approximate position of cross section for next figures. An "x" indicates the region is dry.**

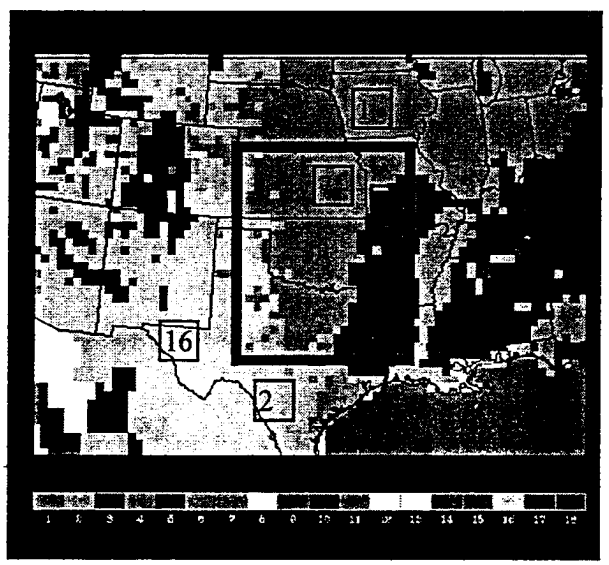


**Figure 5. 11 Vegetation for grid 1 in 11-September 1991 case study. Grid 2 is indicated by the black box and the cross section is indicated by the dashed line. Prominent vegetation types in grid 2 are: 1-Crop/mixed farming, 2-Short grass, 5-Deciduous broadleaf tree, 7-Tall grass, 16-Evergreen shrub and 18-mixed woodland.**

A

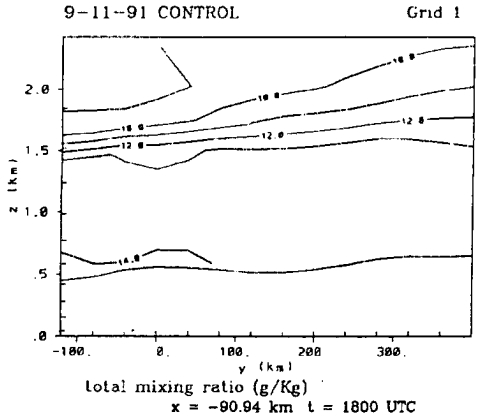


RGDA

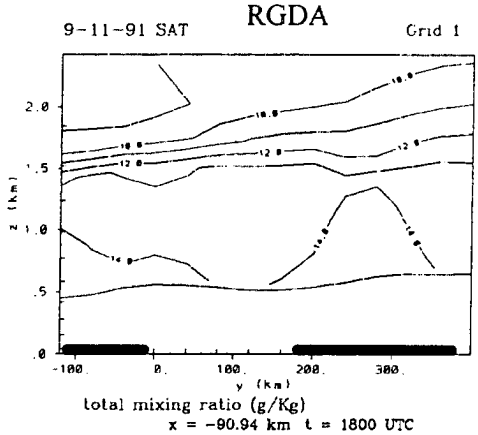


B

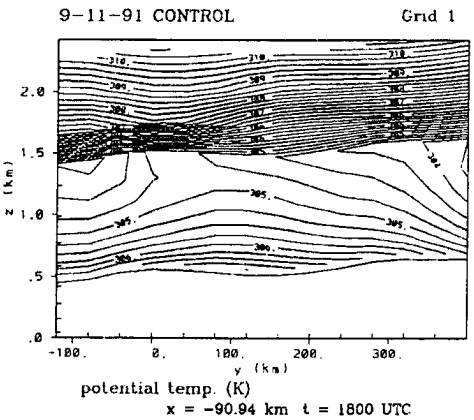


RGDA

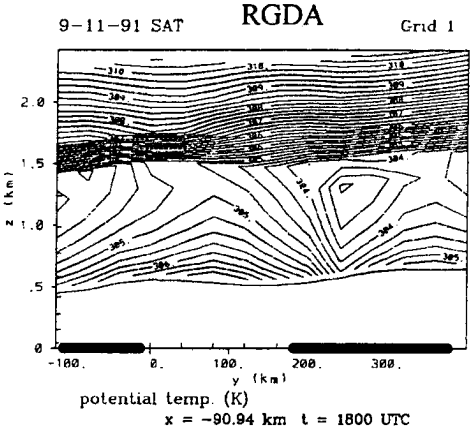


C

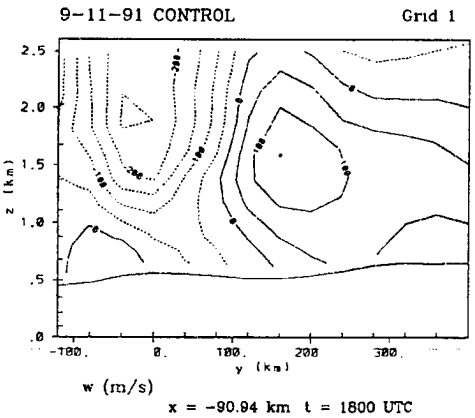


RGDA

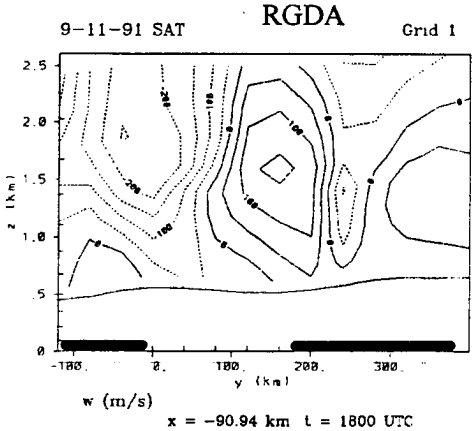

D

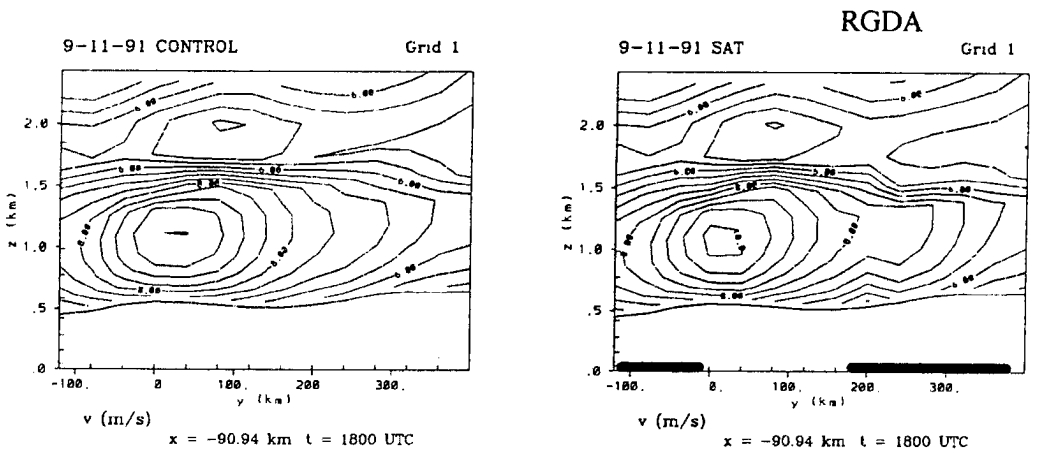


E

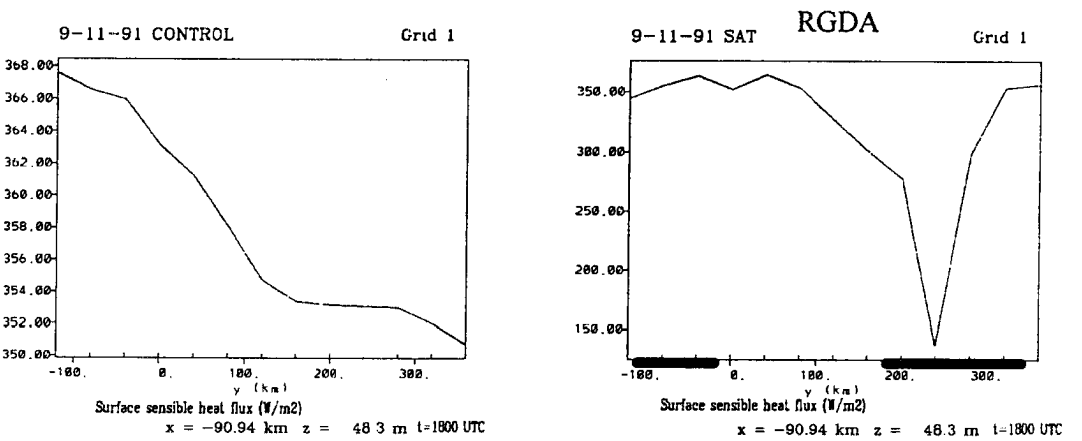


**Figure 5. 12 Total mixing ratio (g/kg), potential temperature (K), vertical wind speed (m/s x $10^5$, southerly wind speed (m/s) and surface sensible heat flux ($W/m^2$) in a north-south cross section for 11 September 1991 case at 18:00z. Black line indicates wet soil.**

Chapter 6

# Conclusions

## *6.1 Summary of all case studies*

All three case studies produced reliable soil moisture fields in the absence of clouds using the RGDA method. However, there were fundamental problems with the assimilation. Complete evaporation of assimilated soil moisture appeared to occur too early in the morning. This may be due to the fact that no significant infiltration of added soil moisture occurs when using sandy clay loam for twelve hour model runs. This caused the assimilation to have a cool, moist bias in the morning hours of the run. Shaw (1995) also found this to occur when using the Antecedent Precipitation Index to initialize soil moisture. It appears to be a problem with the limited soil types allowed in the RAMS model and not the RGDA method itself.

However, the RGDA method can be used to understand land-air interactions even with the bias. Areas of convergence over wet soil regions cannot be predicted with homogeneous soil moisture runs. Soil moisture heterogeneities due to vegetation differences or irrigation cannot be studied using API derived soil moisture amounts. The volumetric soil moisture amounts which can produce reasonable ground surface heating rates are difficult to figure out using an API method without using trial and error.

### *6.2 Accomplishments*

Several new sensitivity tests for the RGDA method were performed. The sensitivity tests dealt with:

1) Top soil layer depth

2) Vegetation fraction

3) Soil type

4) Time of forcing period

5) Extent of forcing (top layer vs full column layer).

The first four tests showed that slightly different soil moisture maps were generated by the RGDA method when the parameters were changed. However, the general pattern of the soil moisture maps was always the same, indicating that small errors in the first four parameters will not greatly affect the soil moisture analysis. For sandy clay loam, it was shown that the top soil layer was not coupled to the bottom ten soil layers in the 8 September 1991 case. Therefore, even large errors in the specification of the bottom ten layers of soil will not greatly affect the RGDA method for sandy clay loam.

Three new case studies were run, bringing the total number of case studies using the RGDA method to four. Each case study evaluated the performance of the RGDA method in comparison to a control run, surface observations from National Weather Service stations, precipitation and radar reports, microwave emissivity maps and visible satellite imagery. The first case study on 2 August 1991 represented a moderately wet region near Lake Texoma. The case study on 6 August 1991 was over wet regions in Kansas in heterogeneous vegetation. The case study on 11 September 1991 had some wet regions in Kansas over fairly homogeneous vegetation.

### *6.3 Results*

The conclusions presented in this section are summarized in Figure 6. 1. This section and the figure discuss the five questions proposed in the introduction of this thesis (pp. 1-2).

The RGDA method was found to be most sensitive to soil type. Sandy soil was found to generate a much longer-lasting soil moisture map than sandy clay loam soil, although the pattern of wet soil moisture regions were the same. A smaller top layer depth in the soil caused the soil moisture map to be drier, although the pattern was again the same. A smaller vegetation fraction caused the soil moisture map to show slightly more moisture.

All three new case studies appeared to have valid soil moisture fields generated in cloud-free vegetated regions. Each case study's soil moisture field was compared to microwave emissivity maps, radar reports and precipitation data. Unfortunately, there were no *in-situ* measurements of soil moisture, but the results thus far using the RGDA method are very promising.

The sensitivity tests for the 6 August 1991 case study (changing the time period of satellite forcing) suggested that RAMS was evaporating the RGDA soil moisture field too quickly. This appears to be due to the lack of a sufficient soil type to use for homogeneous initialization. Sandy clay loam was probably the best possible soil type to use out of the 12 choices in RAMS, but it still can not be expected to be representative of any moderately sized domain. However, from using the RGDA method at different times for 6 August, it appears realistic that all the soil moisture in the top layer was gone by the end of the run (one can see how dry it is in Figure 4 . 14). This means that the total amount of daily evaporation is still reasonable. It is the evaporation time frame that is incorrect.

Because of fast evaporation, it appears that the RGDA method runs cannot generate significantly more realistic surface observations than the control runs. The RGDA method runs

generally have a cool, moist bias in the morning hours. However, in all three cases the value of the maximum surface relative humidity was improved over the control run for the morning.

As each case study was presented, a section was entitled "Usefulness of the RGDA method." This was provided because some may wonder why one would want to use the RGDA method if the surface observations were not significantly improved over the control. The results presented in the "usefulness" section were generally of mesoscale events for which there were not enough NWS stations to resolve. However, those studying mesoscale circulations will need soil moisture included in their modeling and observational networks to better understand lake effect breezes (2 August 1991 case), breezes due to heterogeneous vegetation (6 August 1991) or even breezes in homogeneous vegetation (11 September 1991). It was found that a 2.0% fluctuation in volumetric soil moisture corresponded to a 50 $W/m^2$ fluctuation in surface latent and sensible heat fluxes from the top soil layer using the RGDA method in the 6 August 1991 (wet) case study. In the 2 August 1991 case study (fairly dry), a 2.0% fluctuation in volumetric soil moisture corresponded to an 80 $W/m^2$ fluctuation in the surface heat fluxes.

### *6.3 Ideas for future research*

Future research should include trying the data assimilation with heterogeneous soil type information, similar to Copeland (1995). More research needs to be done to diagnose vegetation fraction and how it changes throughout the year. Also, an improved cloud clearing scheme needs to be developed. More case studies should be attempted over areas with more data (e.g. the Oklahoma Mesonet area). In this way the true effect of heterogeneous soil moisture can be monitored to see if it is the same as the model suggests.

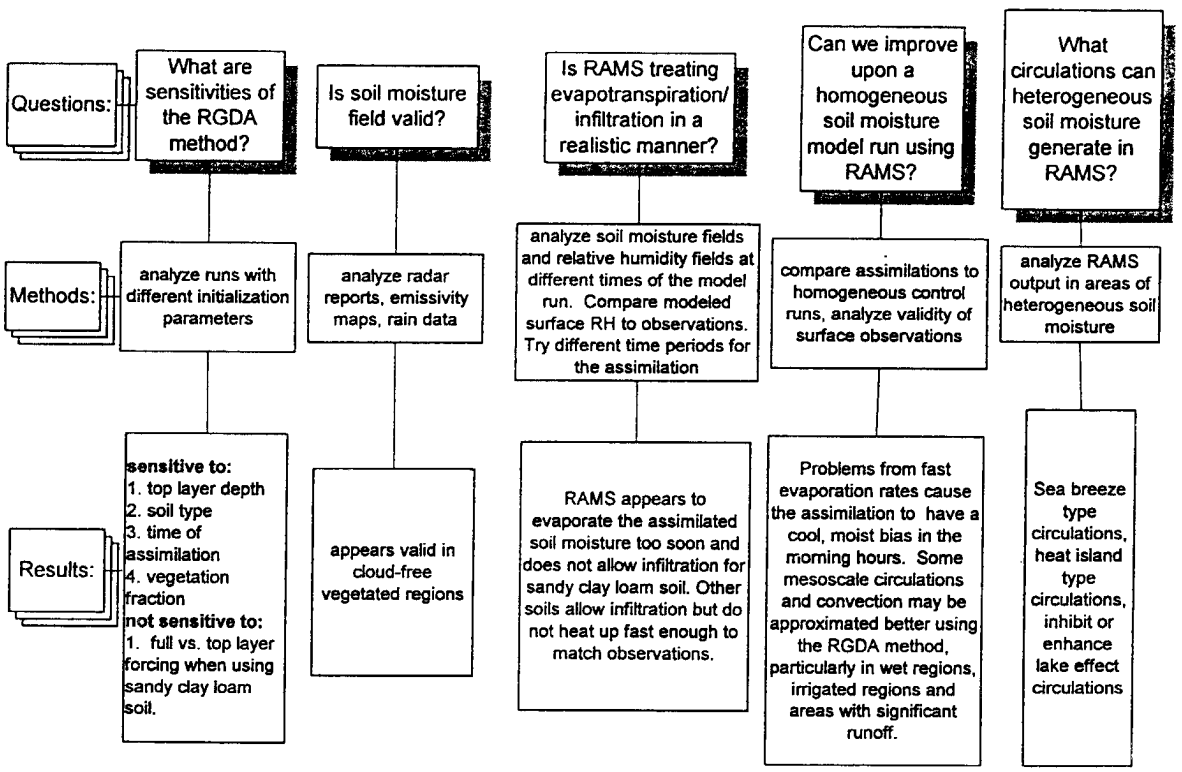


**Figure 6. 1 Flowchart examining major questions studied in this thesis.**

## Bibliography


Achutuni, R., J. Ladue, R. Scofield, N. Grody, R. Ferraro, 1994: A Soil wetness index for monitoring the great floods of 1993, pp. 580 to 583, In: Seventh Conference on Satellite Meteorology and Oceanography, June 6-10, 1994 preprints. American Meteorological Society, Boston Massachusetts 02108-3693.

Avissar, R., and R. A. Pielke, 1989: A parameterization of heterogeneous land surfaces for atmospheric numerical models and its impact on regional meteorology. *Mon. Wea. Rev.*, **117**, 2113-2136.

Blackadar, A. K., 1979: High resolution models of the planetary boundary layer. *Adv. Environ. Sci. Eng.*, **1**, 50-85.

Carlson T. N., J. K. Dodd, S. G. Benjamin and J. N. Cooper, 1981: Satellite estimation of the surface energy balance, moisture availability and thermal inertia. *J. Applied Meteor.*, **20**, 67-87.

Copeland, J.H., 1995: *Impact of soil moisture and vegetation distribution on a July 1989 climate using a regional climate model.* Ph.D. dissertation, Colorado State University, Fort Collins, Colorado, 124 pp.

FAO-Unesco, 1975: **Soil map of the world**, Vol. 2., UNESCO.

Gillies, R. R. and T. N. Carlson, 1995: Thermal remote sensing of surface soil water content with partial vegetation cover for inclusion into climate models. *J. Atmos. Met.*, **34**, 745-756.

Gannon, P., 1978. Influence of earth surface and cloud properties on the south Florida sea breeze, *Tech. Rep. ERL 402-NHEML2*, NOAA, U.S. Dep. Of Commerce, Washington, D. C.

Grasso, L., 1996: *Numerical simulation of the May 15 and April 16, 1991 thunderstorms.* Ph.D. dissertation, Colorado State University, Fort Collins, Colorado, 151 pp.

Jones, A. S., 1996: *The use of satellite-derived heterogeneous surface soil moisture for numerical weather prediction.* Ph.D. dissertation, Colorado State University, Fort Collins, Colorado, 493 pp.

Jones, A. S., K. E. Eis, and T. H. Vonder Haar, 1995: A method for multisensor-multispectral satellite data fusion. *J. Atmos. Oceanic Technol.*, **12**, 739-754.

Klemp, J.B. and R.B. Willhelmson, 1978a: The simulation of three-dimensional convective storm dynamics. *J. Atmos. Sci.*, **35**, 1070-1096.

Lull, H. W., 1964: Ecological and silvicultural aspects. In Handbook of Applied Hydrology, edited by V. T. Chow, McGraw-Hill Book Company, New York., 6.1-6.30.

Mahrer, Y., and R. A. Pielke, 1977: A numerical study of the airflow over irregular terrain. *Beitr. Phys. Atmos.*, **50**, 98-113.

McCumber, M. C. and R. A. Pielke, 1981: Simulation of the effects of surface moisture in a mesoscale numerical model. *J. Geophys. Res.*, 9929-9938.

McFarland, M.J., and C.M.U. Neale, 1991: Land parameter algorithm validation and calibration, pp. 9-11 to 9-39, In: DMSP Special Sensor Microwave/Imager Calibration/Validation, Final Report, Volume 2. Naval Research Laboratory, Washington, DC 20375-5000.

McNider, R. T., A. J. Song, D. M. Casey, P. J. Wetzel, W. L. Crosson, and R. M. Rabin, 1994: Toward a dynamic-thermodynamic assimilation of satellite surface temperature in numerical atmospheric models. *Mon. Wea. Rev.*,**(122 )**, 2784-2802.

Pielke R. A., W. R. Cotton, R. L. Walko, C. J. Tremback, W. A. Lyons, L. D. Grasso, M. E. Nicholls, M. D. Moran, D. A. Wesley, T. J. Lee and J. H. Copeland, 1992: A comprehensive meteorological modeling system - RAMS. *Met. and Atmos. Phys.*, **49**, 69-91.

Segal, M., R. Avissar, M. C. McCumber, and R. A. Pielke, 1988: Evaluation of vegetation effects on the generation and modification of mesoscale circulations. *J. Atmos. Sci.*, **16**, 2268-2292.

Segal, M., W. E. Schreiber, G. Kallos, J. R. Garratt, A. Rodi, J. Weaver, and R. A. Pielke, 1989. The Impact of Crop Areas in Northeast Colorado on Midsummer Mesoscale Thermal Circulations. *Mon. Wea. Rev.*, **117**, 809-825.

Shaw, B.L., 1995: *The effect of soil moisture and vegetation on a great plains dryline: a numerical study.* M.S. thesis, Colorado State University, Fort Collins, Colorado, 93 pp.

Stull, R. B., 1988: *An Introduction to Boundary Layer Meteorology*, Kluwer Academic Publishers.

Tremback, C. J., 1990: Numerical simulation of a mesoscale convective complex: model development and numerical results. Colorado State University, Department of Atmospheric Science., paper no. 465.

USDA, 1991: *Weekly Weather and Crop Bulletin* (July 30, 1991). Produced by the NOAA/USDA Joint Agricultural Weather Facility, Washington, DC.

USDA, 1991: *Weekly Weather and Crop Bulletin* (Aug. 6, 1991).

USDA, 1991: *Weekly Weather and Crop Bulletin* (Sep. 10, 1991).

USDA-SCS, 1981: *Land Resource Regions and Major Land Resource Areas of the United States*, Agricultural Handbook 296, Washington DC.

USGS, 1993: *Seasonal Land Cover Regions map of the US*, Denver CO 80225.

# Appendix

## Appendix: Basic hydrology and land-air interactions seen using the RGDA method.

In this section, the RGDA method is analyzed for the 8 September 1991 case. A very basic overview of hydrology terms is presented and then an attempt is made to explain what is going on during the data assimilation for large spatial scales as well as for a specific wet region and a specific dry region. The model run is the same as the Jones (1996) run except with a smaller top soil layer specified (0.5 cm rather than 3 cm) and only the largest grid is used. Chapter 2 describes the sensitivities to the smaller top layer assumption. The purpose of this appendix is to give a qualitative description of how the RGDA method works.

### *A.1 Basic hydrology important for studying land-air interactions*

The following discussion is based on facts and information obtained from Howard Lull's section in the Handbook of Applied Hydrology (edited by Chow, 1964). This reference, although old, discusses the basics of hydrology that are needed as background to study land-air interactions. Rainfall and moisture can be intercepted by vegetation, infiltrated into soils or evaporated into the air.

#### A.1.1 Interception

Interception refers to rain or moisture absorbed by leaves in a vegetation canopy. This occurs when rain first begins until the maximum surface storage capacity of the leaves is reached.

This storage of moisture by leaves can be evaporate after rain stops and the humidity of air has decreased.

Between 10 and 20 percent of rain during the growing season is intercepted and later evaporated. Because interception only occurs until the leaves have saturated, a short storm always has a larger percentage of its rain intercepted than a long storm in the same area.

### A.1.2 Infiltration

Infiltration refers to the movement of water into the soil and is highly dependent on soil texture and structure. Coarse soils have the most infiltration and bare clay soils has the least. Dry soil allows more infiltration than wet soil. Maintaining large infiltration rates is easiest where there are undisturbed natural forest canopies and decaying vegetation (i.e. tree roots); these types of forest floors soak up water more than bare soil. The compaction of soils (such as by a tractor passing through or due to grazing animals) can reduce infiltration rates by as much as 80%.

Infiltration rates are frequently measured just after the soil has been moistened by rain but before the soil is saturated. Some examples given in the *Handbook of Applied Hydrology* are 0.6 inches/hr after two passes with a tractor in a pasture and 2.36 inches/hr measured in an undisturbed forest region in Minnesota.

### A.1.3 Evapotranspiration

Evapotranspiration combines the effects of water released by plants to the atmosphere (transpiration) and water vapor moving from soil and vegetation (evaporation) to the atmosphere.

Soils from which water evaporates the fastest are the most compact, the most dark and most dominated by medium-sized particles. Frequently just the top layer of soil dries out while lower layers remain moist.

Transpiration is highest with high air temperatures, high winds, saturated leaf tissues, high amounts of light, low atmospheric humidity, and large availability of soil moisture. Average daily evaporation is largest in the summer months (0.18 inches of water in June) and smallest in winter (0.06 inches of water in January).

### A.1.4 Basic hydrology in the RGDA method

In the RGDA method, water is put directly into the top layer of soil and into the vegetation profile. There is no interception by vegetation above the ground. Infiltration is governed by soil type and moisture content only and there is no specification in RAMS involving how compact the soil may be.

Soil moisture is added in the morning hours of the assimilation because there is normally less temperature advection. The atmospheric conditions in which water is added during the assimilation are fairly different from when rainwater is added. During rainstorms water is more likely to infiltrate deeper into soil because the atmospheric humidity is so high. Because the IR sensor on the GOES-7 satellite is only seeing skin temperature, the top layer is the only layer forced by the RGDA method.

The RGDA method gives the value of soil moisture required to generate realistic heating rates. For the API method it is up to the user to decide how this index will correspond to volumetric soil moisture. For example, Grasso (1996) used the API described by Wetzel and Chang (1988), but smoothed and reduced all the values by 10% for one great plains simulation in April. For a great plains simulation in May of the same year, the values were not smoothed or reduced. A certain amount of trial and error seems to be required to use the API, but it is not required to use the RGDA method.

### *A.2 Surface energy budget in the RGDA method*

Recall that the RGDA method is based upon keeping the surface energy budget in balance (equation 1.1). For the vegetation component, this means that the sum of latent and sensible heat flux should be equal to the net incident radiation. For bare and shaded soil components there is also soil heat flux which needs to be accounted for. Soil heat flux is generally much smaller than latent and sensible heat flux terms and so is not analyzed here, although a discussion is found in Jones (1996). Figure A. 1 shows the terms for the vegetation surface energy budget, for a region in the central plains, from 1-D sensitivity tests by Jones (1996). Time is specified so that 6 hours corresponds to local noon. The control run has no satellite forcing. The RGDA method run is the next plot, but satellite forcing was not used until about 0.7z so that the method could begin when the sun had risen. In these graphs, fluxes are negative when put into the atmosphere from the ground. Because the region was initialized as wet and vegetated, the latent heat flux for the control run is fairly high (up to 600 $W/m^2$ into the atmosphere); the sensible heat flux is small in comparison. The second plot shown is for 1 K/hr forcing throughout the day. This forcing is not physically-based; instead it is used to illustrate how the assimilation works to keep the surface energy budget in balance. In the morning hours, 1 K/hr is a relatively low heating rate for the ground, and so the ground remains moist with high latent heat flux values. In late afternoon the ground should not heat up and so 1 K/hr is a relatively high heating rate, making the RGDA method dryer than before. Sensible heat flux increases and latent heat flux decreases, reflecting that the energy budget is always in balance.

### *A.3 RGDA method analyzed using time series plots*

This section will focus on the effect of altering soil moisture during the time period that the RGDA method is used by analyzing ground temperature, soil moisture, temperature, relative

humidity and latent and sensible heat fluxes. These quantities will be studied using time series plots for sample wet and dry regions.

The 8 September 1991 case study was originally done by Jones (1996). The RGDA method generated a realistic soil moisture map (as compared with the API, Crop Moisture Index and microwave surface emissivity maps).

### A.3.1 Ground Temperature and Bare Soil Moisture

#### Adding Soil Moisture

When the ground is originally heating up too fast in RAMS, the RGDA method adds water to the top layer of soil until the heating rate of the ground is correct. An example of a wet area in the 8 September case is in north central Texas (see Figure A.2). A time series is plotted for one grid cell (40 km spacing) to show how the soil moisture was added. This is in Figure A.3.

Note that during the assimilation period from 14:00z to 15:00z (10800-14400 s) the ground temperature becomes relatively constant to match satellite observations. However, immediately following the assimilation period, ground temperature heating rates return to approximately the same as they were before the assimilation took place. This appears to be a problem caused by the RGDA method initializing just the top layer of soil. Because soil moisture is added during the morning and to only the top soil layer, evaporation occurs much faster than infiltration of water into deeper soil layers.

Jones used the assimilation for just the top layer of soil, leaving the rest of the column at 25% soil moisture (this value provides an intermediate ground surface heating rate). However, Jones suggested that better results may be obtained by initializing the full layer. An attempt was made to simulate this and the results of full layer forcing were not significantly different from only top layer forcing. This run was described in section 2.2.

**Subtracting Soil Moisture**

When RAMS doesn't produce a large enough ground surface heating rate, soil moisture is subtracted to make the soil heat faster. As we have seen with the wet case in the previous section, RAMS evaporates soil moisture very quickly as soon as the sun rises. Therefore the effects of the RGDA method are not as obvious in our time series plots for a dry region. The area chosen is in northwestern Kansas.

One can see that there is a very slight increase in the heating of ground temperature and a fast decrease in soil moisture from Figure A.4. The decrease in soil moisture is only slightly more dramatic than it would have been without assimilating satellite heating rates (compare with the evaporation of soil moisture in the moist case after the data assimilation in Figure A.3).

### A.3.2 Effects of data assimilation method on surface latent and sensible heat fluxes

**Adding Soil Moisture**

The data assimilation method is confined to solutions for the partitioning of energetically consistent latent and sensible heat fluxes. Soil moisture added to the surface should increase latent heat flux and decrease sensible heat flux because more energy can go into evaporation when there is plenty of moisture available. One can see this happening in Figure A.5.

The latent heat flux increases from about 60 $W/m^2$ to 500 $W/m^2$ over the one hour assimilation period (10,800-14,400 s). Sensible heat flux decreases from about 200 $W/m^2$ down to near 0 $W/m^2$ in value. Particularly in the sensible heat flux plot, it appears that after the assimilation occurs the flux increases at the same rate as before the assimilation. However, one can see that the maximum value for the sensible heat flux would have had a larger value had there not been any data assimilation.

**Subtracting Soil Moisture**

In a dry region we expect surface latent heat flux to decrease during the assimilation because soil moisture is forced to disappear. However, because the model without the RGDA method evaporates soil moisture very quickly, there is not a large discontinuity in the fluxes (Figure A.6).

### A.3.3 Surface air temperature and relative humidity.

From the earlier figures, it is seen that the RGDA method does not dramatically change anything for dry regions, while the most significant cases are for wet regions. Previous figures focused on quantities associated with the ground surface energy budget. Temperature and relative humidity changes are not directly altered in the RGDA method; instead they are indirect reactions to the assimilation and finally relate the surface boundary conditions to the weather.

One can see from Figure A.7 that surface air temperature is almost steady during the assimilation and that relative humidity increases shortly after the assimilation begins. These are both directly related to the modeled increased latent heat flux. In the dry case there is no obvious discontinuity in the assimilation for either temperature or relative humidity, and so this figure is not shown.

### A.3.4 Surface air temperature with respect to ground temperature.

Figure A.8 shows surface air temperature with respect to time plotted with ground surface bare soil temperature, with both using the RGDA method. Bare soil begins cooler than air temperature, but heats up much faster as the day goes on. The bare soil temperature is more abruptly changed by the RGDA method compared to the air temperature. As the day ends, one can see that bare soil temperature is cooling off faster than air temperature. In this sense, RAMS and the RGDA method are consistent with basic climatology of air and land. The bare soil gets very hot, over 40 °C. This is not unreasonable as there is very little bare soil (10% or less) in

each grid cell of RAMS. The actual ground temperature is a function of bare soil temperature, shaded soil temperature, and vegetation temperature.

Figure A. 9 illustrates the relationship between vegetation temperature, shaded soil temperature, bare soil temperature and effective ground temperature with air temperature. The figure for the vegetated region contours the air temperature at the midpoint of the first two model layers (24.0 and 72.0 m). The vegetation temperature is shown at 0m and the shaded temperature is shown at -0.15 m. The figure for the shaded soil region has the shaded soil temperature plotted at 0 m and -0.15 m, and the figure for the bare soil region has the bare soil temperature plotted at 0 m and -0.15 m. The figure for ground temperature incorporates all three components. It assumes that at 0 m the vegetation comprises 40% of the grid cell, the shaded soil comprises 50% of the grid cell and the bare soil comprises 10% of the grid cell. At -0.15 m, 90% of the grid cell is shaded soil and 10% is bare soil. All figures are for the 8 September 1991 wet region with the RGDA method occurring between 15 and 16z. From these figures one can see the difference in temperature between the ground and the air above it as the day progresses in the model run. The bare soil heats up quickly and is much warmer than the air temperature by 20z, whereas the shaded soil and the vegetation have heating rates and temperatures similar to air temperature. The incorporation of bare soil, shaded soil and vegetation components is the model's most realistic interpretation of ground temperature vs. air temperature. The ground heats slightly faster than air temperatures, but never gets as warm as only the bare soil component.

### *A.4 Summary.*

The RGDA method is capable of drastically changing surface soil moisture values, ground temperatures and the partitioning between latent and sensible heat fluxes. There has been very little ground truth in this chapter because Jones (1996) does a detailed job of comparing the modeled 8 September 1991 case to observations. This section is only meant to illustrate how the

RGDA method works. Table A.1 and Table A.2 show typical wet region and dry region reactions to the assimilation. In the wet region, ground temperature was kept constant during the RGDA method by adding about 10% more volumetric soil moisture. Before the assimilation sensible heat flux was more than three times the value of the latent heat flux at the surface. After the assimilation, flux at the surface was entirely composed of latent heat release. In the dry region the original values of latent and sensible heat were equal. By the end of the assimilation sensible heat flux was about three times the value of latent heat flux. It is difficult to tell from the tables alone that the assimilation is more affective at altering wet regions than dry regions; however the figures presented earlier make it clear that wet regions are most affected by the data assimilation.

**Table A.1 Typical wet region reaction to the RGDA method.**

| | *Before RGDA* | *After RGDA* | *Maximum during run* |
|---|---|---|---|
| Ground temperature | 302.5 K | 302 K | 317 K |
| Soil moisture | 20% | 30% | 30% |
| Latent heat flux at surface | 60 $W/m^2$ | 500 $W/m^2$ | 500 $W/m^2$ |
| Sensible heat flux at surface | 200 $W/m^2$ | 0 $W/m^2$ | 450 $W/m^2$ |

**Table A.2 Typical dry region reaction to RGDA method.**

| | *Before assimilation* | *After assimilation* | *Maximum during run* |
|---|---|---|---|
| Ground temperature | 297 K | 302.5 K | 313 K |
| Soil moisture | 21% | 15% | 25% |
| Latent heat flux at the surface | 50 $W/m^2$ | 65 $W/m^2$ | 85 $W/m^2$ |
| Sensible heat flux at the surface | 50 $W/m^2$ | 220 $W/m^2$ | 375 $W/m^2$ |

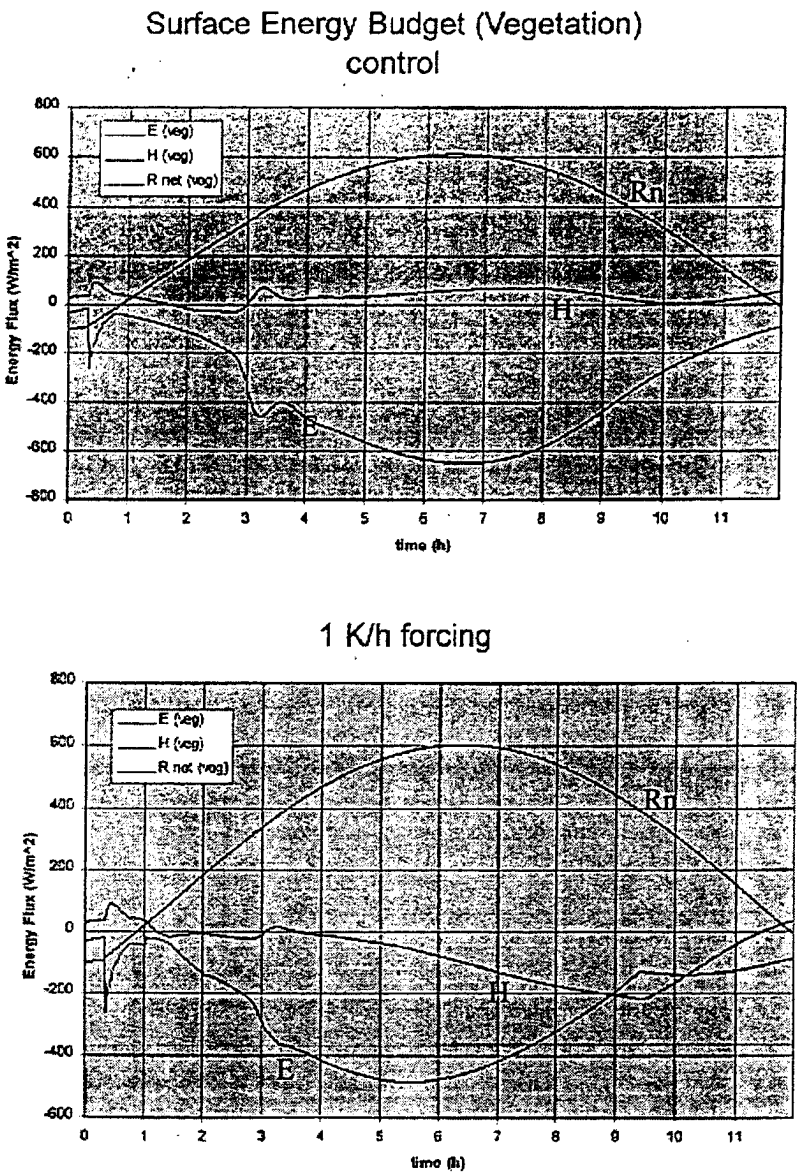


**Figure A. 1 Surface energy budget terms for the vegetation component of the surface, from Jones (1996).**

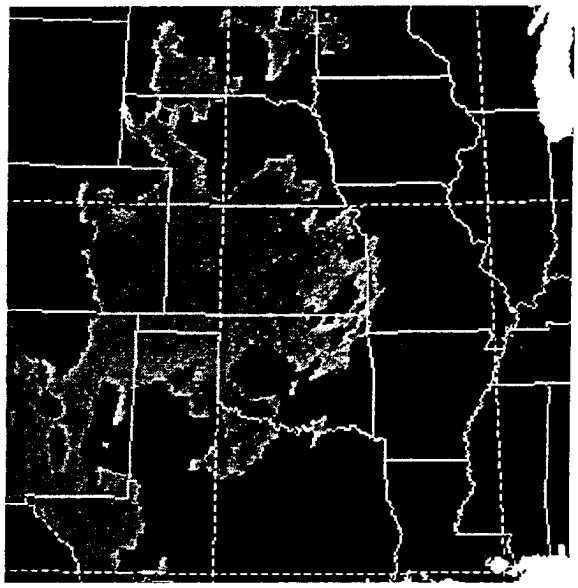

**Figure A.2 Cloud-cleared microwave emissivity map for channel 7, 8 September 1991, 15:30z. Dark areas are low emissivities (probable wet areas), cloud cleared regions are black.**

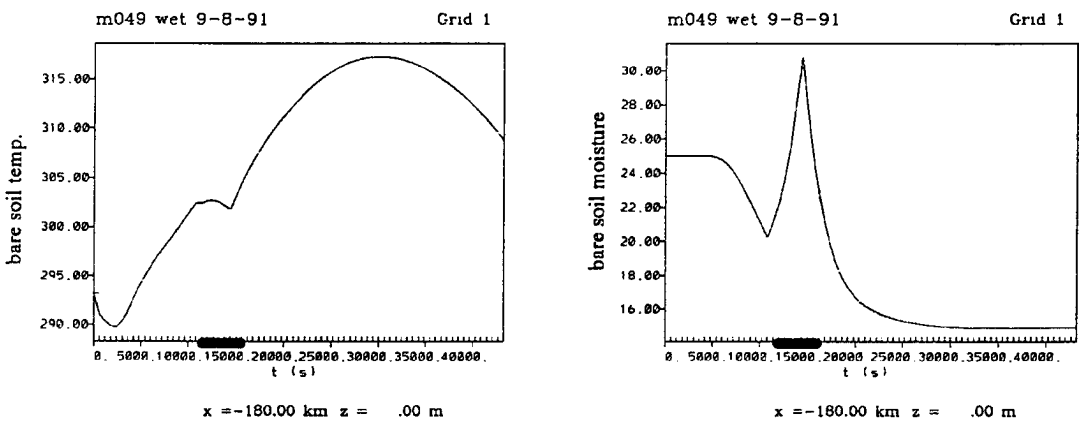


**Figure A.3 The ground temperature and the percent bare soil moisture plotted with respect to time for a moist region on 8 September 1991. Approximate period of assimilation (10800s-14400s) is underlined.**

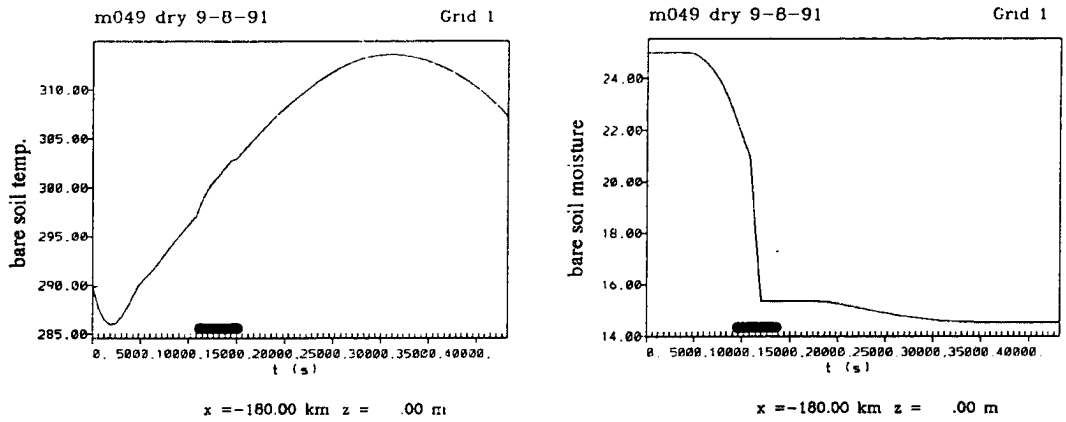


**Figure A.4 The ground temperature and the bare soil moisture percent for a dry area using the RGDA method.**

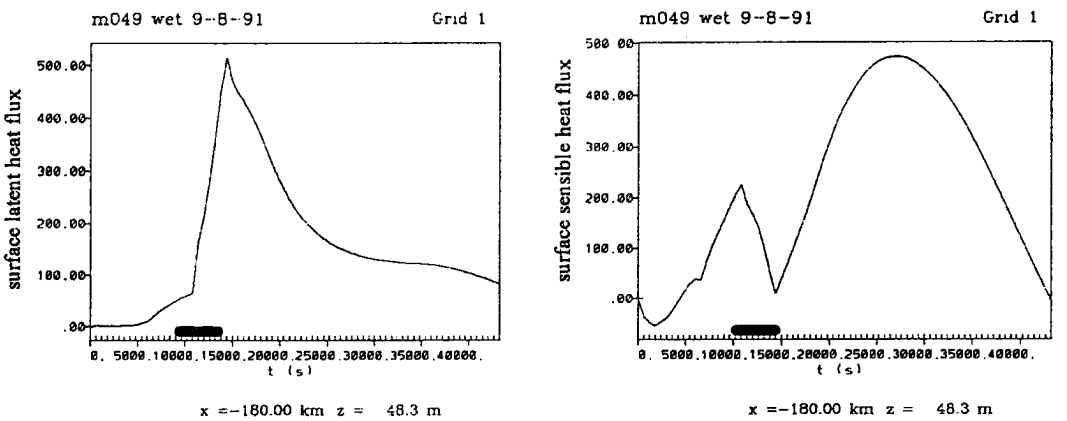


**Figure A.5 Surface latent and sensible heat fluxes with respect to time for a wet region in the RGDA method.**

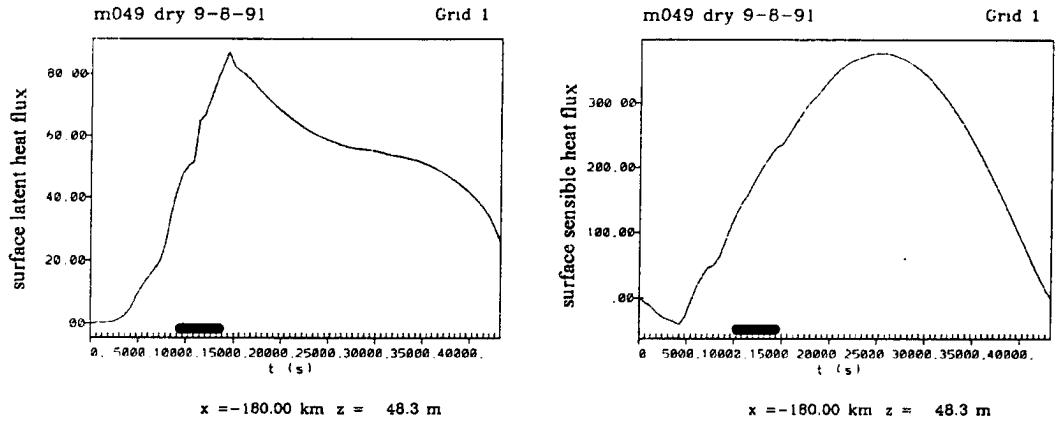


**Figure A.6 Surface latent and sensible heat fluxes for a dry region using the RGDA method.**

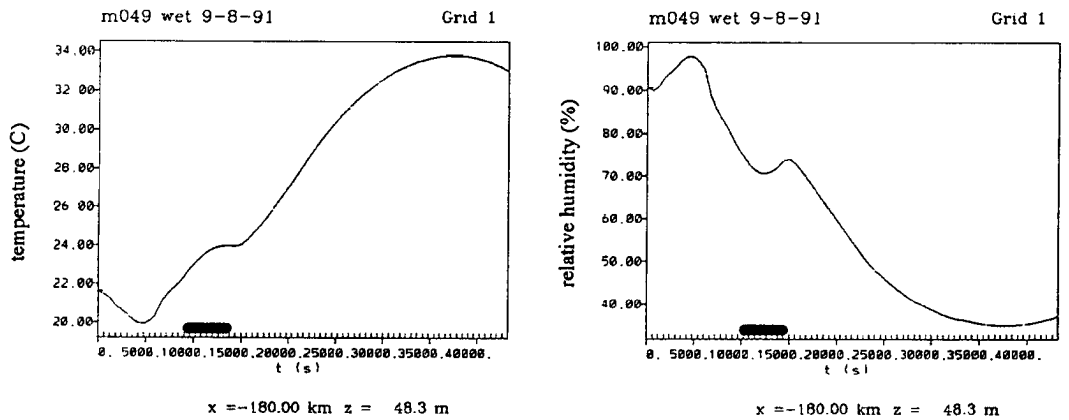


**Figure A.7 Temperature and relative humidity near the surface for a wet region in the RGDA method.**

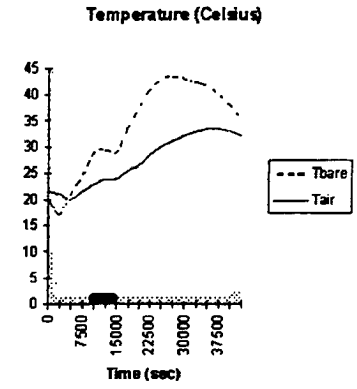


**Figure A.8 Temperature of bare soil and temperature of the air just above the bare soil for a wet region using the RGDA method for the 8 September 1991 case.**

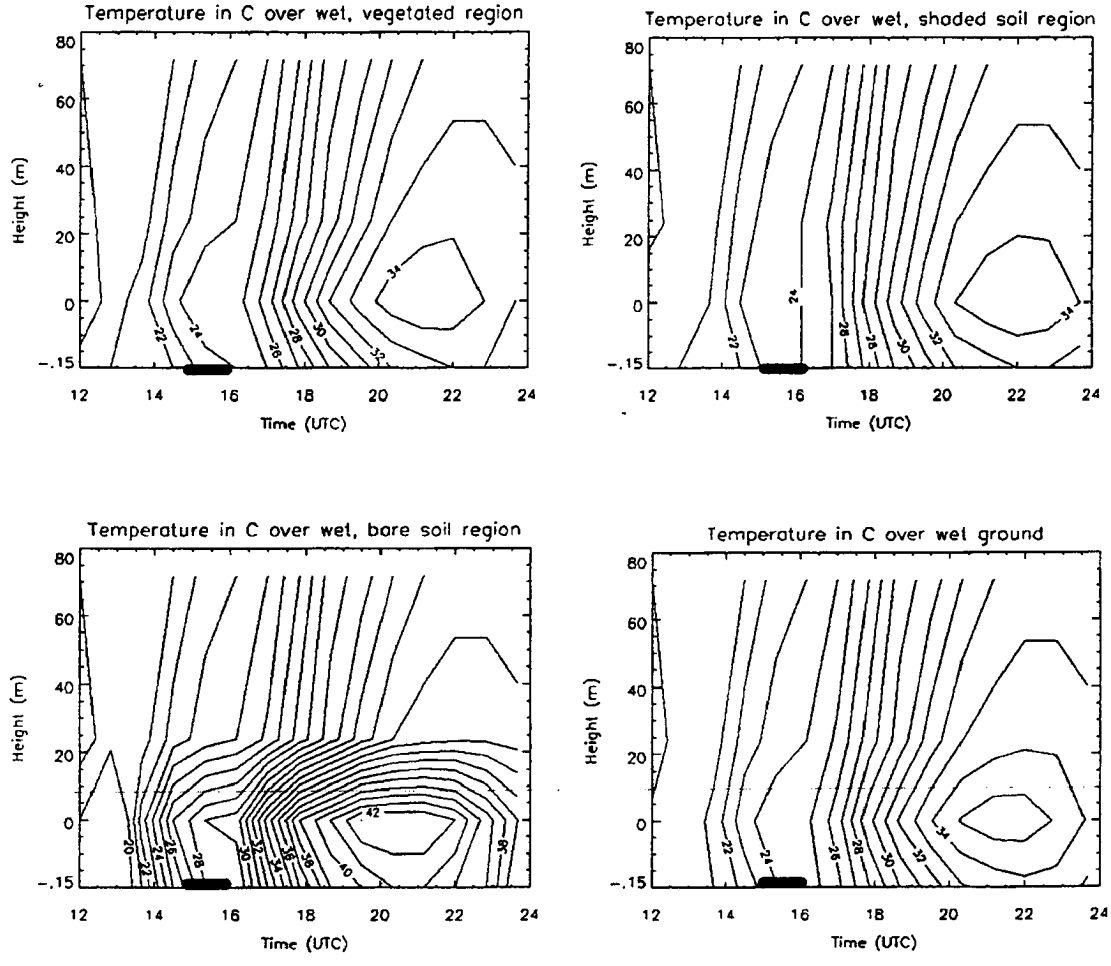


**Figure A. 9 Temperature in Celsius for a wet region using the RGDA method between 15 and 16z (not to scale).**